Quality Assessment of Wind Estimation within Precipitation Using a Three-Beam Radar

MSc Thesis

Esther Oberle

The cover image is a picture showing Cabauw Experimental Site for Atmospheric Research (CESAR) in the Netherlands. The meteorological tower can be seen in the left and the Transportable Atmospheric Radar (TARA) in the right part of the picture. The image is an edited screenshot taken from Google Earth Street View (`https://earth.google.com/web/`, © 2018 Google).

Quality Assessment of Wind Estimation within Precipitation Using a Three-Beam Radar

by

Esther Oberle

to obtain the degree of Master of Science
at the Delft University of Technology,
to be defended publicly on Thursday December 6, 2018 at 13:30 AM.

Student number:	4627598	
Project duration:	March 12, 2018 – December 6, 2018	
Thesis committee:	Ir. C.M.H. Unal,	TU Delft, supervisor
	Prof.dr.ir. H.W.J. Russchenberg,	TU Delft
	Dr. M. Schleiss,	TU Delft
	Dr. L. Nuijens,	TU Delft
	Dr. F.C. Bosveld,	KNMI

TU Delft

Abstract

Wind is an important indicator of circulation related processes in the atmosphere. Accurate wind information is used as an input for weather and circulation models. Wind data with a high temporal and spatial resolution are useful for research on the microphysics of the atmosphere, which is the area of application for the three-beam Transportable Atmospheric Radar (TARA) located at Cabauw Experimental Site for Atmospheric Research (CESAR) in the Netherlands. Although some comparisons were performed using radiosondes, no thorough quality assessment of the wind estimation results has been done so far. During this research, the quality assessment is performed for the estimation of the wind speed and direction during the Analysis of the Composition of Clouds with Extended Polarization Techniques (ACCEPT) campaign, which took place in October and November 2014. This research shows that the wind estimation is working well during precipitation and a TARA-based criteria for the data selection to guarantee the quality of the wind retrievals is identified in the form of the coefficient of variation for the mean Doppler velocities.

The quality assessment of the results of the TARA wind estimation is done by comparing the wind retrievals to the measurements of the meteorological tower at a height of 200 m above the surface at minute resolution. For the assessment to be performed, an effective way of removing clear air measurements is needed, which is done for the whole ACCEPT-campaign using a rough selection of time steps including rain. This approach showed that the wind estimation is working well during precipitation and shows that an improved data selection is needed.

Several approaches towards improving the data selection for the wind estimation of TARA are performed. The most successful is the use of the coefficient of variation, which is defined as the standard deviation divided by the mean. This coefficient is calculated for the mean Doppler velocities, which are the input for the wind estimation algorithm. Comparing the results of the coefficient of variation method to the one based on rain selection shows that both return good results. This leads to the conclusion that the coefficient of variation is useful to improve the data selection.

Acknowledgements

Completing this master thesis would not have been possible without the help of many people. I would like to thank my supervisor Christine Unal for all the valuable input and always finding time for answering my questions. Further, I would like to thank the other members of my assessment committee – Herman Russchenberg, Marc Schleiss, Louise Nuijens and Fred Bosveld – for reading my reports and providing feedback during progress meetings. I would also like to thank the great group of my fellow GRS students who were also working in the PhD room for all the discussions during coffee and lunch breaks. Last but not least, I would like to thank my family for always supporting me.

Contents

List of Figures

List of Tables

List of Abbreviations

ACCEPT	Analysis of the Composition of Clouds with Extended Polarization Techniques
CESAR	Cabauw Experimental Site for Atmospheric Research
FFT	Fast Fourier Transform
FMCW	Frequency Modulated Continuous Wave
MB	TARA Main Beam
MIRA	Millimeter Wave Radar
OB1	TARA Offset Beam 1
OB2	TARA Offset Beam 2
RHI	Range Height Indicator
RMSE	Root Mean Square Error
SNR	Signal to Noise Ratio
TARA	Transportable Atmospheric Radar

List of Symbols

α	Elevation angle of TARA main beam or angle for ground truth simulation	[°]
Δt	Time between transmission and recieving of an electromagnetic wave	[s]
γ	Angle between MB and OB1, and MB and OB2	[°]
λ	Wavelength	[m]
μ	Mean	
σ	Standard deviation	
θ	Offset angle from zenith	[°]
Φ_N	Azimuth of TARA	[°]
B	Frequency bandwidth	[Hz]
c	Speed of light	[m/s]
C_V	Coefficient of Variation	[-]
C_z	Radar constant	
D	Wind direction in reference to North	[°]
D_1	Distance between V_{OB1} and zenith	[m]
D_2	Distance between V_{MB} and zenith	[m]
D_H	Equivolume spherical diameter of the hydrometeor	
e	Error wind speed or direction between TARA and the tower	[m/s],[°]
e_{vy}	Error in V_y-direction	[m/s]
f	Frequency	[Hz]
f_b	Beat frequency	[Hz]
f_c	Frequency change	[Hz]
f_D	Doppler shift of the target	Hz
$f_{b,D}$	Doppler beat frequency	[Hz]
h	Fixed height above ground	
N	Number of estimation values considered	
$N(D_H)$	Hydrometeor size distribution	
P_r	Received power	[W]
R	Range	[m]
r	Radius which correpsonds with the wind speed for the ground truth	[m/s]
R_{max}	Maximum range	[m]

R_{xy}	Correlation of two variables	
T	Sweep time	[s]
t	Number of time steps	
T_0	Time between two consecutive pulses transmitted by the radar	[s]
U	Velocity component in West-East direction	[m/s]
V	Velocity component in South-North direction	[m/s]
v_f	Fall velocity	[m/s]
V_M	Horizontal wind speed	[m/s]
v_r	Radial velocity	[m/s]
V_u	Velocity component in West-East direction	[m/s]
V_v	Velocity component in South-North direction	[m/s]
V_w	Vertical velocity	[m/s]
V_x	Horizontal wind component in TARA reference system	[m/s]
V_y	Horizontal wind component in TARA reference system	[m/s]
V_z	Vertical mean Doppler velocity	[m/s]
v_D	Mean Doppler velocity	[m/s]
V_{fall}	Fall velocity	[m/s]
v_{max}	Maximum unambiguous velocity	[m/s]
V_{MB}	Main beam mean Doppler velocity	[m/s]
V_{OB1}	Off set beam 1 mean Doppler velocity	[m/s]
V_{OB2}	Off set beam 2 mean Doppler velocity	[m/s]
W	Vertical velocity	[m/s]
z	Reflectivity	$[mm^6 m^{-3}]$

1 Introduction

Incoming solar radiation is the main driver of circulations in the atmosphere. The difference between the amounts received at the equator compared to the poles gives rise to zonal temperature differences, leading to pressure differences resulting in air movements which are measured as wind. Wind is an indication for many processes in the atmosphere and it is difficult to measure in-situ at different heights and over larger areas in the atmosphere (Marshall and Plumb, 2008).

Among other applications, accurate wind information is needed as inputs for weather and circulation models as well as for real-time warning systems (Benjamin et al., 2004). Using wind profilers – measuring in clear air and rain – has been a common practice for these applications which use time resolutions of around 30 minutes to a few hours. Another application for vertical wind profiles is studying microphysics within clouds and precipitation. While for weather and circulation models the time as well as spatial resolution does not need to be very good, it is important when studying microphysics. This is the area of application of the three-beam Transportable Atmospheric Radar (TARA) located at the Cabauw Experimental Site for Atmospheric Research (CESAR). There is a standard wind profiler at CESAR. However, the three-beam precipitation radar TARA profiling the troposphere with high temporal and spatial resolution may complement the wind profiler in the case of precipitation.

The main content of this master thesis research will be an approach of using and validating the wind estimation data from the rain radar TARA during precipitation and clouds with high time resolution compared to the common practice of wind profiler studies. The Introduction will include a section introducing the principle of radar wind profilers and TARA, including the main differences. Previous research in mainly two categories including high and low time resolution applications will then be followed by a section about TARA and the Analysis of the Composition of Clouds with Extended Polarization Techniques (ACCEPT) campaign. The conclusion of the Introduction Chapter includes the research questions.

1.1. Previous Research Using Wind Profiles

There are two main types of application discussed in the following sections. The first type of applications that are introduced use relatively low temporal resolutions. These include weather and circulation models. These types of application use averaging in order to solve the issues caused by the beams measuring different media. Also, the research areas are mostly larger compared to high spatial and temporal resolution case studies which TARA is designed for. The second type of applications is thus focused on using relatively high time resolution and discussing results obtained by other research done. Examples include research on thunderstorms and tropical cyclones as well as studies concerning microphysics within cloud and precipitation.

1.1.1. Weather and Circulation Models

As mentioned above, for wind profilers one approach of solving problems due to beam divergence or looking at a heterogeneous media is to average the data over relatively long time periods. For case studies looking at microphysics of the media observed this is not a solution, but in cases where the time

resolution is less important, this approach is sufficient. An example for this are weather and circulation models as well as observing larger scale weather phenomenon.

A study using wind profilers was performed by Zhong et al. (1996) in the Great Plains of the United States. In this study a combination of Wind Profiler and modelling were used to observe the summertime low-level jet successfully and in better spatial and temporal resolution than previous studies (Zhong et al., 1996). Another paper analyses the value of wind profilers for weather forecasting and comes to the conclusion that through the good temporal resolution the short-term forecasts profit a lot from wind profiler data available at up to 6 minutes time resolution (Benjamin et al., 2004). A challenge was found in the form of migrating birds by Wilczak et al. (1995) which consists of errors introduced when using time periods of an hour for averaging of the vertical wind profiles. It was found that migrating birds are the cause of relatively large errors found in wind profiler data averaged over the period of one hour (Wilczak et al., 1995). In Europe a study was conducted using a network of 13 wind profilers with the intention of validating the use of the wind data in weather models. The time and spatial resolutions vary mostly due to the different sensor properties of the wind profilers. The data is available at 12 minutes time resolution, but was found to be usable at 30 minutes averaging intervals. A vertical resolution of 300 metres was found to be feasible. The main conclusion was that the results justify the use of the data obtained in the network as input in weather models (Nash and Oakley, 2001).

To conclude, for studies looking at larger scale phenomenon or weather models, the time resolution is not the most important aspect. The next section looks at research done which uses higher time resolution or work done on improving the usable time resolution for vertical profiles of the horizontal wind.

1.1.2. Thunderstorms and Tropical Cyclones

The applications discussed in this section compared to the ones in the previous section are mostly concerning case studies which need higher time and spatial resolution than weather and circulation models. Studies concerning microphysics in the atmosphere mostly concern specific case studies and depend on high time resolution because averaging smooths out variabilities of wind speed and direction observations which might exactly be the thing that someone is trying to observe. Other examples are studies concerning fast-evolving phenomenons such as thunderstorms. To observe the relatively fast evolution of thunderstorms and tropical cyclones it is necessary to be able to look at high time as well as high spatial resolution data. There are numerous case studies looking at land falls of tropical cyclones as well as evolution of thunderstorms which use wind data in high time and spatial resolution. The meaning of high time and spatial resolution in the individual cases will be discussed below.

An example is the application of two mobile Doppler radars that were used to measure outflow winds of thunderstorms. In this study two Doppler radars were used and the measurement method was validated using data from a meteorological tower. The mode used was Range Height Indicator (RHI) and the time resolution was in the range from seconds to a maximum of 10 minutes averaging. The method of using two Doppler radars for vertical profiles of the horizontal wind speed and direction was successfully validated with the data from the tower (Gunter and Schroeder, 2015). Another example is a case study in Hong-Kong where three wind-profilers were used along with anemometers to gain insight into tropical cyclone structures. Depending on range and sensor the spatial resolution can be in a range from 60 meters to several kilometres. While the actual time resolution is 10 minutes, the profiles used consisted of 30 minutes mean wind speed and direction during the passage of two tropical cyclones. The separate profiles of the sensors as well as a combination was analysed in this study and conclusions on the evolution and characteristics of the passage of the tropical cyclones could be made (He et al., 2016). Hong-Kong was subject of another research paper which focused on obtaining vertical wind profiles during typhoons, monsoon and thunderstorms. The profiles were a combination of anemometer measurements combined with Doppler radar profiler measurements. The spatial resolution was ranging between 60 and 200 metres the time resolution was found for each range gate to be at 10 minutes for the speed and 2 minutes for the direction of the wind. While it was possible to make an analysis of the profiles of typhoons and monsoons with fitting models to composites of the obtained profiles, the thunderstorms were analysed on the base of separate profiles that were normalised with boundary layer wind speeds. It was found that the vertical wind profiles obtained from the combination of the different instruments could be used to conclude on the nature of mean vertical wind profiles in the case of typhoon and monsoon (Shu et al., 2017). An important short term weather phenomenon that could benefit from high time and spatial resolution is the observation of downbursts

which can cause a lot of damage. In a study conducted in southern Germany polarisation radars were used to observe downbursts and consider the possibility of momentary downburst detection (Dotzek and Friedrich, 2009).

However it is important to mention that high time resolution is not equal to high accuracy in the observation with a high time resolution. This is the reason that a validation needs to be done in a first step before an attempt at improving the time resolution is made for the Transportable Atmospheric Radar (TARA) wind speed and direction estimation data.The aim is to obtain techniques to improve the usable time resolution while having a good accuracy of the wind measurements, which can be used not only for TARA, but also for other multi-beam radars.

1.2. Vertical Profiles of Horizontal Wind Estimated by Radars

During this master research project the main objective is to validate and analyse the wind retrievals from a precipitation radar situated in the Netherlands at CESAR. For a better understanding of this topic it is useful to introduce commonly used techniques to retrieve three-dimensional wind estimates. This will be done in the following subsections which include a description on how vertical profiles of the horizontal wind in the atmosphere are retrieved using radar.

The acronym radar stands for radio detection and ranging. A pulse radar measures ranges based on the time between an electromagnetic pulse that has been sent out and the time it takes for a reflected echo to return. A Frequency Modulated Continuous Wave (FMCW) radar measures the frequency shift between transmitted and received electromagnetic signals to obtain the range information. The Doppler effect, i.e. the frequency change at fixed range caused by an object moving relative to the radar makes it possible to measure velocities in the radial direction of a radar beam (Milrad, 2018). These mean Doppler velocities can then be translated into estimates of the horizontal wind speed and direction in reference to North.

After an introduction to wind profilers, a section comparing them to and introducing TARA will follow. The following subsections discussing wind profilers and TARA will not go into much detail. The important aspects of radars concerning the main topic of this report – wind retrieval using the three-beam rain radar TARA – will be discussed in more detail later on in Chapter 2.

1.2.1. Wind Profiler

A radar wind profiler is set up with multiple beams. One of them is looking at the zenith while the other beams have a slight offset. This makes it possible to obtain a 3D wind field (Wilczak et al., 1995). A set up of the measurement principle of a wind profiler is shown in Figure 1.1 and the resulting equations to obtain the three dimensional wind velocity field during precipitation are explained below. The measurement principle of the wind profiler includes one beam directed at the zenith, meaning that the vertical velocity is directly measured. Further the other two beams consist of a component of the fall velocity of the hydrometeors and the horizontal wind. Time averaging is used in the case of wind profilers to solve the problem of looking at different media. A problem which becomes more significant with distance away from the radar antenna, as the beams diverge (CIE4608 - Lecture Atmospheric Observation, 2017).

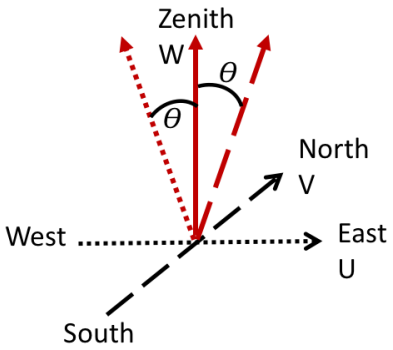

Figure 1.1: Working principle of a Wind profiler. The beams (red arrows) are observing the movement of particles in the atmosphere. One beam is looking at the zenith (solid red line) while the other beams (number depending on the system) are looking in slightly offset directions.

To obtain the three-dimensional wind vector (V, U, V_z) the following equations are used. V_v results from the beam measuring at an angle offset, θ, from the zenith in South-North direction, V_u the component measured at an offset angle from the zenith in West-East direction and W_w is the component measured looking at the zenith (see Figure 1.1 for reference). V_w is a combination of the vertical wind ,W, as well as the fall velocity, v_f.

$$\begin{aligned} V_v &= V \cdot sin(\theta) + (W + v_f) \cdot cos(\theta) \\ V_u &= -U \cdot sin(\theta) + (W + v_f) \cdot cos(\theta) \\ V_w &= (W + v_f) \end{aligned} \tag{1.1}$$

V and U are the horizontal wind components South-North and West-East, respectively.

At CESAR such a wind profiler is present which uses averaging periods of 30 minutes. Unfortunately, the data are not available in the CESAR-database.

1.2.2. The Transportable Atmospheric RAdar (TARA)

The Transportable Atmospheric Radar (TARA) is a precipitation radar used to study the microphysics of clouds and precipitation in the Netherlands. It measures using three beams and the mean Doppler velocities are estimated for all three beams (see Figure 1.2). Contrary to a wind profiler, TARA does not have a beam that is looking at the zenith. This means that none of the wind components are directly observed. Analogue to the procedure of the wind profiler the three mean Doppler velocity measurements (one from each beam of TARA) are translated into the components along the X-, Y- and Z-axis and rotated around the Z-axis in order to be able to reference the wind estimates to the north and be able to compare the results to other sensors. See subsection 2.4.2 for the equations, and the exact details of the wind estimation procedure for TARA are explained and discussed in Chapter 2.

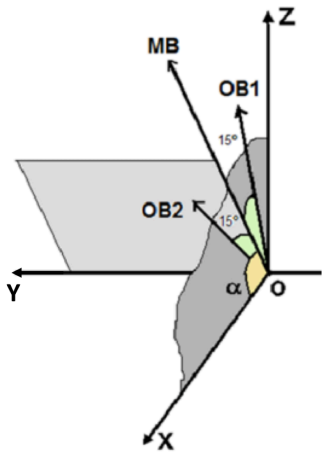

Figure 1.2: TARA setup measurement cycle and reference system (Unal et al., 2012). The main beam measures with an azimuth of 246.5° and this means the X-axis is aligned with the same azimuth. The Z-axis is looking at the Zenith and the Y-axis is perpendicular to the other two. MB = Main Beam, OB1 = Offset Beam 1, OB2 = Offset Beam 2.

TARA and the processing algorithms used so far are designed to measure precipitation and clouds. This means that while wind speed and direction estimates are expected to be usable in cloud and precipitation, this is probably not the case for clear-air measurements.

Further, the way in which the wind algorithm is designed (see subsection 2.4.2) several assumptions are made. The dynamics as well as the microphysics in the measurements are assumed to be originating from the same media for all three beams. This means that it is further expected that the wind estimation during stratiform rain (stable conditions) is more accurate compared to when a more heterogeneous medium is observed. While the wind profiler mainly attempts to solve the problem of observing different media in the different beams by using longer averaging periods, the aim of using TARA wind estimates is to get higher resolution wind profiles in order to study microphysics within

cloud and precipitation. Because it is an FMCW system, the transmitted power is sometimes reduced to avoid receiver saturation in the case of heavy precipitation. However, this also means that the Signal to Noise Ratio (SNR) is then decreased for these periods of times. Measurements with low wind speeds will also be more susceptible to errors as the relative impact of errors in wind estimate is larger, compared to the same error for higher wind speeds. This could be approached by defining a minimum wind speed for the estimates to be considered in the analysis.

1.3. Horizontal Wind Measured by Anemometer

The data which will be analysed during this master thesis is obtained using TARA which is located at Cabauw Experimental Site for Atmospheric Research (CESAR) in the Netherlands. At CESAR other measurement instruments are located and continuously measuring. For the time span of the Analysis of the Composition of Clouds with Extended Polarization Techniques (ACCEPT) campaign there are data available from the cup anemometers located on the meteorological tower at CESAR with time resolutions of either 1- or 10-minute averages. The measurements are taken at different heights along the tower. The first measurement is at 40 m above ground followed by 80, 140 and 200 m. The 1-minute averages are validated while the 10-minute averages available are validated as well as gap-filled. Gap-filled means that the data for missing days are interpolated (Bosveld, 2018). These measurements are considered as the ground truth for the validation of the TARA wind estimation results. The 10-minute data from the tower is available on the CESAR-database. Access to the server containing the 1-minute data from the tower was provided by Fred Bosveld (KNMI).

1.4. TARA and ACCEPT

The Transportable Atmospheric Radar (TARA) is designed to measure precipitation, but due to the fact that it uses three beams it is additionally possible to estimate wind speed and direction in rain and cloud as explained shortly in subsection 1.2.2 above and in detail in Chapter 2 subsection 2.4.2. The wind data provided publicly from TARA on the CESAR-observatory website at the moment is at the resolution of approximately three seconds. First positive comparisons during study cases of rain were carried out using radiosonde measurements, which showed the potentiality of TARA to measure vertical profiles of the horizontal wind. However, further assessment has to be carried out. The wind estimation algorithm currently used for TARA wind estimation is shortly presented in Unal et al. (2012), but the quality of the results has not been analysed so far. TARA observes in time height indication mode. This means that the measurements are taken at fixed azimuth and elevation in consecutive time steps. This radar is a research radar to investigate the microphysics and dynamics of the measured precipitation system (rain and clouds) at high time and spatial resolution.

The Analysis of the Composition of Clouds with Extended Polarization Techniques (ACCEPT) campaign took place at CESAR in October and November of 2014. Additionally to the permanent sensors also other sensors such as Millimeter Wave Radar (MIRA) were measuring during the campaign. MIRA is looking in vertical direction, while TARA is measuring at an elevation of 45°. This means that only the vertical component can be verified using MIRA. For the horizontal wind speed and direction, the anemometer located on the tower at 200 m above the surface – which is located at a distance of 300 m from TARA – can be used. While the tower data is available from the surface until 200 m the measurements from TARA can only be used from approximately 200 m upwards. This is due to the fact that the near-field measurements of TARA cannot be used. The configuration and exact details of the set-up of the instruments will be discussed further in Chapter 2.

Although some of the studies retrieve data at high time resolution, the ones mentioned in the section on previous research so far do not consider the possibility of using high time resolution Doppler radar data on the order of one minute or less. Either the mean wind is used or a system is found to filter out ambiguities without detection of their cause. Another aspect is that papers were mainly written on specific case studies. During this project the whole period of the ACCEPT campaign will be considered for the assessment of quality of the wind estimation performed using TARA.

While the wind profiler uses 30 minute averages, TARA has the possibility of using a time resolution of up to 3 seconds. The longer time periods used for averaging for the wind profiler could also be applied to the TARA wind estimation. The reason why this is not done is that for studies involving microphysics of clouds and precipitation, the time resolution should be as high as possible. Previous research involving TARA used 10 minute averages (Unal, 2015), 30 and 90 second averages (Pfitzen-

maier et al., 2018) as well as comparisons of different averaging periods between 10 and 540 seconds (Pfitzenmaier et al., 2017).

To be able to assess the quality of the wind estimation of TARA, data as ground truth is needed. The wind data from the cup anemometer of the meteorological tower is used, which is available at 1- and 10-minute averages. This is a reason why the 1-minute data will be used unless there are some large problems with the data that give a reason to also consider the 10-minute data. The preference of using the 1-minute averages instead of the 10-minute averages is also due to the fact that a lot of fluctuations are averaged out and more data is lost when applying the same data selection methods to larger time spans. For example, when there is 1 minute of good data in a 10-minute interval with mostly low reflectivity or signal to noise ratio (SNR) values then this data will also be removed. But this also applies for the opposite, if averages of 10 minutes are taken with one strong outlier in the data due to low SNR or reflectivity, this will result in a biased average wind speed, but it might be removed when considering averages of 1 minute while the usable data will remain.

1.5. Research Questions

The main topic of this master project is to assess the retrieval of wind estimates obtained using the Transportable Atmospheric Radar (TARA). This topic was approached using the following research questions.

- What is the current quality of the TARA wind estimation?
  - How to remove clear air measurements?
  - What is the quality of the wind retrieval during precipitation?
  - What is the impact of a non-homogeneous medium?
- How can the usable wind estimates be selected based on TARA only?

These research questions will be approached using Matlab to analyse and present the data stored during the period of the ACCEPT-campaign in October and November of 2014. This data includes the observations from the meteorological tower, the wind profiler, radiosonde measurements and TARA-data recorded at CESAR.

The structure of this report follows the order of the research questions. After an introduction of the wind estimation using TARA in Chapter 2, the quality of the wind estimation is assessed in Chapter 3. Chapter 4 then focusses on data selection using TARA-based variables only. In Chapter 5 and 6 the main conclusions and recommendations are presented. After the Bibliography the Appendix includes tables with the detailed results of the assessment and data selection.

2

Wind Estimation TARA

The topic of (Doppler) radar is broad and a lot of details could be discussed. In this section the most important concepts relevant to this research project will be explained. In particular this means that first there is an explanation of how the mean Doppler velocity is obtained. This will then be followed by a more specific setting of the radar TARA used to retrieve the data for this master thesis during the ACCEPT campaign.

Following that more technical details concerning the retrieval of the three dimensional wind estimates using the mean Doppler velocity measured by the three beams of TARA will be explained and compared to the system of equations used for wind profilers. This is important to understand the concepts behind the algorithm used, especially because it will be discussed later on. Another section then introduces the sensors which are used for the validation and analysis of the current quality of the wind estimates obtained by TARA.

The chapter is then concluded with a section discussing possible problems that could be encountered when estimating wind using TARA. These include beam divergence, clutter, the orientation of TARA.

2.1. General Properties Radar

A radar is an active system that can be used in meteorology to measure properties of the atmosphere from the ground at a good spatial resolution and coverage as well as good temporal resolution. Microphysics as well as movements of particles can be observed. Radar stands for Radio Detection and Ranging. A pulsed radar in essence works with sending out electromagnetic waves that reflect from an object and the resulting return signal is received by the radar antenna (Doviak and Zrnic, 2006).

An electromagnetic wave such as the one sent out by a radar has an electric field and a magnetic field which are perpendicular to each other. It can be oriented in a way that makes it possible to obtain shape information, which also means microphysical information about the medium observed. The polarization is defined as the direction of the electric field of the electromagnetic wave transmitted and received by a radar. The transmission and reception can either be using the same or a different polarization. Measuring phase and phase-differences gives information of velocity and position while the polarization can give information about the shape of observed objects. The radar frequency defines to what size of particles the radar is most sensitive, while the transmitted amplitude of the electric field defines the sensitivity. (Lecture Atmospheric Observation 2017).

The frequency f of the electromagnetic wave sent out by a radar is related to the wavelength λ with the speed of light $c = 3 \cdot 10^8 ms^{-1}$.

$$c = \lambda \cdot f \ [m] \tag{2.1}$$

The time between sending and receiving of an electromagnetic wave, Δt , can be measured and translated into a range R, where scatterers are located using the following equation.

$$R = \frac{c \cdot \Delta t}{2} \; [m] \tag{2.2}$$

The maximum range that can be measured unambiguously depends on the time between two consecutive pulses transmitted by the radar, T_0.

$$R_{max} = \frac{c \cdot T_0}{2} \; [m] \tag{2.3}$$

The maximum possible velocity measured unambiguously also depends on T_0 and is given by the following relation.

$$v_{max} = \pm \frac{\lambda}{4 \cdot T_0} [ms^{-1}] \tag{2.4}$$

The disadvantages of a pulsed radar include the fact that a short pulse duration means that high pulse power is needed and that there is a blind range during time of transmission of the pulse.

The received power, P_r, depends on the power transmitted, the gain, wavelength, reflectivity z and the range.

$$P_r = \frac{C_z \cdot z}{R^2} \; [W] \tag{2.5}$$

where C_z is the radar constant and in the Rayleigh scattering regime

$$z = \int D_H^6 N(D_H) \; dD_H \; [mm^6 m^{-3}] \tag{2.6}$$

where D_H is the equi-volume spherical diameter of the hydrometeor and $N(D_H)$ the hydrometeor size distribution.

In contrast to a pulsed radar a Frequency Modulated Continuous Wave (FMCW) wave radar does not send separate pulses but transmits continuously with a varying frequency (see Figure 2.1). The range is then measured from the frequency shift between the transmitted and received signal. Using a Fourier transform the signal is translated from time domain to beat frequency spectrum. Each beat frequency can be related to a range (see equation 2.8) (Lecture ET4169 - Microwaves Radar and Remote Sensing, 2017).

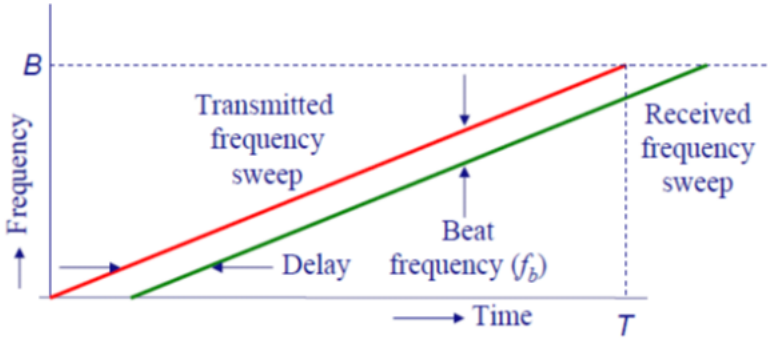

Figure 2.1: FMCW principle (Source: Lecture ET4169 - Microwaves, Radar and Remote Sensing, 2017)

The beat frequency f_b is given for a stationary target by the equation below. B is the frequency bandwidth on transmission while T is the sweep time (see Figure 2.1).

$$f_b = \frac{2 \cdot R \cdot B}{c \cdot T} \; [Hz] \tag{2.7}$$

In case of a moving target a frequency shift, i.e. a Doppler shift of the beat signal will occur. Only the radial component per beam can be measured while movements perpendicular to the looking direction of the radar will not be measured. The resulting Doppler beat frequency, $f_{b,D}$, will be smaller for an object moving towards the radar or larger for an object that is moving away from it (Lecture slides ET 4169 - Microwaves radar and remote sensing, 2017). The equation for the Doppler beat frequency of a moving target is given below.

$$f_{b,D} = \frac{2 \cdot R \cdot B}{c \cdot T} \pm \frac{2 \cdot v_r \cdot f_c}{c} \; [Hz] \tag{2.8}$$

The second fraction of the right part of the equation corresponds to the Doppler shift of a moving target, f_D, with v_r being the radial velocity and f_c the change in frequency.

$$f_d = \frac{2 \cdot v_r \cdot f_c}{c} \; [Hz] \tag{2.9}$$

Using a Fast Fourier Transform (FFT) on a time series of measurements at fixed range a Doppler spectrum at each range bin can be calculated. From this the Doppler frequency spectrum can be derived. The mean Doppler frequencies can then be translated to mean Doppler velocities using the following equation.

$$v_D = -\frac{f_d \cdot \lambda}{2} \; [ms^{-1}] \tag{2.10}$$

The Transportable Atmospheric Radar (TARA) is located at Cabauw Experimental Site for Atmospheric Research (CESAR). CESAR is a site used for atmospheric research, where different measurement instruments with different lengths of time series data are co-located. TARA is a rain radar which has been first used in 2000 (Heijnen et al., 2000) and received an update of the system in 2011 (Unal et al., 2012) which included the capability of real-time processing for the mean Doppler velocities of the three beams and with that the wind retrieval. The topic of this research project is depending on the fact that TARA measures using three beams. It means that the mean Doppler velocities in three different directions can be measured. Those three mean velocities can then be used to estimate the wind. The details for the specifications and measurement principles can be found in the following sections.

2.2. The Transportable Atmospheric RAdar (TARA)

TARA is a FMCW radar profiler with a central frequency of 3.3 GHz. More details on the specification of TARA during the ACCEPT-campaign can be found in Table 2.1. TARA measures at a fixed azimuth and elevation of 45° for the main beam. The main beam is polarimetric while the two offset beams are not. Figure 2.2 repeats Figure 1.2 for convenience.

The first offset beam measures at the same azimuth as the main beam but with an elevation of 60°. The second offset beam measures at an elevation of 43.1° and also a different azimuth. The azimuth for the main beam and the first offset beam is 246.5° while the second offset beam measures at 267.3°. The two planes (OB1 - MB to OB2 - MB) are perpendicular to each other. The orientation was chosen in order to minimize ground clutter and obstacles while measuring. In addition these azimuth angles are related to the West-South-West direction where most of the storms come from.

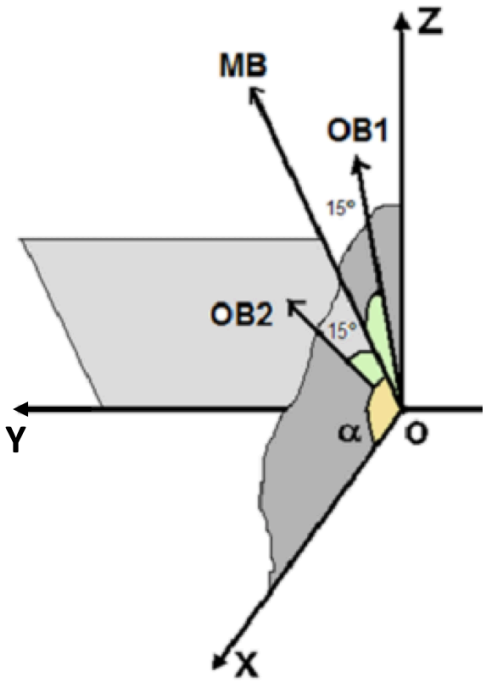

Figure 2.2: This figure repeats Figure 1.2 for convencience, which shows the TARA measurement cycle and reference system (Unal et al., 2012). The main beam measures with an azimuth of 246.5° and this means the X-axis is aligned with the same azimuth. The Z-axis is looking at the Zenith and the Y-axis is perpendicular to the other two.

All the data files (NetCDF format) are archived on hard discs. In the CESAR database, the main beam reflectivity, the horizontal wind (velocity and direction) and the vertical velocity, are provided with the height resolution 21.2 m and time resolution of approximately 3 seconds. The vertical extent from the ground starts at 127.3 m above ground and reaches as far as 10458.1 m above ground. In this thesis work, the full set of processed data (TARA-5_cycle_Processed_Data) will be used including mean Doppler velocities for all the beams and polarimetric measurements of the main beam.

Table 2.1: Table showing the setup of TARA during ACCEPT (Pfitzenmaier et al., 2017). HH means horizontal transmit and receive, VV means vertical transmit and receive. HV means vertical transmit and horizontal receive.

Radar		
Type	FM-CW	
Central frequency	3.298 GHz	S-band
Transmitted power	100 W	Automatic decrease by step of 10 dB in case of receiver saturation (moderate to extreme precipitation)
Signal generation		
Sweep time	0.5 ms	
No. of range bins	512	
Range resolution	30 m	Height resolution is 21.2 m
Time resolution	2.56 s	
Polarimetry		
Polarisation	VV HV HH	Main beam only (single receiver channel)
Measurement cycle	VV HV HH OB1 OB2	Main beam + 2 offset beams
Doppler		
No. Doppler bins	512	
Doppler resolution	0.036 ms^{-1}	
Max. unambiguous velocity	$\pm$ 9.1 ms^{-1}	
Max. velocity main beam	$\pm$ 45.5 ms^{-1}	After spectral polarimetric dealiasing (Unal and Moisseev, 2004)
Max. velocity offset beams	$\pm$ 45.5 ms^{-1}	After spectral dealiasing
Antennas		
Beam width	2.1°	
Gain	38.8 dB	
Near field	≤ 200 m	
Beams	Elevation	Azimuth related to the North
Main beam	45°	246.5°
Offset beam 1	60°	246.5°
Offset beam 2	43.1°	267.3°
Clutter suppression		
Hardware	Antennas	Low side lobes
Processing	Doppler spectrum	Spectral polarimetry (main beam)

2.3. Quicklooks of TARA Data

In this subsection some plots of the data obtained during the ACCEPT-campaign using TARA are shown. These quicklooks provided with the TARA-data were used in a first step to decide which days of the ACCEPT-campaign are interesting to look at further.

The case presented below is the 7.11.2014. This was mainly chosen as on this day there is a variety of measurement types. There are parts with clear air, clouds and precipitation. A part of this day will be discussed further in the rest of the chapter and compared to a case on the 3.11.2014. The case of the 3.11.2014 was chosen because during that time series there was strati-form precipitation measured only. Thus these two case studies can be used to compare the results for stable against variable conditions during measurements of TARA

In the three figures below (Figure 2.5, 2.6 and 2.7) an example of mean Doppler velocities for the three beams of TARA can be found.

Figure 2.3 below show quicklooks showing reflectivity measurements taken by TARA on 7.11.2014. While the polarimetric clutter suppression for the main beam works quite well (Unal, 2009), for the other two beams the clutter suppression is not as good. The zoomed in part from Figure 2.4 shows in more detail the time period between 06:00 and 13:00 on the 7.11.2014.

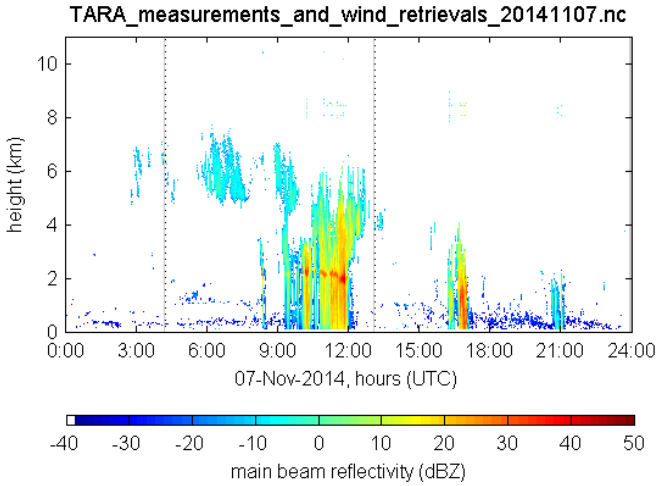

Figure 2.3: Quicklook of the main beam reflectivity for TARA on 7.11.2014. The vertical dotted lines show the time periods for raw data sets available on the day. See the figure discription for Figure 2.4 below for more details on what can be observed in the figure. These data are supplied to the CESAR database with a time resolution of approximately 3 seconds.

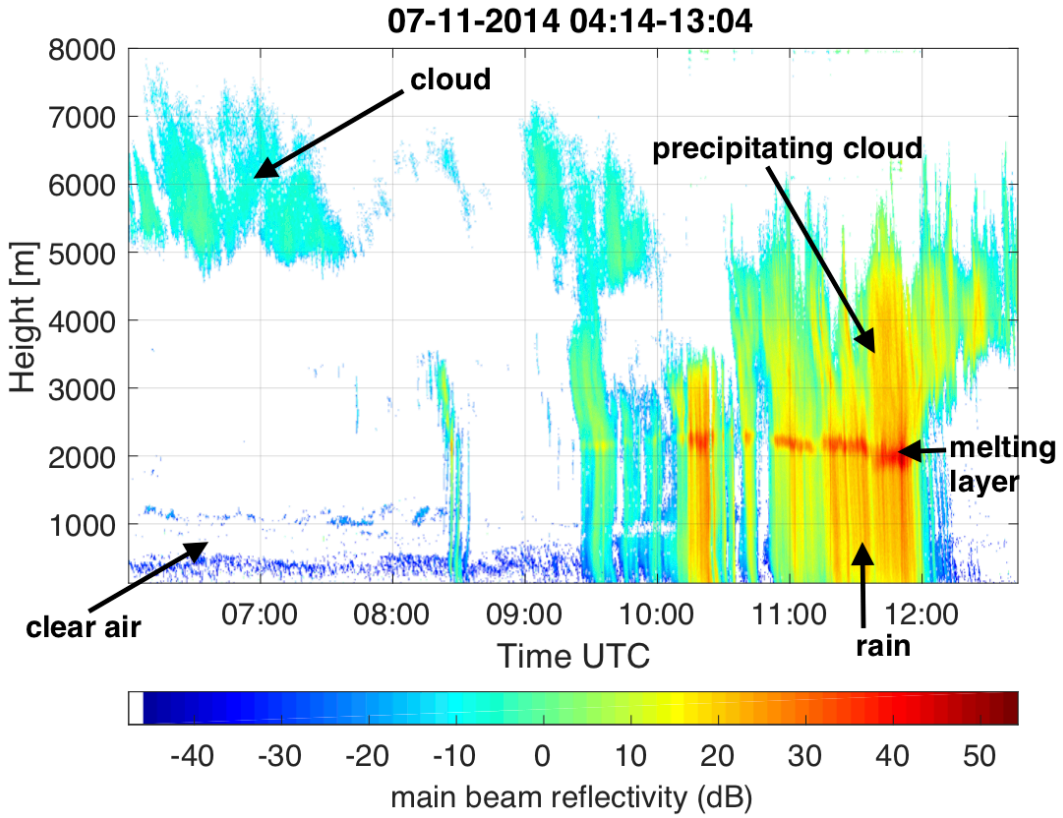

Figure 2.4: Zoom in of the main beam reflectivity on 7.11.2014 between 06:00 and 13:00. The plot shows different components of the atmosphere that can be observed.

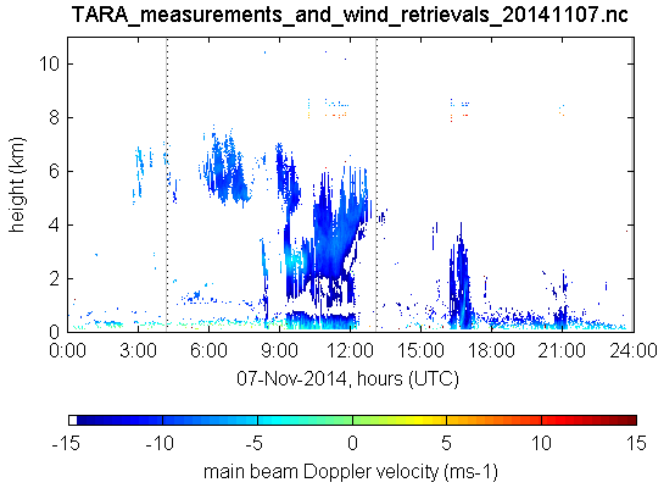

Figure 2.5: Main beam Doppler velocity measured on 7.11.2014 during ACCEPT-campaign

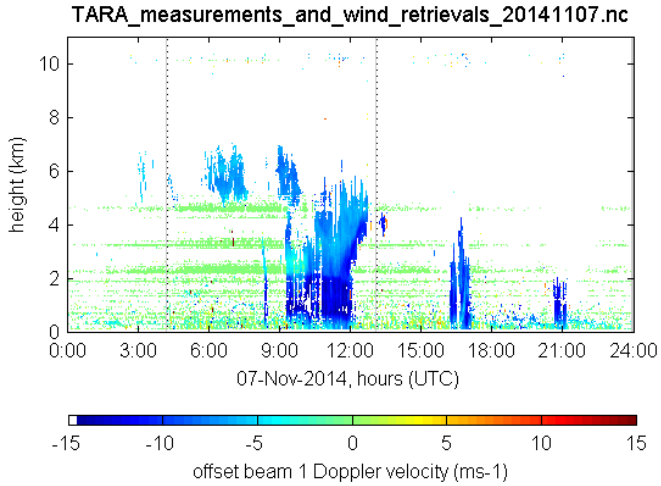

Figure 2.6: Offset beam 1 Doppler velocity on 7.11.2014 during ACCEPT-campaign

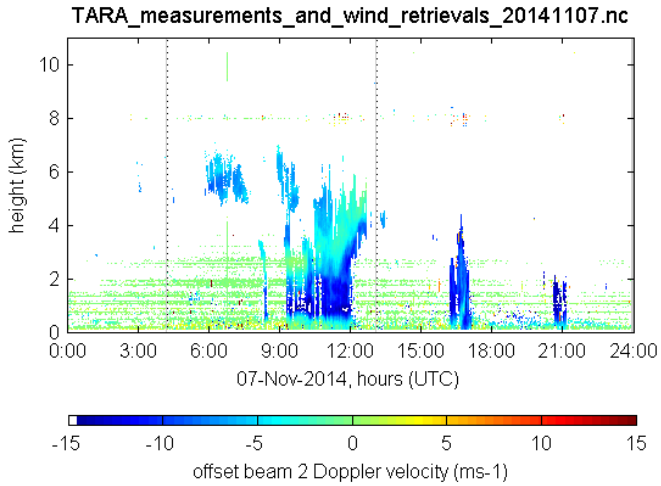

Figure 2.7: Offset beam 2 Doppler velocity on 7.11.2014 during ACCEPT-campaign

2.4. Wind Estimation Algorithm

In the case of wind estimation from the output of the mean Doppler velocities of a three-beam radar in the form of a wind profiler or the precipitation radar TARA different algorithms are applied. The following subsections will first introduce the wind estimation algorithm for the wind profiler and in the next subsection the algorithm used for TARA will be introduced.

2.4.1. Wind Profiler

The equations introduced for the wind profiler wind estimation in Subsection 1.2.1 (see equation (1.1)) can be rewritten as shown below, with $V_w = V_z = W + v_f$ which is the velocity component along the vertical axis V_z is measured directly by the wind profiler, because one of the three beams points towards the zenith. The other two beams are measuring at an offset angle θ away form the vertical in either the South-North,V, or West-East, U, direction.

$$\begin{bmatrix} V_v \\ V_u \\ V_w \end{bmatrix} = \begin{bmatrix} sin(\theta) & 0 & cos(\theta) \\ 0 & -sin(\theta) & cos(\theta) \\ 0 & 0 & 1 \end{bmatrix} \cdot \begin{bmatrix} V \\ U \\ V_z \end{bmatrix} \tag{2.11}$$

$$\begin{bmatrix} V \\ U \\ V_z \end{bmatrix} = \begin{bmatrix} sin(\theta) & 0 & cos(\theta) \\ 0 & -sin(\theta) & cos(\theta) \\ 0 & 0 & 1 \end{bmatrix}^{-1} \cdot \begin{bmatrix} V_v \\ V_u \\ V_w \end{bmatrix} \tag{2.12}$$

With $\theta = 15°$ this results in the equations for (V,U and V_z) below.

$$\begin{aligned} V &= 3.8637 \cdot V_v + -3.7321 \cdot V_w \\ U &= -3.8637 \cdot V_u + 3.7321 \cdot V_w \\ V_z &= V_w \end{aligned} \tag{2.13}$$

In the case of the wind profiler the components for the West-East and the South-North direction are decoupled. This means that each component is measured directly by one beam. Only the vertical Doppler Velocity has to be the same in the three distinct radar resolution volumes. This is not the case for TARA as will be explained in the subsection below.

2.4.2. TARA

The coordinate system used for TARA has the X-axis aligned with the azimuth of the main beam and the Z-axis is aligned to the zenith. The Y-axis is then found at an angle of 90° of both other axes. The mean Doppler velocity measurements of all the beams can thus be represented in relation to the X-,Y- and Z-axis. In a further step a geometrical transformation is performed to obtain the 3D wind estimates from the velocity vectors originally represented in the local TARA coordinate system. The information about the wind estimation retrieval from the three-dimensional velocity field written in (Unal, technical report).

The following equations can be found for the relationship between the mean Doppler velocities for each beam (V_{MB}, V_{OB1},V_{OB2}) and the wind components in X-, Y- and Z-direction. V_x and V_y are the components of the horizontal wind and V_z is the vertical Doppler velocity consisting of the mean fall velocity of the hydrometeors and the mean vertical wind. This approach is based on the assumption that the three beams contain the same horizontal wind and vertical Doppler velocity at fixed height. In case of looking at different media due to beam divergence this assumption is a potential source of error in the wind estimation.

The relationship between the mean Doppler velocities and V_x, V_y and V_z are given below. In this case α is the elevation of the main beam and has a value of 45° and γ equals 15°.

$$\begin{aligned} V_{MB} &= V_x\ cos(\alpha) + V_z\ sin(\alpha) \\ V_{OB1} &= V_x\ cos(\alpha+\gamma) + V_z\ sin(\alpha+\gamma) \\ V_{OB2} &= V_x\ cos(\alpha)\ cos(\gamma) + V_y\ sin(\gamma) + V_z\ sin(\alpha)cos(\gamma) \end{aligned} \tag{2.14}$$

Rewriting the equations to matrix form and for V_x, V_y and V_z leads to the following transformation matrix that will be multiplied with the vector for the mean Doppler velocities of the three beams.

$$\begin{bmatrix} V_x \\ V_y \\ V_z \end{bmatrix} = \begin{bmatrix} cos(\alpha) & 0 & sin(\alpha) \\ cos(\alpha+\gamma) & 0 & sin(\alpha+\gamma) \\ cos(\alpha)cos(\gamma) & sin(\gamma) & sin(\alpha)cos(\gamma) \end{bmatrix}^{-1} \cdot \begin{bmatrix} V_{MB} \\ V_{OB1} \\ V_{OB2} \end{bmatrix} \tag{2.15}$$

$$\begin{bmatrix} V_x \\ V_y \\ V_z \end{bmatrix} = \begin{bmatrix} \frac{-sin(\alpha+\gamma)}{sin(\alpha)cos(\alpha+\gamma)-cos(\alpha)sin(\alpha+\gamma)} & \frac{sin(\alpha)}{sin(\alpha)cos(\alpha+\gamma)-cos(\alpha)sin(\alpha+\gamma)} & 0 \\ \frac{-cos(\gamma)}{sin(\gamma)} & 0 & \frac{1}{sin(\gamma)} \\ \frac{cos(\alpha+\gamma)}{sin(\alpha)cos(\alpha+\gamma)-cos(\alpha)sin(\alpha+\gamma)} & \frac{-cos(\alpha)}{sin(\alpha)cos(\alpha+\gamma)-cos(\alpha)sin(\alpha+\gamma)} & 0 \end{bmatrix} \cdot \begin{bmatrix} V_{MB} \\ V_{OB1} \\ V_{OB2} \end{bmatrix} \tag{2.16}$$

with $sin(\alpha)cos(\alpha+\gamma) - cos(\alpha)sin(\alpha+\gamma) = -sin(\gamma)$ the result is:

$$\begin{bmatrix} V_x \\ V_y \\ V_z \end{bmatrix} = \begin{bmatrix} \frac{sin(\alpha+\gamma)}{sin(\gamma)} & \frac{sin(\alpha)}{-sin(\gamma)} & 0 \\ \frac{-cos(\gamma)}{sin(\gamma)} & 0 & \frac{1}{sin(\gamma)} \\ \frac{cos(\alpha+\gamma)}{-sin(\gamma)} & \frac{cos(\alpha)}{sin(\gamma)} & 0 \end{bmatrix} \cdot \begin{bmatrix} V_{MB} \\ V_{OB1} \\ V_{OB2} \end{bmatrix} \tag{2.17}$$

Using the values for $\alpha = 45°$ and $\gamma = 15°$ gives the following result.

$$\begin{bmatrix} V_x \\ V_y \\ V_z \end{bmatrix} = \begin{bmatrix} 3.3461 & -2.7321 & 0 \\ -3.7321 & 0 & 3.8637 \\ -1.9319 & 2.7321 & 0 \end{bmatrix} \cdot \begin{bmatrix} V_{MB} \\ V_{OB1} \\ V_{OB2} \end{bmatrix} \tag{2.18}$$

$$\begin{aligned} V_x &= 3.3461 \cdot V_{MB} - 2.7321 \cdot V_{OB1} \\ V_y &= -3.7321 \cdot V_{MB} + 3.8637 \cdot V_{OB2} \\ V_z &= -1.9319 \cdot V_{MB} + 2.7321 \cdot V_{OB1} \end{aligned} \tag{2.19}$$

Finally the wind estimates need to be transformed from being in a local to a global coordinate system (see Figure 2.8 below). This means leaving the V_z component as it is and rotating the other two components to reference them to the north.

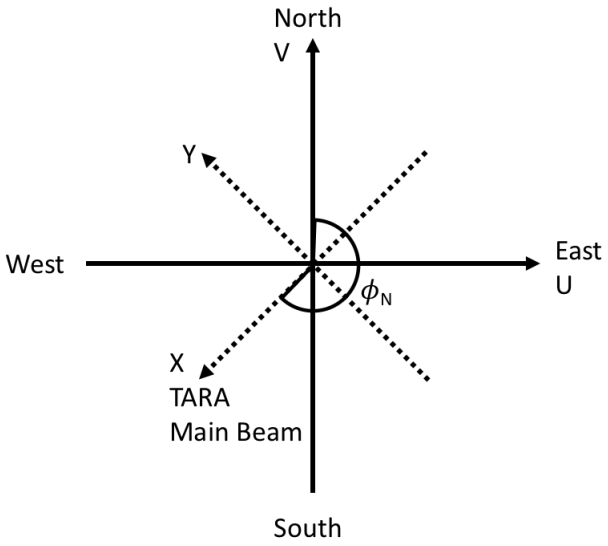

Figure 2.8: Shows the relation between the local reference system of TARA in relation to the global reference system. The rotation done is around the Z-axis.

$$\begin{bmatrix} V \\ U \\ V_z \end{bmatrix} = \begin{bmatrix} cos(\Phi_N) & -sin(\Phi_N) & 0 \\ sin(\Phi_N) & cos(\Phi_N) & 0 \\ 0 & 0 & 1 \end{bmatrix} \cdot \begin{bmatrix} V_x \\ V_y \\ V_z \end{bmatrix} \tag{2.20}$$

Because of the looking direction of TARA, the estimation of V, U and V_z requires the same medium (microphysical and dynamical) at fixed height.

Using the azimuth of TARA, $\Phi_N = 246.5°$, to calculate the transformation matrix results in the following relation.

$$\begin{bmatrix} V \\ U \\ V_z \end{bmatrix} = \begin{bmatrix} -0.3987 & 0.9171 & 0 \\ -0.9171 & -0.3987 & 0 \\ 0 & 0 & 1 \end{bmatrix} \cdot \begin{bmatrix} V_x \\ V_y \\ V_z \end{bmatrix} \tag{2.21}$$

$$\begin{aligned} V &= -0.3987 \cdot V_x + 0.9171 \cdot V_y \\ U &= -0.9171 \cdot V_x + -0.3987 \cdot V_y \\ V_z &= V_z \end{aligned} \tag{2.22}$$

The last step towards obtaining the horizontal wind speed is to calculate the square root of the squared sum.

$$V_M = \sqrt{V_x^2 + V_y^2} = \sqrt{V^2 + U^2} \tag{2.23}$$

The wind direction is related to the tangent of U and V. Inverting the relation leads to the direction.

$$tan\ D = \frac{-U}{-V} \tag{2.24}$$

$$D = tan^{-1}\frac{-U}{-V} \tag{2.25}$$

The wind direction in meteorological applications is defined as from where it is coming from in reference to the North. The direction is converted from radians to degrees and is obtained between and interval of $-180°$ to $+180°$. In the next step $360°$ is added to the values below zero to obtain an interval between 0 and $360°$.

An example of the wind estimation done as explained above can be found in Figure 2.9 and 2.10. The two Figures show quick looks provided with the TARA data. Note that the clutter present in Figures 2.6 and 2.7 does not result in a wind estimation because there are no data in the main beam display (Figure 2.5). This means that only when there is reflectivity in all three beams a wind estimation will be done. But in case of clutter in the precipitation this can still be the cause of errors due to the clutter in the offset beams. For the other radar variables, the polarimetric main beam is used.

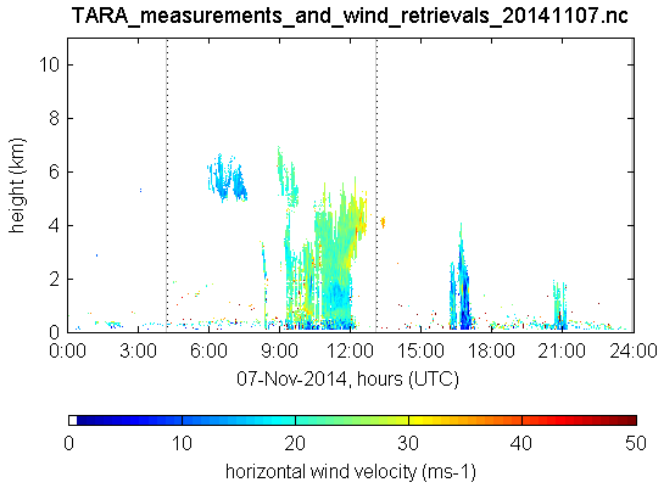

Figure 2.9: Quicklook of TARA wind speed estimation produced on 7.11.2014 during real time processing.

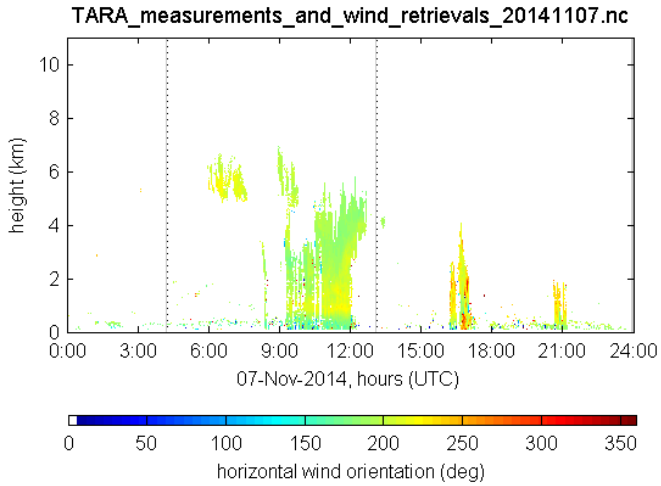

Figure 2.10: Quicklook of TARA wind direction estimation produced on 7.11.2014 during real time processing.

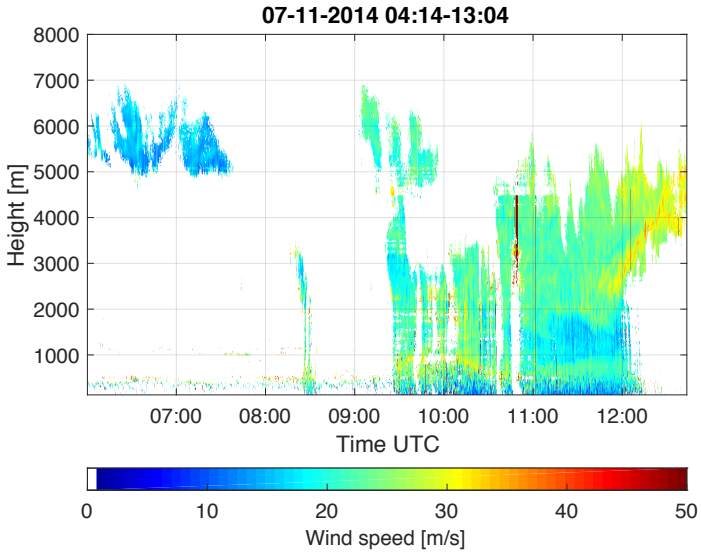

Figure 2.11: Zoom in of the main beam reflectivity on 7.11.2014 between 06:00 and 13:00. The plot shows different components of the atmosphere that can be observed.

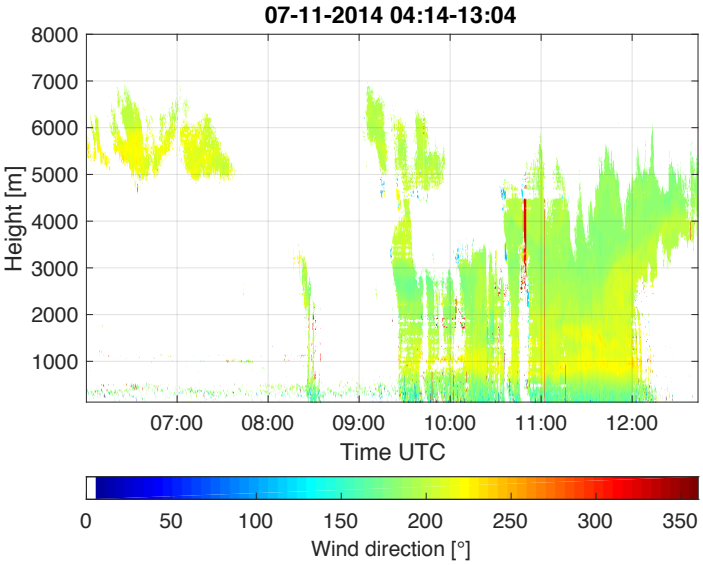

Figure 2.12: Zoom in of the main beam reflectivity on 7.11.2014 between 06:00 and 13:00. The plot shows different components of the atmosphere that can be observed.

2.5. Possible Problems when Retrieving Three-Dimensional Wind Fields

A number of problems can be expected when only applying a geometrical system of equations to estimate a three-dimensional wind field. These include – amongst others – clutter suppression problems for the two offset beams. When clutter and precipitation overlap this clutter may lead to biased mean Doppler velocities, which is the input variable for the wind retrieval. Another factor is that the wavelength of TARA is chosen to measure mainly precipitation. This means that it can be expected that the clear air measurements can be less accurate.

Another aspect is that there needs to be sufficient strength of the the power returned compared to the noise. The Signal to Noise Ratio (SNR) is a measure of this ratio. Sufficiently above noise level would be a SNR above 10 dB. This means that the power received from e.g. precipitation is 10 times more than the noise power.

Clutter might have a high SNR due to large reflection surface or radar system artefacts. This means that while the wind estimation is done when there is a large signal to noise ratio, the value observed might still be wrong. Thus even when the signal to noise ratio is sufficient this does not exclude the possibility that the wind estimation might be of insufficient quality. This is mainly true if there is clutter found in precipitation. For the cluttered clear air measurements, it is expected that the data will be filtered out because missing data from the main beam prevents the estimation of the wind.

Another effect to be considered is beam divergence. This means that the further away from the radar the range considered the further away are the actual locations of the three beams used to measure the mean Doppler velocities. This also means the further away the measurement considered, the higher the possibility of measuring different media which could lead to different fall velocities and different dynamics for the three beams. The problem of beam divergence is not expected to be a problem at the altitudes used to compare the wind estimation from TARA to the tower measurements which are taken up to 200 m. The beam divergence at 200 m between the MB and the OB1 for example is given by the following equation. D_1 is defined as the distance from the zenith to the OB1 and D_2 the distance from the zenith to MB. Figure 2.13 gives an overview of the variables concerned in the calculation.

$$\begin{aligned} tan(30°) &= \frac{D_1}{200\ m} = 115.5\ m \\ tan(45°) &= \frac{D_2}{200\ m} = 200\ m \\ D_2 - D_1 &= 200\ m - 115.5\ m = 84.5\ m \end{aligned} \tag{2.26}$$

This shows that at a low altitude the distance is not larger than for example the distance to the tower anemometer (approximately 300 m (Bosveld, 2018)) to which the data is compared to. The next calculation is done for an altitude of 1 km.

$$\begin{aligned} tan(30°) &= \frac{D_1}{1000\ m} = 577.4\ m \\ tan(45°) &= \frac{D_2}{1000\ m} = 1000\ m \\ D_2 - D_1 &= 1000\ m - 577.4\ m = 422.6\ m \end{aligned} \tag{2.27}$$

Here the distance is already larger than the distance between the tower and TARA.

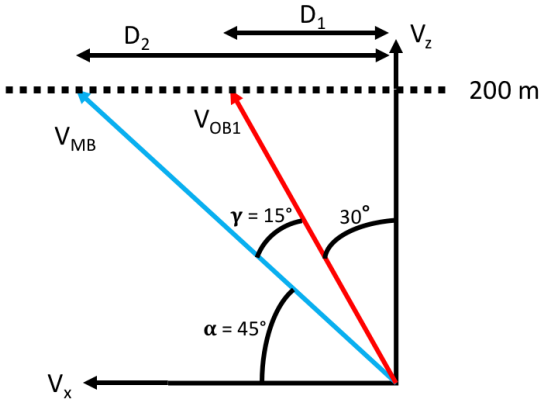

Figure 2.13: Showing the concept of how the beam divergence is calculated between the main beam and offset beam 1

The orientation of TARA also needs to be taken into account as it might be more or less sensitive to errors when different directions are considered. During the ACCEPT-campaign most of the usable cases represent wind directions of $180°$ until $360°$. The impact of the direction on the estimation will be discussed later in Section 3.5.

3

Assessment Wind Estimation TARA

Following the chapter introducing the wind estimation algorithm used for TARA, the assessment of the wind estimates is discussed in this chapter.

First, two case studies will be introduced. The one for the 3.11.2014 shows stratiform precipitation while in the one for the 7.11.2014 the conditions are more heterogeneous. The results of the case studies will be compared to the tower anemometer at 200 m above the surface.

Three types of measurements are present in the TARA data: clear air, cloud and precipitation. Clear air measurements are measurements taken when there is no precipitation but there is still sufficient power returned to estimate the wind. These echoes are related to contrast in refractive index. Because there are some large outliers in the wind estimation of TARA – especially during clear air – the second section will be concerned with finding a way to remove clear air measurements using different methods. This makes it possible to assess the quality of the wind retrieval during precipitation. During precipitation, the retrieval is expected to be best because these are the cases for which the TARA processing algorithms are designed. The application of a SNR threshold in order to remove clear air measurements did not prove to be successful without also removing usable data. Therefore the next step was to investigate the retrieval of wind during rain. These periods of rain were found by a rough detection of melting layer presence.

Comparisons of the methods will be done in detail for the two case studies and a summary of the results for all the usable cases during ACCEPT-campaign are also presented.

The methods mentioned above showed a bias in wind estimation errors which was then further investigated using simulations. These simulations were performed by defining the ground truth and introducing errors in order to investigate the effects of i.e. different fall velocities in the different beams.

3.1. Case Studies 3.11.2014 and 7.11.2014

For the assessment of the TARA wind estimation, two case studies were selected. The SNR plots for the 3.11.2014 and 7.11.2014 are shown below in Figures 3.1 and 3.2. Both figures show the plots of the Signal to Noise Ratio (SNR) for both cases.

While the case studies presented in this section, during this report mean values for the whole ACCEPT-campaign will be presented. These tables are based on usable data only, unless it is indicated otherwise. The usable cases were selected based on several steps. In a first step the quick-looks of the TARA data were considered. Cases which did not contain any useful measurements in the form of clouds or precipitation were removed. The other cases were considered if the errors in wind estimation compared to the tower anemometer were below 40 m/s and also not increasing when applying the filtering methods explained further on in this chapter.

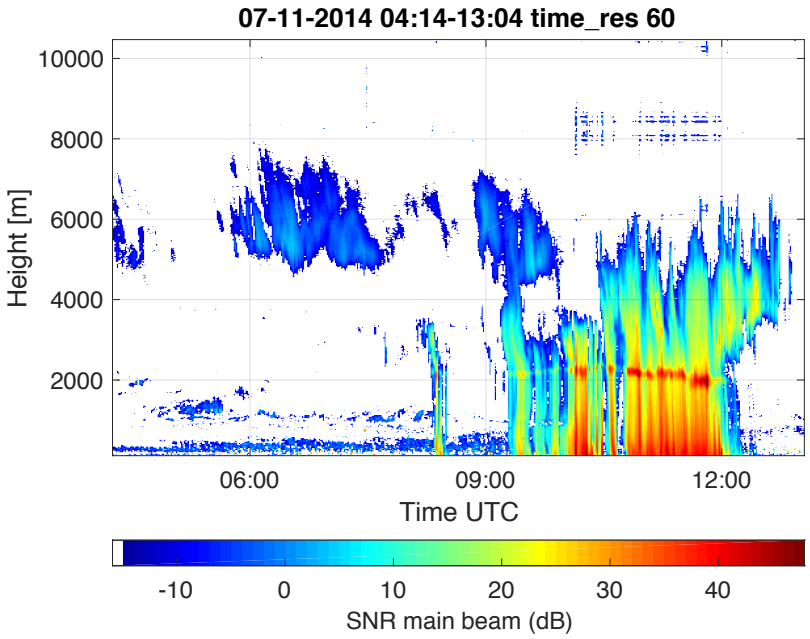

Figure 3.1: Shows the SNR for the 7.11.2014 plotted for all heights.

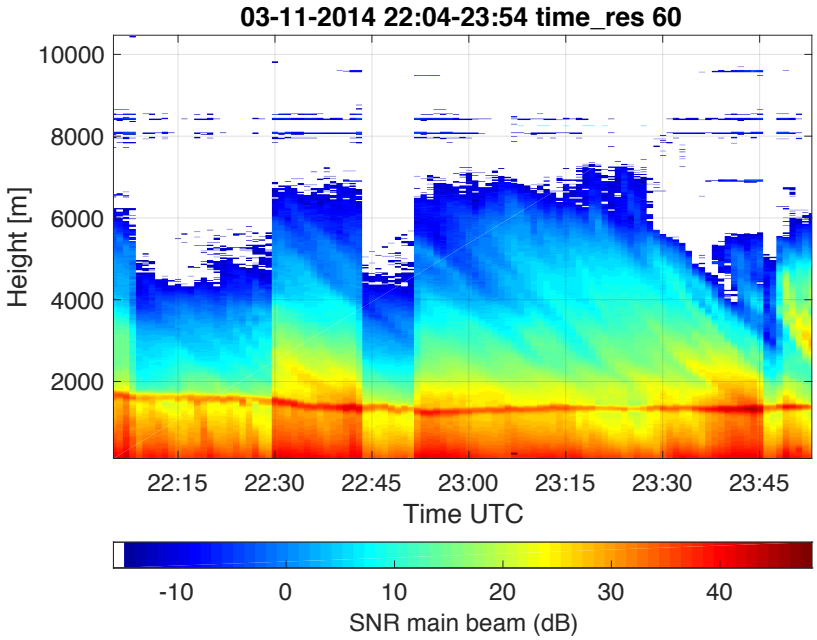

Figure 3.2: Shows the SNR for the 3.11.2014 plotted for all heights.

3.1.1. Validation Using Data from the Meteorological Tower

To assess the current quality of the TARA wind estimation it is necessary to make a comparison to other observations in order to validate the results obtained. Applied methods to improve the quality such as removal of unusable data also need to be validated. This can in this case be done using other sensors that are located CESAR. Near the ground the data of the anemometer located on the meteorological tower at 200 m above the surface will be used.

The tower is located at CESAR at a distance of approximately 300 m from TARA. There is data available at 2, 10, 20, 40, 80, 140 and 200 m above ground (Bosveld, 2018). TARA wind estimates are available at 191 and 212 m approximately. The average of these two values will be used for the

comparison to the time series recorded by the anemometer located on the tower at 200 m above ground.

While TARA measures with a time-resolution of 3 seconds on average the data available for validation from the tower is available at time resolutions of 1- and 10-minute intervals. All data of the tower anemometer are validated, the 10-minute data is also gap-filled. This means that missing data is interpolated (Bosveld, 2018). For the 1-minute averages there are no gaps found for the time period of the ACCEPT-campaign (October and November 2014). For the validation of the TARA data at an height of 200 m above ground, the tower data is considered to be the ground truth. Averaging for the TARA data was performed using the tower time steps as boundaries. The code for the averaging was an edited version of the one previously used by Brukx (2015), which also included removal of statistical outliers.

A measure of the standard deviation of residuals is given by the value of the Root Mean Square Error (RMSE). Usually used to evaluate the difference between a model and observations in the case of this research instead of the model the tower data is used. The RMSE is calculated with the following formula.

$$RMSE = \sqrt{\frac{\sum_{t=1}^{N} e_{t,h}^2}{N}} \tag{3.1}$$

Where e is the difference in wind speed or direction between TARA and tower at a certain time step t and fixed height h above ground. N is the number of estimation values considered while t is the number for the time steps.

Validation and error identification give a value for the accuracy of the TARA wind estimation results. But the size of these errors and the quality needs to be evaluated using a reference for accuracy. The evaluation of the wind estimation will be done using state-of-the-art values found in the literature. For the wind speed accuracies are around 1-2 ms^{-1} and for the wind direction values between 5 to 10° are given (Balaji et al., 2017, Gage et al., 1991, Gunter and Schroeder, 2015, Park and Lee, 2009, Vaughan and Hooper, 2015). When comparing the results for the filtering out of unusable data, these values are included in the plots for the visual interpretation (see Figures 3.8 to 3.13).

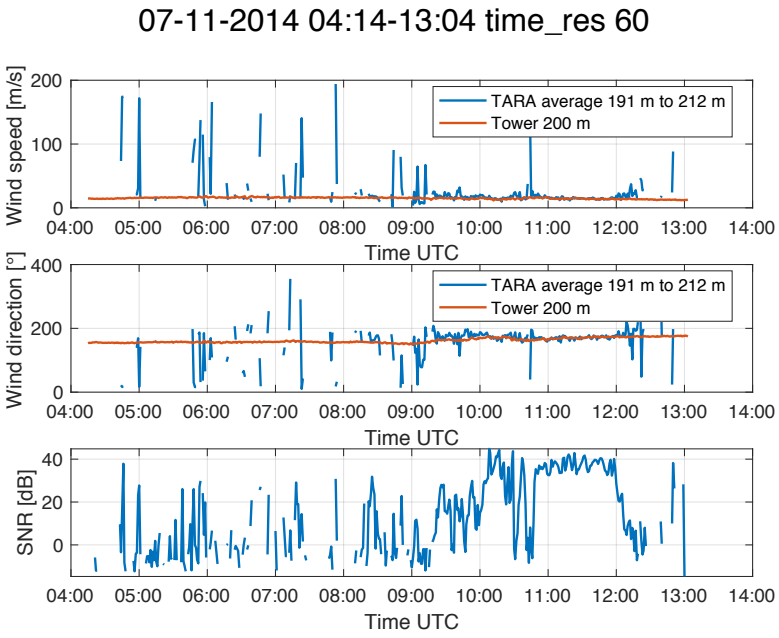

Figure 3.3: Figure showing the time series of TARA on 7.11.2014. The top plot shows the wind speed of TARA and of the tower at an average of 60 seconds. TARA shows a larger variability than the tower. The same is true for the wind direction shown in the middle plot. The bottom plot shows the SNR for the time series. Negative values of SNR are possible due to the processing done.

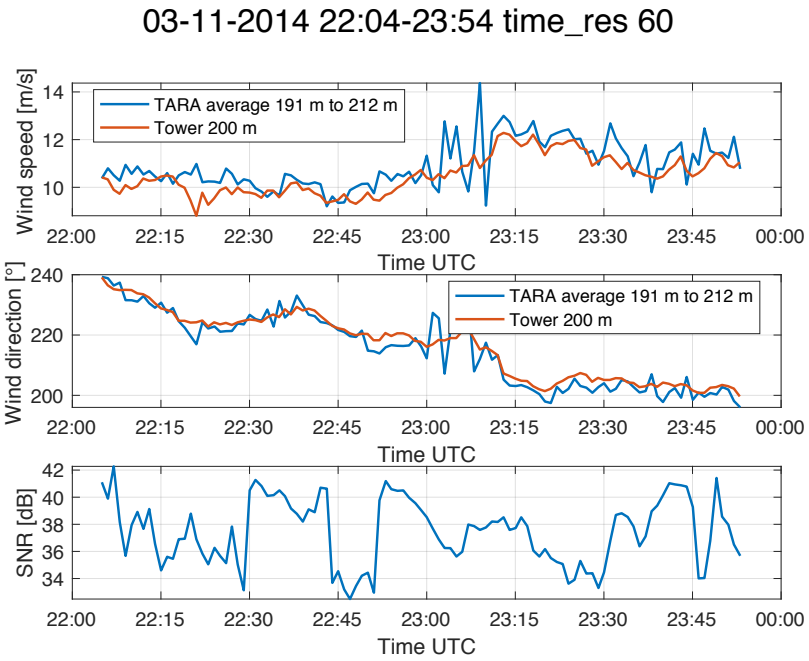

Figure 3.4: Figure showing three plots with time series observed on 3.11.2014, all using a resolution of 60 s. The top plot shows the wind speeds measured using TARA and the anemometer of the tower. The plot in the middle shows the same but for the wind direction and the bottom plot is the SNR for the same time period as observed using TARA. The situation during this observation period is stable and the variations in wind speed and direction smaller compared to the time series on 7.11.204 (see Figure 3.3).

3.2. Removal of Clear Air Measurements Using the SNR of the Main Beam

The first step in threshold definition for the signal to noise ratio as mentioned in the previous section is to find a way to remove data based on the fact of low reflectivity making a retrieval of accurate velocity vector estimates unlikely. The reason for this is the correlation visible in Figure 3.3 that the wind speed values show large outliers in the case of low signal to noise ratio. Thus, it makes sense to apply a filtering based on the signal-to-noise ratio and then check the results. If the results of this approach are promising, then a way has to be found to identify the threshold to be used. This means to identify which threshold removes what part of the values present in from the recorded time series (drizzle, cloud, clear air, rain).

The signal to noise ratio of the main beam was chosen instead of the reflectivity of the main beam as the signal to noise ratio is a more objective value for decisions. While the reflectivity in certain parts of the observed medium might be low, the signal to noise ratio itself might still be high enough. Removing those parts will most likely lead to losses mostly in the cloud.

The results shown in figures are different for the case of the 7.11.2014 (Figure 3.5) compared to the 3.11.2014 (Figure 3.6). For the first case some of larger outliers for the TARA are removed others remain and the rmse increases. This is likely due to the fact that as the threshold is increased more good data is removed and the relatively large outliers that remain have a larger impact with less good data left. In the second case of the 3.11.2014 the RMSE remains the same for all thresholds applied and none of the relatively small outliers when comparing to the previous case were removed.

To conclude it became clear that this method of filtering is not the best approach to resolving the issues of large outliers which might be e.g. caused by clutter. In the following sections another approach to filtering the usable data will be discussed which is based on only using the data obtained during periods of rain.

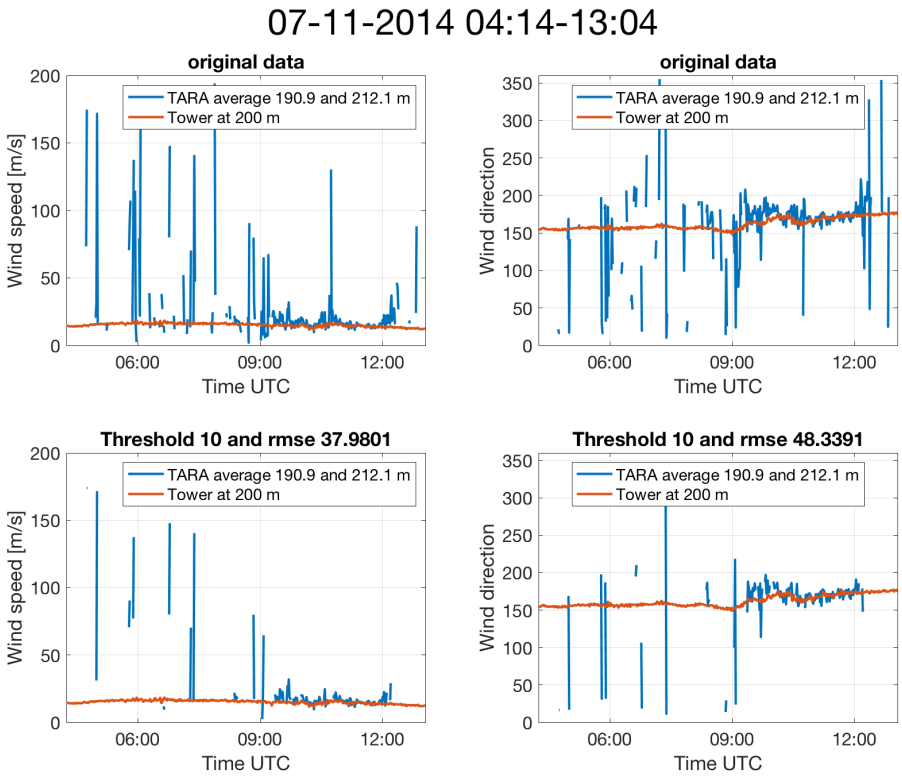

Figure 3.5: This figure shows a time series measured by TARA and the tower anemometer at a resolution of 60 s average. The increase in threshold for the SNR results in removal of some of the outliers while other relatively large wind speed outliers remain.

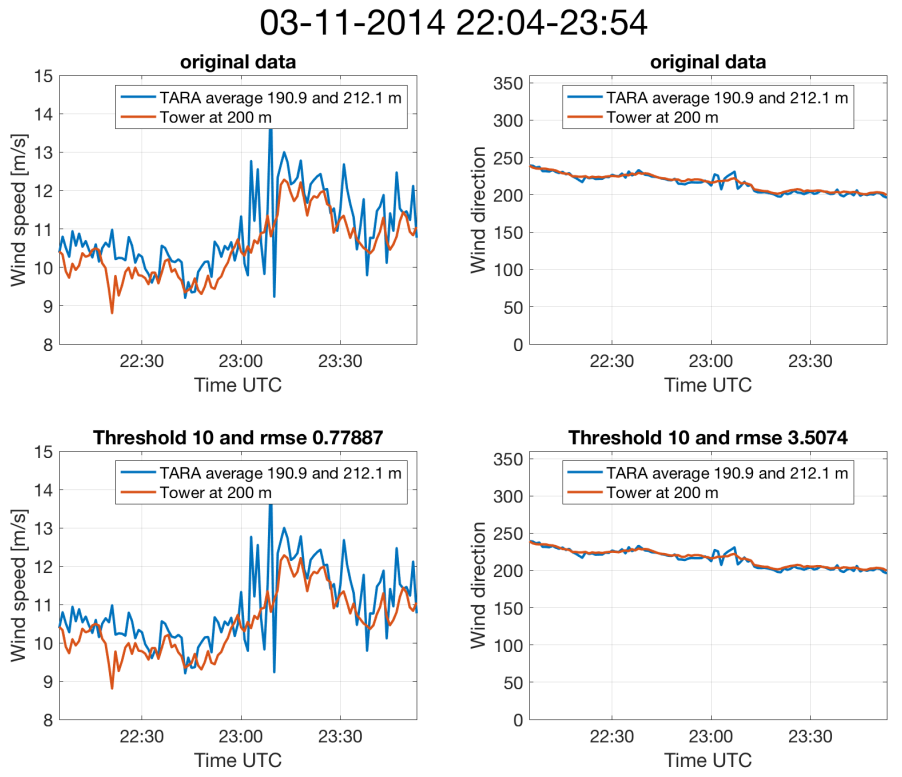

Figure 3.6: Figure shows different thresholds of SNR that were applied to the time series on 3.11.2014. In this case the threshold does not have a visible impact on the outcome, the RMSE remains the same for all of the plots.

3.3. Selection of Rain Events Based on Melting Layer Presence

Due to the fact that the removal of clear air measurements using a SNR was not as successful as expected and that the result was that unusable as well as usable data were removed with increasing threshold while some large outliers with SNR remained. In order to test the algorithm in cases where the conditions are actually what the algorithm of TARA is designed for, a rough selection of precipitation events was developed. If there are already problems found with these data, those problems need to be solved before the clear air or cloud wind estimation results obtained using TARA can be investigated.

In the matlab-code the way to approach this topic is to identify the presence of a melting layer for each time step and eliminating data with no precipitation. The data is averaged first for the time interval of 1 or 10 minutes. Which averaging interval is used, is based on the tower anemometer set used for validation. After this the threshold is applied to the maximum found for all heights at a given time interval. Given the 10 highest values of a time-bin are below 30 dB, then this whole time-bin will be removed from the analysis. The SNR-value chosen for this filtering was based on qualitatively looking at the data and identifying which value corresponds to the melting layer. This then gives the possibility of only keeping the usable data and comparing it to the tower and computing the RMSE.

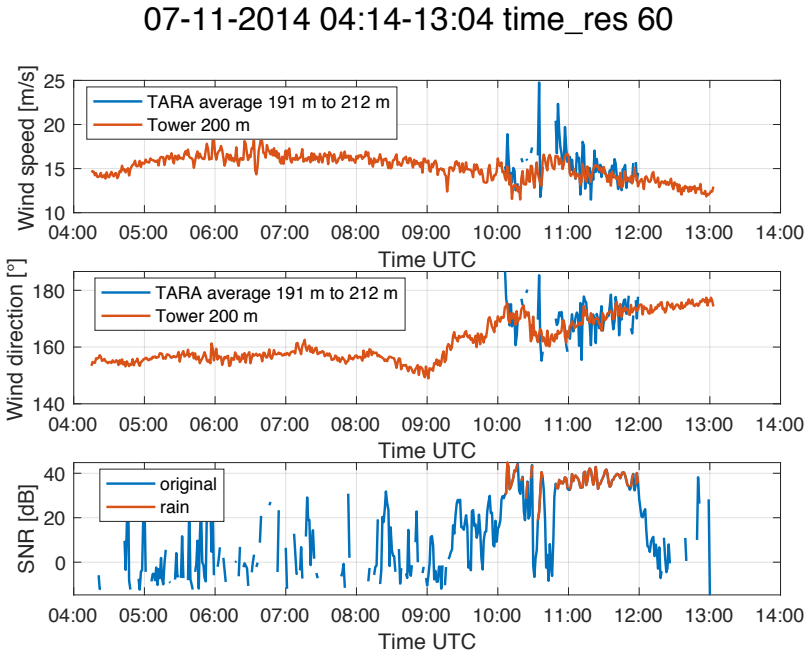

Figure 3.7: Figure showing three plots of the time series on 7.11.2014. While the whole time series for the anemometer data is shown in the plot, only the TARA-data during the rain events are shown. In the top plot the wind speed time series is shown. While there are still differences, a lot of the large outliers have been removed (compare to Figure 3.3). The middle plot shows the wind direction, here also the full time series for the tower anemometer is shown. In the bottom plot the SNR is shown.

For the case of 7.11.2014 this method of only using data during a period with a melting layer presence works better while for the 3.11.2014 the same result is achieved as when applying a threshold which means that all data remain. This is the reason why only the result for the 7.11.2014 is shown in a figure (see Figure 3.7). For the 3.11.2014 all data remained, thus the figure was not reproduced here (see Figure 3.4 for comparison). The following subsection a comparison will be made between results obtained using an SNR-threshold and rain event selection which also includes quantitative values (see Table 3.1 in subsection 3.4.1 below).

3.4. Results and Discussion

Two methods were used in a first part of assessing the results of the wind estimation of TARA. The method of removing clear air measurements using SNR thresholds as well as only keeping data during rain periods will be compared below. Following the comparison of the results for the two case studies, the results for all the usable cases during the ACCEPT-campaign are presented in a table and discussed.

3.4.1. Comparison Results Filtering Techniques

In a first attempt of filtering the wind estimation results retrieved using TARA a threshold of signal to noise ratio was applied. This method was not as successful as expected which lead to the application of a rough filtering out of data not obtained during precipitation. The comparison of the results of both methods is the topic of this subsection. For each of the two case studies (7.11.2014 and 3.11.2014) the same methods were applied and a summary of the results in numbers can be found in Table 3.1 below. The figures below first show the original data (Figures 3.8 and 3.11), followed by a plot of each methods. The SNR- threshold results can be found in Figures 3.9 and 3.12 and the results after filtering for precipitation data in 3.10 and 3.13.

For the case of the 7.11.2014 (Figures 3.8, 3.9 and 3.10) there is a large improvement when comparing the original and SNR-threshold result to the rain event result. For the case of the 3.11.2014 (Figures 3.13, 3.12 and 3.13) there are no large changes but this is due to the reason that the data considered on this day were recorded during a stable precipitation situation (see Figure 3.4). This means that Figures 3.11, 3.12 and 3.13 show the same outcome.

For both cases it can be concluded that the mean error in wind speed shows a positive bias, i.e. overestimates the wind. Most of the directions show a mean negative value for the differences between TARA and the tower (see Table 3.1). This can also be seen during the other usable data from the ACCEPT-campaign. The quantitative results can be seen in detail in Appendix A and below in Table 3.3 the mean values are presented. The identification of this positive bias in the wind speed estimation results leads to the next step in the research which is investigating possible causes of this bias. This investigation will be done by performing simulations using the wind estimation algorithm used for the processing of the TARA-data.

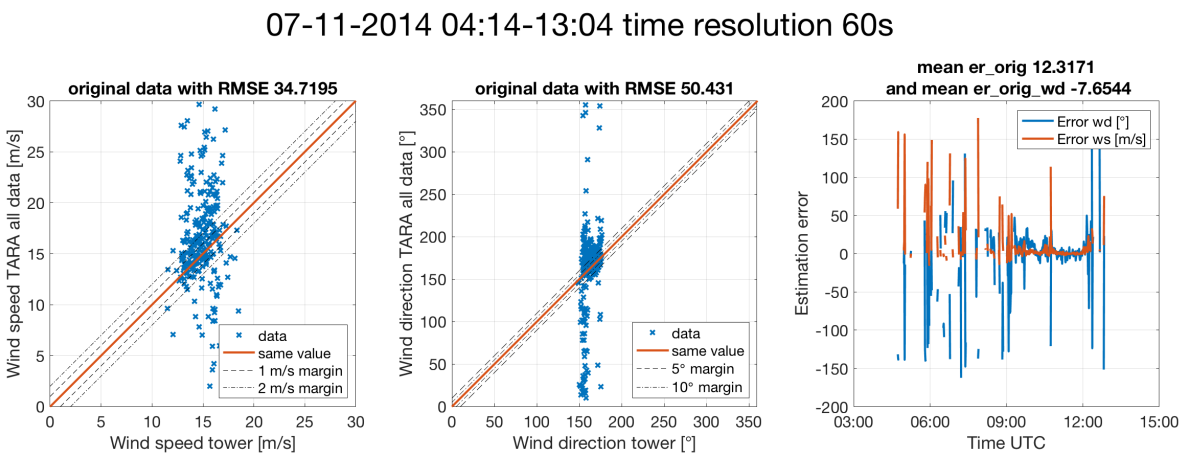

Figure 3.8: This figure shows three plots for the time series on 7.11.2014. The left plot is the wind speed measured by the tower plotted against the wind speed estimated using TARA. The middle plot is the same for the wind direction and the right plot shows the error in wind speed and direction.

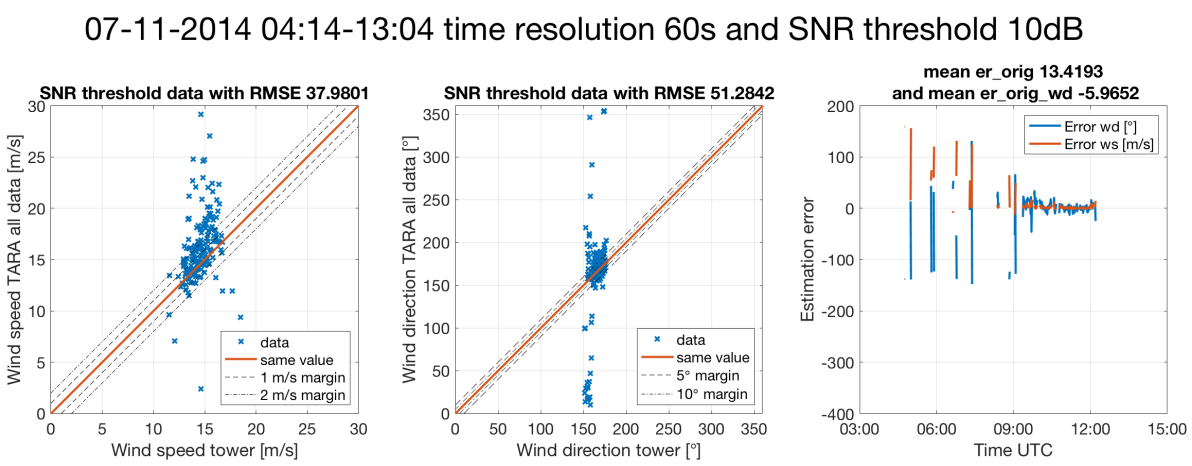

Figure 3.9: This figure shows the same three plots as Figure 3.8 but after application of a SNR-threshold of 10 dB.

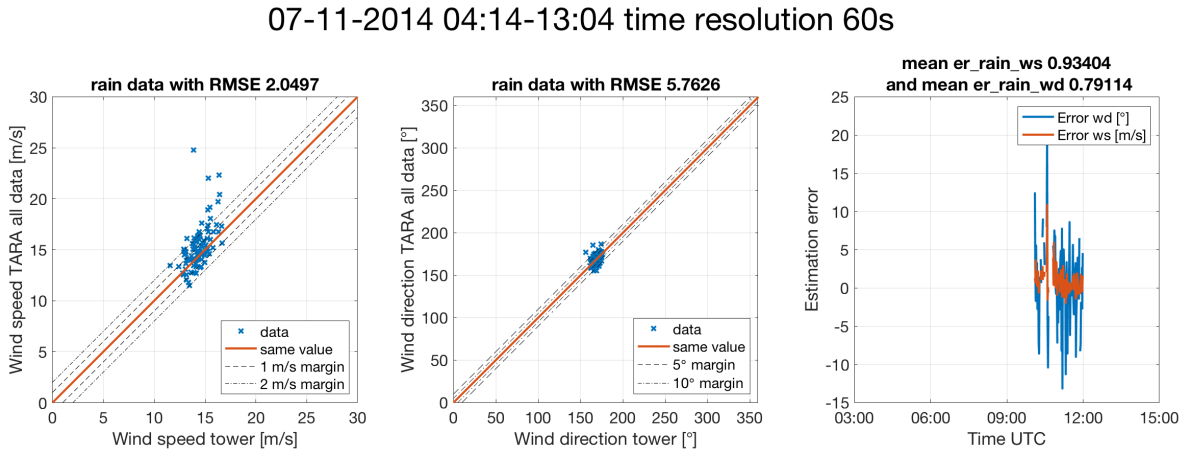

Figure 3.10: This figure also shows the time series of the 7.11.2014 in the same manner as the two figures above (Figures 3.8 and 3.9). The difference is that in this case only the wind speed and direction estimated during rain events were used which resulted in a reduction of the errors.

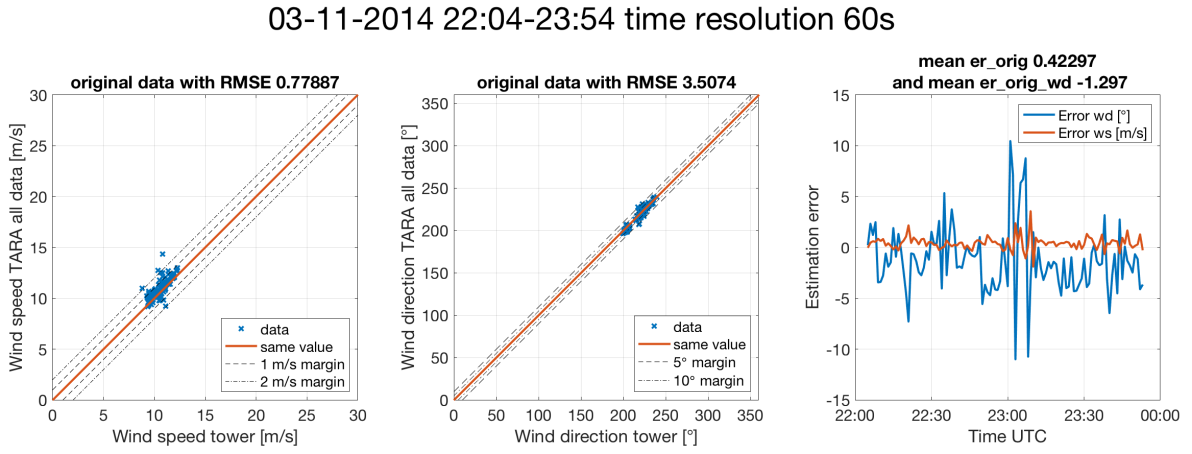

Figure 3.11: This figure shows three plots of the data for the time series obtained on 3.11.2014. The left plot shows the tower wind speed plotted against the wind speed estimation from TARA. The plot in the middle shows the same for the wind direction. The plot on the right shows the difference between TARA and the tower.

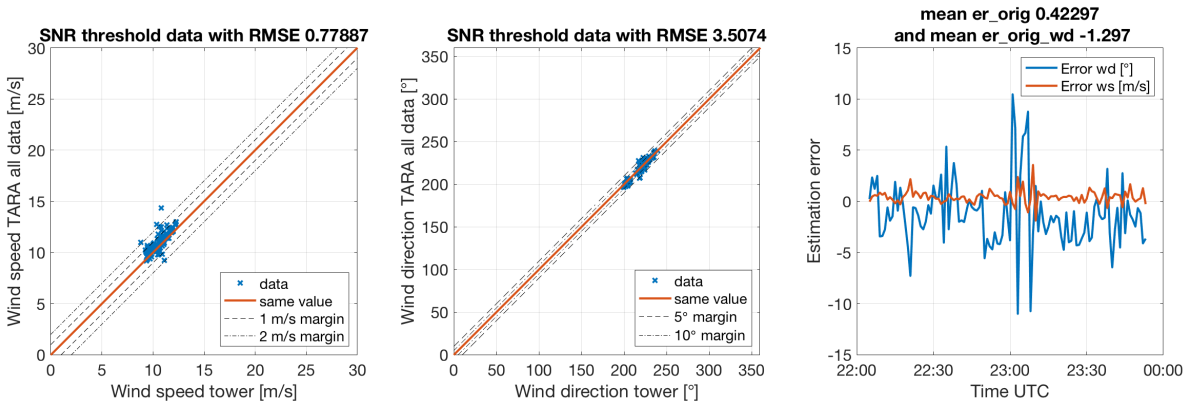

Figure 3.12: This figure shows the time series on the 3.11.2014 with an applied threshold in SNR of 10 dB. The left plot shows the wind speed measured by the tower plotted against the wind speed estimation from TARA. The plot in the middle shows the same for the wind direction. The difference between TARA and the tower can be found in the plot on the right.

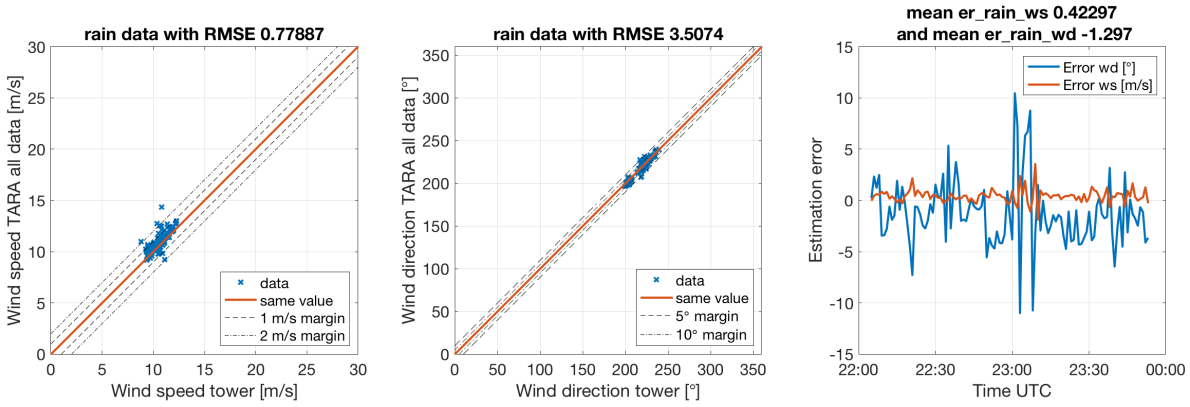

Figure 3.13: This figure shows the time series during rain for the 3.11.2014. The left plot shows the wind speed measured by the tower against the wind velocity estimation of TARA. The plot in the middle shows the same for the wind direction. The plot on the right shows the difference between the estimation from TARA and the tower.

3.4.2. Time Resolution

One important part of the quality assessment is to be able to make a recommendation of what time resolution can be used for the wind estimation performed by TARA. In Tables 3.1 and 3.2 the results for the two case studies using different time resolutions are presented. Table 3.1 shows the results for using an averaging period of 1 minute while for Table 3.2 a resolution of 10 minutes was used. While the results using 10 minutes averaging periods for both cases show lower RMSE and mean error values it can be argued that still it is better to use the 1 minute averages. This is because although the values are larger, they still remain in the 1-2 m/s and 5-10° range which was found in the literature. Another argument for using the 1 minute averages is that more data is kept which is more useful in the case of performing studies on the microphysics of the medium observed.

Table 3.1: Shows the comparison of the results obtained for the two case studies compared above. The averaging time period was in this case 60 seconds. The table includes the mean ws errors as well as the mean wind direction errors.

07.11.14	rmse		mean error	
	wind speed [m/s]	wind direction [°]	wind speed [m/s]	wind direction [°]
original	34.7	50.4	12.3	-7.7
SNR threshold 10dB	38.0	51.3	13.4	-6
rain	2.0	5.8	0.9	0.8

03.11.14	rmse		mean error	
	wind speed [m/s]	wind direction [°]	wind speed [m/s]	wind direction [°]
original	0.8	3.5	0.4	-1.3
SNR threshold 10dB	0.8	3.5	0.4	-1.3
rain	0.8	3.5	0.4	-1.3

Table 3.2: This table shows the mean values of all usable cases during the ACCEPT-campaign with an averaging period of 600 seconds. Detailed values can be found in the table included in Appendix A.

07.11.14	rmse		mean error	
	wind speed [m/s]	wind direction [°]	wind speed [m/s]	wind direction [°]
original	32.3	46.3	16.4	-6.7
SNR threshold 10dB	50.5	78.7	25.9	-26.8
rain	1.1	2.9	0.8	-0.4

03.11.14	rmse		mean error	
	wind speed [m/s]	wind direction [°]	wind speed [m/s]	wind direction [°]
original	0.5	2.1	0.4	-1.6
SNR threshold 10dB	0.5	2.1	0.4	-1.6
rain	0.5	2.1	0.4	-1.6

3.4.3. Results for All Usable Cases During the ACCEPT-Campaign

While before only two case studies were considered, the results of the assessment of the wind speed and direction estimation for all the usable case studies during the ACCEPT-campaign are given in this subsection. The detailed tables can be found in Appendix A and the mean values are presented in Table 3.3. Looking at the mean values for the whole ACCEPT-campaign it can be found that the results during rain events for the wind speed and direction estimates are better for the 600 second averages compared to the 60 second resolution. A mean positive bias for the wind speed could be identified as well as a mean negative bias for the wind direction when considering the result for the whole campaign.

Table 3.3: This table shows the mean values of all usable cases during the ACCEPT-campaign. Detailed values can be found in the table included in Appendix A.

	rmse		mean error		mean wind speed [m/s]		mean wind direction [°]	
resolution 60 s	wind speed [m/s]	wind direction [°]	wind speed [m/s]	wind direction [°]	tower	TARA	tower	TARA
original	12.4	28.1	5.5	-6.2	13.5	18.9	216.3	207.7
rain	2.4	8.3	1.1	-1.6	13.6	14.7	216.3	214.7

	rmse		mean error		mean wind speed [m/s]		mean wind direction [°]	
resolution 600 s	wind speed [m/s]	wind direction [°]	wind speed [m/s]	wind direction [°]	tower	TARA	tower	TARA
original	9.2	20.0	5.4	-5.8	13.5	18.9	216.6	210.0
rain	1.3	2.8	1.1	-1.0	13.5	14.6	216.4	215.3

3.5. Error Simulations

For this section the goal is to investigate the effect of certain wind speeds, direction and fall velocities on the wind speed and direction estimation errors, while the assumption of the same fall velocities the three measuring beams does not hold.

To test the wind retrieval algorithm a simulation was done. In a first step the ground truth will be defined and the Doppler velocities will be calculated using different fall velocities for the three beams. The obtained mean Doppler velocities will then be used to estimate the three-dimensional wind field using the algorithm currently employed for TARA that assumes that all beams measure the same medium i.e. measure the same fall velocity of the particles.

This approach is focused on introducing an error into one beam, but it is important to remember that there are many other sources of errors like spatial changes in dynamics which need further investigation.

3.5.1. Definition of Ground Truth and Simulations

The first step for starting the simulation is to define the ground truth. This ensures that the exact error resulting from different fall velocities can be calculated. Using the values for the wind speeds V_x, V_y will be estimated from V and U that are defined. The fall velocity will be defined for the different beams separately.

$$\begin{bmatrix} V_x \\ V_y \\ V_z \end{bmatrix} = \begin{bmatrix} cos(\Phi_N) & -sin(\Phi_N) & 0 \\ sin(\Phi_N) & cos(\Phi_N) & 0 \\ 0 & 0 & 1 \end{bmatrix}^{-1} \cdot \begin{bmatrix} V \\ U \\ V_z \end{bmatrix} \tag{3.2}$$

$$\begin{bmatrix} V_x \\ V_y \\ V_z \end{bmatrix} = \begin{bmatrix} cos(\Phi_N) & sin(\Phi_N) & 0 \\ -sin(\Phi_N) & cos(\Phi_N) & 0 \\ 0 & 0 & 1 \end{bmatrix} \cdot \begin{bmatrix} V \\ U \\ V_z \end{bmatrix} \tag{3.3}$$

For the V_{mb} and V_{ob1} the same fall velocity will be assumed while for the V_{ob2} another value for V_z will be used. We also assume that the vertical wind is negligible. Using the V_x and V_y that were calculated and the defined fall velocities V_z and V_z' (for the V_{ob2}) the mean Doppler velocities will be calculated. The reason for choosing to use a different fall velocity for the V_{ob2} is that the other two beams are looking at the same azimuth while V_{ob2} is not. Thus it is more likely that V_{ob2} is looking at a different media at the same height.

$$\begin{aligned} V_{MB} &= V_x\ cos(\alpha) + V_z\ sin(\alpha) \\ V_{OB1} &= V_x\ cos(\alpha + \gamma) + V_z\ sin(\alpha + \gamma) \\ V_{OB2} &= V_x\ cos(\alpha)\ cos(\gamma) + V_y\ sin(\gamma) + V_z'\ sin(\alpha)cos(\gamma) \end{aligned} \tag{3.4}$$

The estimation of the wind from the calculated mean Doppler velocities will then be done according to Section 2.4.2. In this case the ground truth is known so the differences can be calculated and it can be tested how large the impact of changing speeds, direction and fall velocities is.

Different values for the two components U and V, keeping $U^2 + V^2 = const$, result in different wind directions. This can be used to test the dependency of the accuracy of the estimation on the direction. Most of the data obtained during ACCEPT-campaign had mean wind speed values between 5 to 15 m/s. This will be used to choose the values for the ground truth. More specifically the V and U were defined for the use in matlab as shown in Figure 3.14. The actual results of the ground truth definition can be seen in Figure 3.15.

The differences in fall velocity have an impact in this case because of the way the simulation is done. It will first be assumed that there is a difference in fall velocity for the three beams to obtain V_{MB}, V_{OB1}, V_{OB2} from the V,U,V_{fall} components. With this the wind will be estimated but assuming that the fall velocity is the same for all three beams. Doing this will show what differences can be found with this approach.

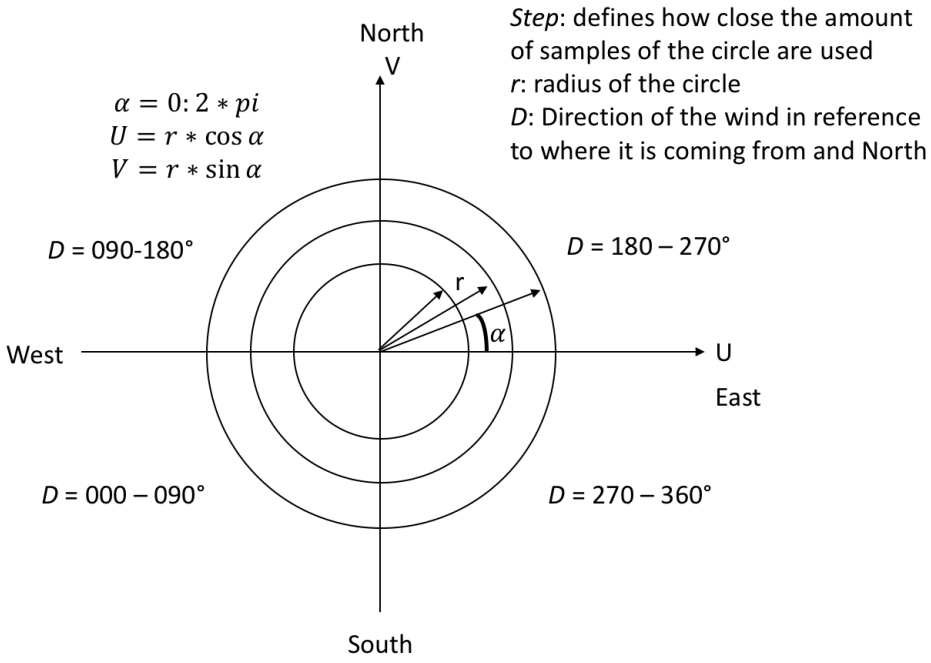

Figure 3.14: This figure shows the concept behind the definition of the ground truth used for the error simulation. The idea is to include all wind directions as well as different wind speeds. This can be done by creating wind vectors that result in circles as shown in this figure. The wind direction is defined as reference to North in and the direction of which it is coming from.

Figure 3.15 below shows the wind speed and direction used for the simulation. In this case a step in radius of 1 m/s is chosen. The re-estimation was performed as discussed above. The results of the simulation will be discussed in the following results and discussion section.

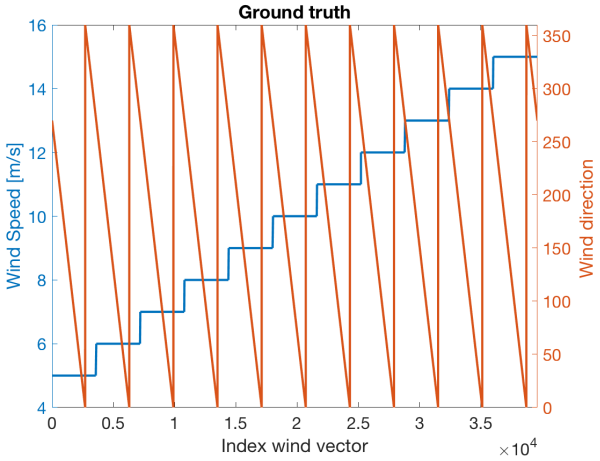

Figure 3.15: This plot shows the result of the wind speed and direction when estimating the wind using the U and V as defined in Figure 3.14 above. Note that this plot shows a variety of wind speeds to show the principle of how the ground truth is defined for the simulation. In the figures below there is only one wind speed considered.

3.5.2. Results and Discussion

As explained above, an error was introduced to V_{ob2} during the simulation using the wind estimation algorithm. Looking at the equations in Subsection 2.4.2 shows that this error will only have an effect on the V_y-component as this is the only one where V_{OB2} is a part of (see equation 2.19). This equation is repeated in equation 3.5 for convenience. Thus it can be expected that the errors for wind speed and direction are smallest when the wind is in the direction of the main beam (246.5°) as there the V_{OB2}-component is zero and largest perpendicular to the main beam.

The results of the simulation are shown below. The first plot (Figure 3.18) shows the influence of the wind speed on the accuracy of wind speed and wind direction estimation for different fall speeds in V_{OB2}. Following this there are two figures showing the influence of the wind direction on the accuracy of the wind speed and direction estimation (Figures 3.20 and 3.21). A summary of the differences for wind speed and direction estimation errors found is related to fall velocity differences in Figure 3.23. There were some unexpected results, thus there will also be a section explaining these results with example calculations based on the wind estimation algorithm found in subsection 2.4.2.

Introducing an error in V_{OB2} means that the only component affected is V_y. This can be seen in the equations 2.19 reproduced below.

$$\begin{aligned} V_x &= 3.3461 \cdot V_{MB} - 2.7321 \cdot V_{OB1} \\ V_y &= -3.7321 \cdot V_{MB} + 3.8637 \cdot V_{OB2} \\ V_z &= -1.9319 \cdot V_{MB} + 2.7321 \cdot V_{OB1} \end{aligned} \tag{3.5}$$

Figure 3.16 shows what happens to V_y when using different fall velocity difference. It can be seen that there is a constant offset for V_y caused by the error introduced V_{OB2}. The exact values for this offset in relation with the fall velocity difference are shown in Figure 3.17.

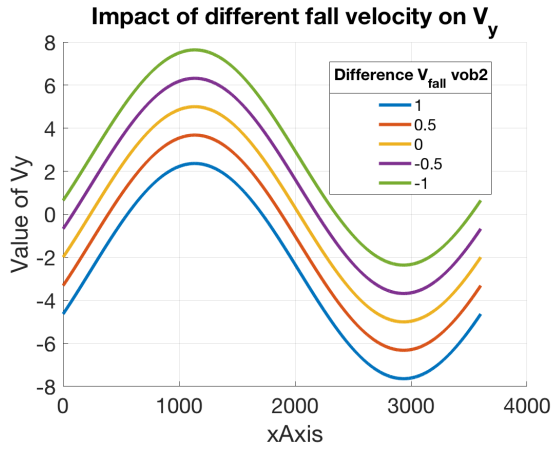

Figure 3.16: This figure shows the different values for V_y when different fall velocities are used in V_{OB2} for the estimation algorithm.

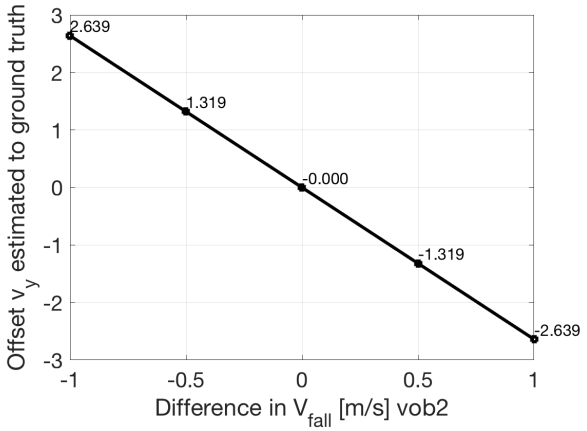

Figure 3.17: Shows the values for the offset in relation to the fall velocity difference.

The effect of this under- or over-estimation of V_y on the wind estimation results will be discussed in the following subsections. The first one will be concerned with the influence of the wind speed on the estimation error for wind speed and direction. The second subsection will look at the influence of the direction on the wind speed and direction estimation error. The last subsection will discuss the relation of a positive bias to the RMSE of a wind speed or direction estimation error.

Influence Wind Speed

Figure 3.18 shows the influence of the wind speed on the errors made when applying the wind estimation algorithm under the assumption of equal fall velocity while this is not the case. In the left part of the figure the relationship between wind speed and wind speed error for different fall velocity differences is shown. The wind speed does not have an influence on the error made for the wind speed, while the wind speed error increases with the fall velocity difference. The increasing spread is due to the fact that the error is not the same for all wind directions. The influence of the wind direction on the estimation will be discussed further below.

The right part of Figure 3.18 shows the influence of the wind speed on the wind direction estimation. With increasing difference in fall velocity the errors become larger. But also a second effect can be found, the error decreases with increasing wind speed. To conclude, the wind speed does not have an influence on the spread and maximum of the wind speed estimation error. However the wind speed has an influence on the spread and maximum wind direction estimation error.

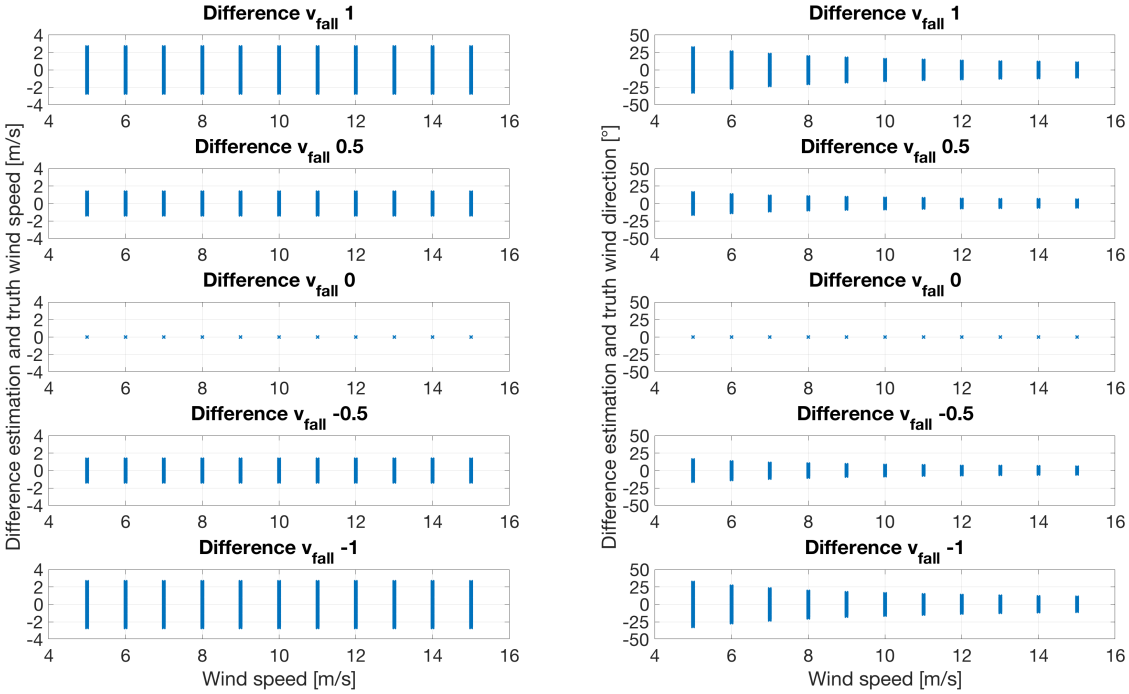

Figure 3.18: Figure showing two plots. On the left the wind speed is plotted against the difference between wind speed estimation and truth for different fall velocity differences. The right side shows the wind speed plotted against the difference between estimation and truth for the wind direction. This is also done for different fall velocities.

This wind speed dependence of the wind direction estimation error is caused by the relative impact of the same error for different wind speeds. When the same error in e_{vy} is applied to a larger value for V_y the effect is relatively smaller than for a smaller wind speed. Figure 3.19 shows this influence graphically.

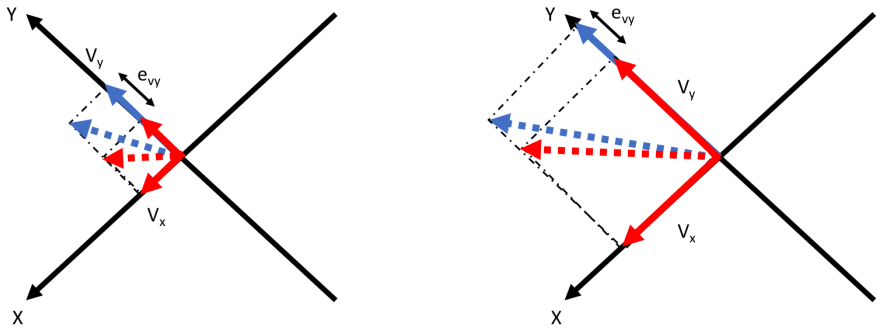

Figure 3.19: Shows what happens to the wind direction when the V_y changes by the same amount e_{vy} for smaller and larger wind speed i.e. larger and smaller V_x and V_y values. The red arrows depict the ground truth and the blue line is the change value of V_y. The left part of the figure shows the situation for an error in V_y of the same order of magnitude as its actual value. The right side of the figure shows the impact the same error has on a larger value of V_y. The change in angle for the left side is larger than the right side, thus the wind direction estimation error is smaller for the right side compared to the left side although the error in V_y is the same.

Influence Wind Direction

Figure 3.20 shows the influence of the wind direction on the wind direction estimation accuracy. It was expected that the smallest error is to be found in direction of the main beam which would be a wind direction of $246.5°$ or $66.5°$. Instead an absolute minimum is found at $156.5°$ and $336.5°$ which means that they are perpendicular to the axis of the main beam. The reason for this will be explained after introducing the figures.

The influence of the wind direction on the wind direction estimation error is shown in Figure 3.20 below. It can be seen that when there is no error in fall velocity there is also no error in wind direction estimation as it would be expected. The larger the fall velocity error, the larger also the maximum errors in wind direction estimation get. The minima can be found at the wind direction looking perpendicular to the main beam orientation.

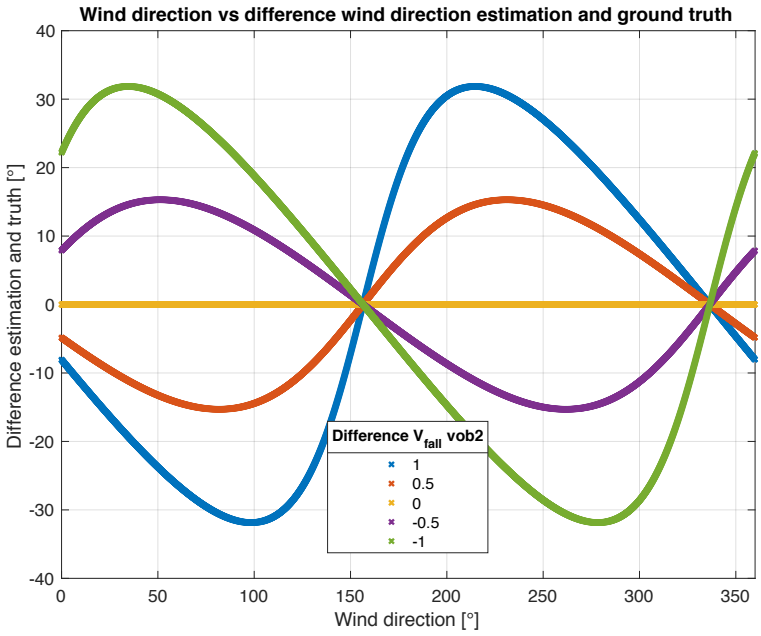

Figure 3.20: Figure showing the wind direction plotted against the difference between estimation and truth for the wind direction. The errors were introduced in the form of different fall velocities in offset beam 2. Re-estimation of the wind was then again done assuming that the fall velocities are equal. Thus this lead to under- as well as overestimation of the fall velocity in V_{OB2} which are the differnent colors, explained in the legend as difference in fall velocity V_{OB2}. The wind speed for this plot was 5 m/s.

The influence of the wind direction on the wind speed estimation accuracy is shown in Figure 3.21 below. Here the largest error can be found at the same positions as the minima in Figure 3.20. Also in the case of the relation of the wind direction with the wind speed error the absolute minima is not found in the looking direction of the main beam i.e. where the V_y was expected to be zero.

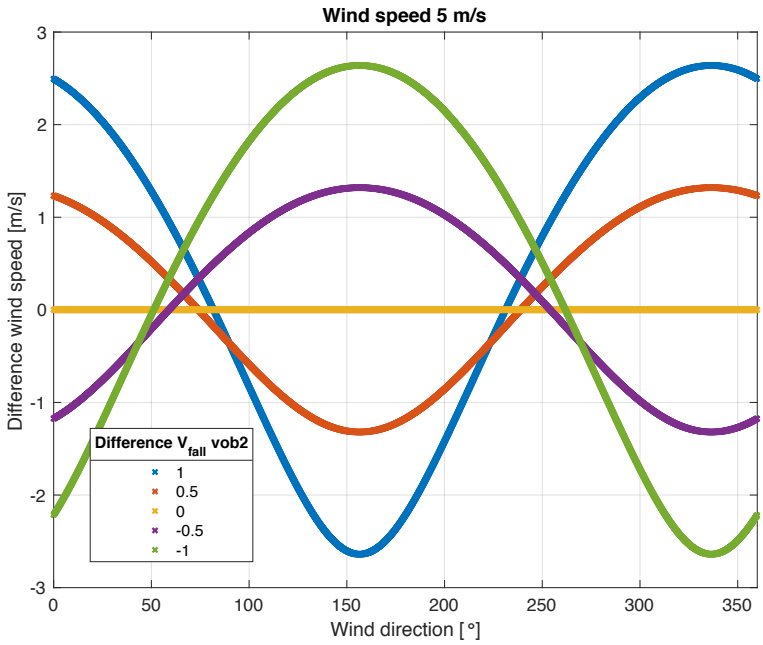

Figure 3.21: Plot showing the wind direction plotted against the wind speed estimation to truth differences of the wind speed. This is done for different fall velocities in V_{OB2} and using a wind speed of 5 m/s.

As already explained above, the only effect of the error introduced in V_{OB2} is on the V_y component in the form of a constant offset. The effect of this offset of V_y explained above compared to the original value of the ground truth results in a shift relative to V_x. Figure 3.22 shows the effect of a change in V_y with either a value of zero for V_x (left part of the figure) or V_x being non-zero. In a case where V_x is zero the offset of V_y only has an effect on the estimated speed, while there will be no error observed for the estimation of the direction.

Looking at the right part of Figure 3.22 shows the case where V_x is non-zero. As an example, consider that the ground truth is that the wind is in the direction of the main beam i.e. in X-direction. In such a case V_x would then be the wind speed defined as ground truth while V_y should be zero. But due to the fact that there is an offset in V_y, the maximum value of V_x does no longer correspond with the value of zero for V_y. The value of non-zero for V_y not only introduces an error in the wind speed, but mainly an error in wind direction.

Theoretically this explanation also holds for when V_y is zero even with the relative shift compared to V_x. The result should be no error in the direction as well as an under- or overestimation of the wind speed. But this is not the case for these examples as V_y is never exactly zero which is caused through how the ground truth is defined (Smallest absolute value for $V_x = 1.7764 \cdot 10^{-15}$ and for $V_y = 0.0032$). The reason that the minimum for $V_x = 0$ (i.e. perpendicular to the main beam) can be identified in Figure 3.20 is that there the errors change from negative to positive (or the opposite) and thus a value for zero appears to be present. Zooming into the plot shows that also there no zero error for the wind direction is found.

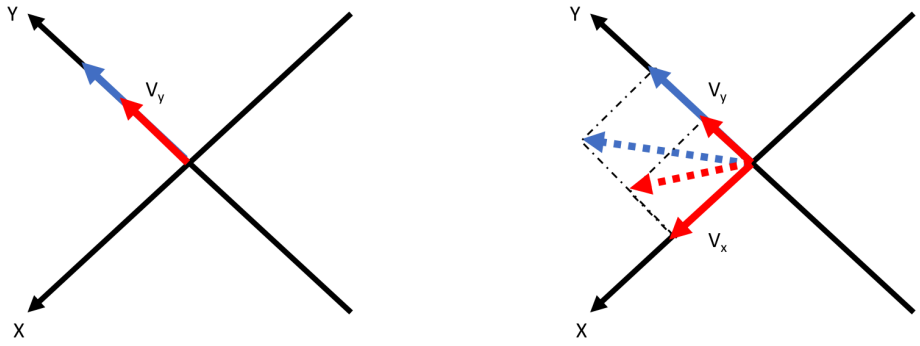

Figure 3.22: Shows what happens to the wind vector when the V_y changes while V_x remains constant. The red arrows depict the ground truth and the blue line is the change value of V_y. The left part shows what happens if V_x is zero which is a change in wind speed while the wind direction estimate remains constant. The right part of the figure shows what happens when V_x is non-zero. Additionally to an error in the wind speed estimation there is now also an error in the wind direction estimation.

Figure 3.23 below shows the difference in fall velocity plotted against the mean difference wind speed and direction estimation. For the wind speed in any case a difference in fall velocity results in a positive bias for the estimation results compared to the ground truth. Figure 3.21 shows that the maximum errors are the same positive and negative which could suggest that there should not be a positive bias found for the wind speed estimation error. But looking more closely at the figure shows that the positive values for the wind speed estimation error are over a larger interval of directions compared to the negative errors.

For the wind direction the mean difference is either positive or negative depending on the either positive or negative value for the fall velocity difference. To conclude these results suggest that the positive bias discovered when looking at the accuracy of the TARA-data is possibly caused by the assumption that the fall velocity for all three beams is the same.

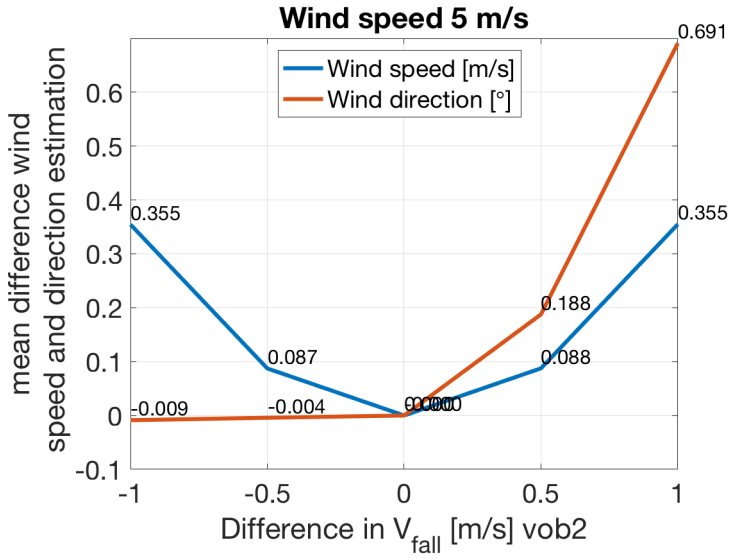

Figure 3.23: Plot showing the relation between the fall velocity differences and mean difference in wind estimation and ground truth for wind speed and direction. The y-Axis does thus have two units either [m/s] or [°].

Bias vs. RMSE

It could be argued that biases such as the ones shown in Figure 3.23 could be acceptable but the mean error does not say much about the overall accuracy. While some errors might be acceptable others might be too large (see maximum wind speed estimation error in Figure 3.21 for example). As a measure to better be able to choose the error acceptable in the fall velocity the RMSE has been

computed as well and is displayed in Figure 3.24 below. Even with a small difference of fall velocity of 0.5 m/s the RMSE of the wind speed is already close to 1 m/s while the wind direction has already reached a RMSE of more than 10 degrees.

Comparing these results to the TARA wind estimations can be done using the data shown in Table 3.1. The RMSE values in wind speed were 2.0 m/s (7.11.2014) and 0.8 m/s (3.11.2014) and the ones for the wind direction were 5.8° (7.11.2014) and 3.5° (3.11.2014). Both the wind speed and the direction are calculated using the same values for U and V values. Thus Figure 3.24 also shows the difference in error propagation for wind speed and direction. Thus an error in fall velocity of 0.5 m/s translates to an wind speed RMSE of 0.9, but the RMSE for the wind direction has a value of 10.8° which is already above 10°.

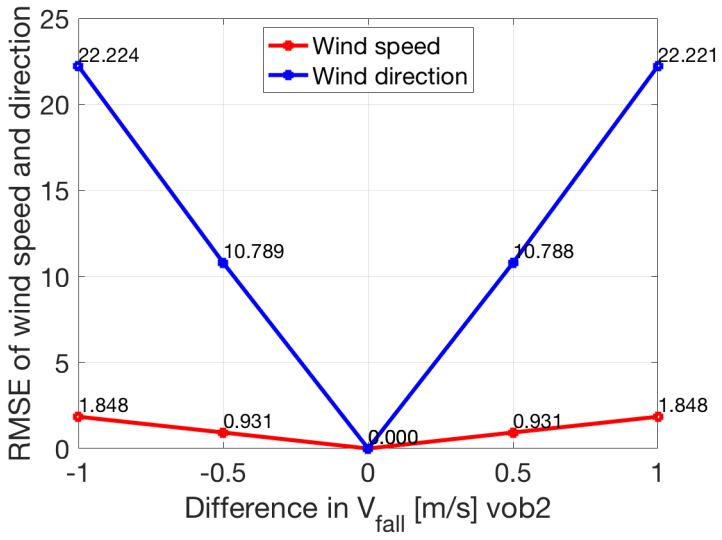

Figure 3.24: This plot shows the RMSE for the wind speed and direction for the simulation.

4

TARA-data Selection

Following the quick assessment of the wind estimation in the previous chapter it became obvious that there are some large error sources when the wind estimation is performed in situations for which the algorithm is not designed for. In particular this means situations where the dynamics and the micro-physics in the three beams are different. Due to this it is important to find a way to identify when these conditions are present and to identify the usable data.

Due to the fact that there are no sensors at CESAR that can be used to compare the results of the TARA wind estimation at all heights and at high time resolution, the criteria for the selection of the usable data need to be based on TARA-data only. While the selection of rain events based on melting layer presence proved to be sufficient for a quick assessment of the results of the wind estimation, this approach of data-selection had certain drawbacks. These drawbacks include that when selecting the whole data of a time step still some unusable data might be present, as melting layer presence does not mean that the data is usable at all heights above the surface.

Several approaches will be shown in this chapter in order to select the most suitable variable – based on TARA only – which can be used to select the usable data. The same two case studies as in Chapter 3 will be considered as well as an additional time period on the 3.11.2014. In the first section below the additional case study will be introduced. Following this the dependence of the wind estimation results on the SNR will be discussed. A way to increase the SNR is to use time averages. Following this conclusion the idea of re-estimation of the wind speed and direction using averaged mean Doppler velocities was developed. As this was not successful for all cases, there was a need to find a better way of data selection.

It was expected that the correlation of the mean Doppler velocities for the three beams could be useful for the data selection. Why this is not possible, will be explained in the next section. The last section will be concerned with using the mean Doppler velocities and computing the Coefficient of Variation which is defined as the normalization of the standard deviation by the mean. Vertical wind profiles of the horizontal wind will be presented which can be used for a qualitative assessment.

4.1. Case Studies 3.11.2014 and 7.11.2014

The two case studies from the previous chapter will again be used for the data selection approaches in the following sections (see Section 3.1 for more details). An additional time period for the 3.11.2014 will be introduced in this subsection.

In the previous chapter, the averaging included a method of removing statistical outliers. While this was appropriate to perform a quick assessment of the algorithm performance, in this following chapter, the averaging of the wind speed and direction estimates was done using all data. This is the reason why the original values of the RMSE and mean errors are slightly different from the results of the assessment of the wind estimation algorithm performance of the previous chapter, as well as the results shown in Appendices A and B. The reason for this change is to find a data selection method which reliably works on all outliers in the data.

For some of the plots and sections presented in this chapter only the time series of the wind speed is presented. Although the propagation of errors for the wind speed and direction is different caused by

the calculation from U and V (see Subsection 2.4.2 - TARA wind estimation), an error on U and V will result in an error in wind speed and direction. This is the case unless one of the components is exactly zero which would mean only an error in wind speed (see the Section 3.5 - Error simulation).

4.1.1. Introduction Additional Case Study on 3.11.2014

In addition to the two case studies introduced in the previous chapter (see Section 3.1) another time period for the 3.11.2014 will be considered in this chapter. The reason to introduce an additional case was the fact that while the 7.11.2014 (see Figure 3.3) showed very large outliers and the results for the 3.11.2014 (see Figure 3.4) showed a good result, but there is no case in between. For this reason another time period on the 3.11.2014 was added which is presented in Figures 4.1 and 4.2.

Figure 4.1 shows the SNR for the additional case study and in contrast to the 7.11.2014 (see Figure 3.1) during the whole time series there is light precipitation near the surface. Comparing Figure 3.3 to Figure 4.2 below also shows that for the 3.11.2014 the values of the SNR are mainly above zero while for the 7.11.2014 a lot of values below zero can be found. This is mostly the case for the clear air measurements on 7.11.2014 (see Figure 3.1). This difference between the two cases can also be seen when comparing the top plots of Figures 3.3 and 4.2. The differences in wind speed estimation between TARA and the tower are much larger in value for th 7.11.2014 compared to the second time period considered on the 3.11.2014.

Comparing the figures for all three case studies (Figures 3.3, 3.4 and 4.2) with a focus on the relationship between the SNR and the accuracy of the wind speed estimation it becomes evident that there is a relatively large value of SNR required for an accurate wind speed estimate. This will further be discussed in the next subsection.

Summarizing, this added case consists of variable rain (SNR = 0 to 40 dB) while the other study case on the same day is related to rain (SNR = 32 to 42 dB).

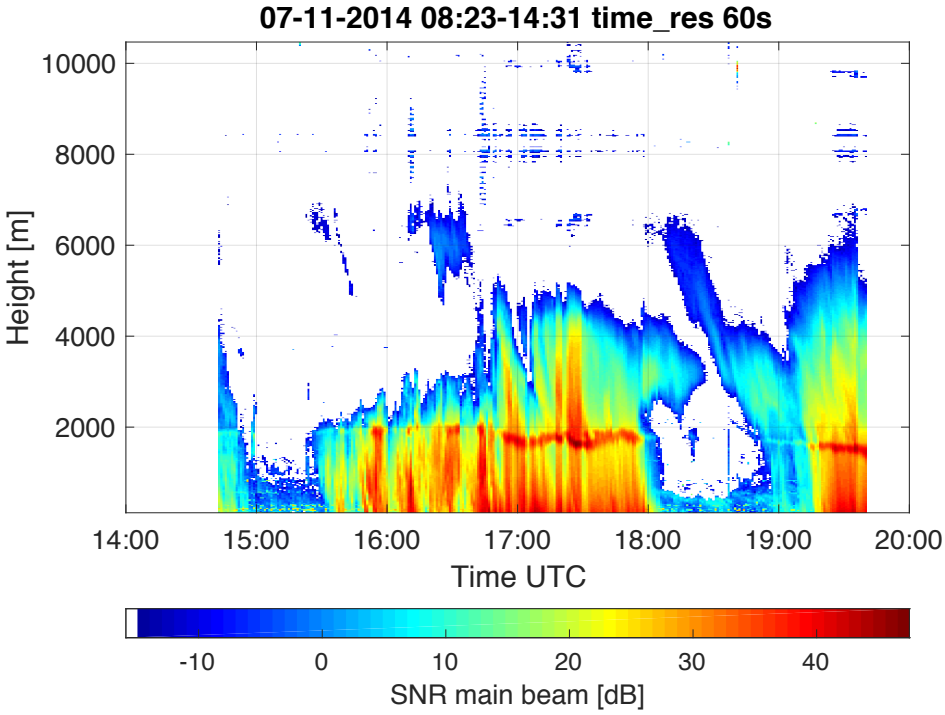

Figure 4.1: This figure shows an additional case study on the 3.11.2014. The plot shows the SNR for this case.

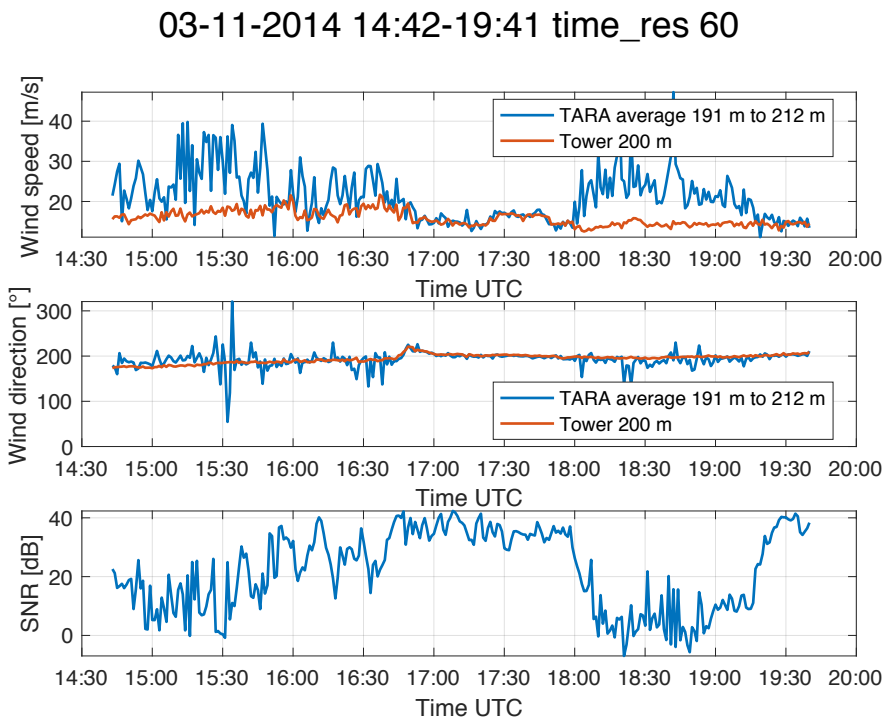

Figure 4.2: Figure showing three plots with time series observed on 3.11.2014, all using a resolution of 60 s. The top plot shows the wind speeds measured using TARA and the anemometer of the tower. The plot in the middle shows the same but for the wind direction and the bottom plot is the SNR for the same time period as observed using TARA.

4.2. Influence of SNR on the wind estimation accuracy

When comparing the time series for the three case studies considered (see Figures 3.3, 3.4 and 4.2), it becomes evident that a relatively large value for the SNR is required for an accurate wind estimation of TARA. Figures 4.3, 4.5 and 4.7 show this relation in more detail. For a better overview of the relation between estimation errors and SNR-values, Figures 4.4, 4.6 and 4.8 show scatter plots with the SNR on the x-Axis and the wind speed and direction errors along the y-Axis.

While for the 7.11.2014 the wind estimates are close to the tower values when the SNR is above 30 dB, some of the largest outliers can be found for values below zero (see Figure 4.3). This would suggest that a simple filtering based on the SNR should be sufficient for the data selection. However some of the large outliers in the case of the 7.11.2014 also have large values in SNR (see scatter plot in Figure 4.4). This is probably caused by residual clutter and it means that the SNR criteria cannot hold in case of clear air measurements (see Figures 3.8 and 3.9). For the case studies on the 3.11.2014, one shows SNR-values which are constantly above 30 dB and small differences between the TARA wind speed estimation results compared to the tower measurements. This can also be seen in the scatter plot presented in Figure 4.6. The second case considered for the 3.11.2014 (see Figure 4.7) shows a case which is between the other two. While there are parts with high SNR (between 17:00 - 18:00 and after 19:30) and accurate wind estimation, there are also still overestimations in the other parts of the time series. In contrast to the case of the 7.11.2014 are on the order of tens of m/s compared to hundreds of m/s. As can be seen in the scatter plot shown in Figure 4.8 there are no large outliers above 30 dB SNR.

To conclude, the SNR is an important criteria for the quality of the wind estimation in the case of rain (3.11.2014). In the case of clear air measurements (7.11.2014) with probably residual clutter, the SNR criteria cannot hold, therefore data selection only keeping rain, melting layer and cloud is necessary.

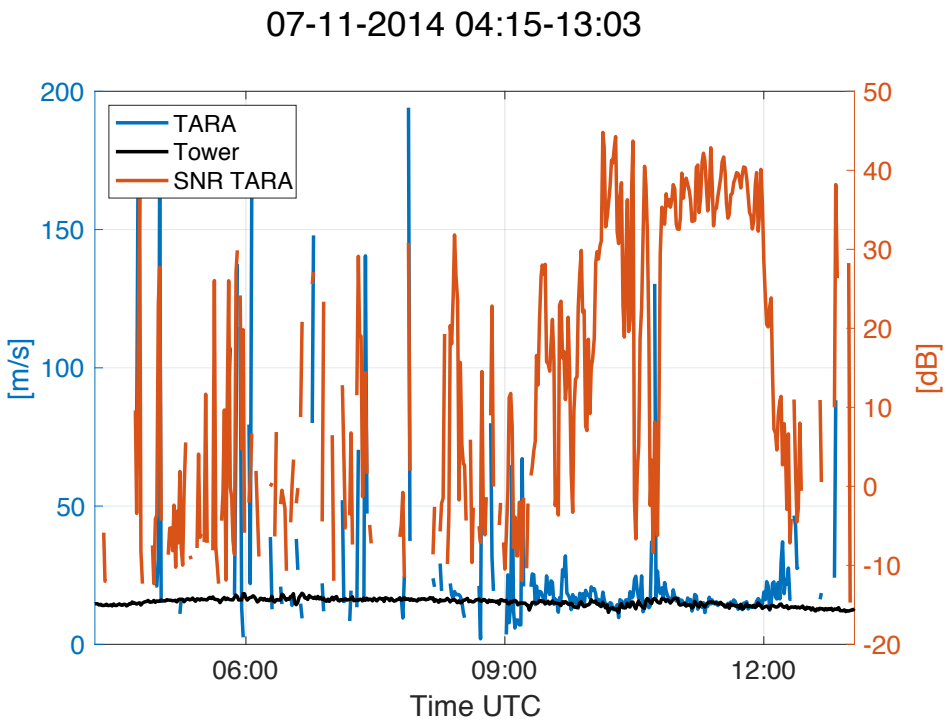

Figure 4.3: This figure shows a plot of the time series for the case study on the 7.11.2014. The blue line shows the wind estimate of TARA and the black line the wind speed measured by the tower. In the same plot the SNR is shown with the scale on the right side of the plot in dB.

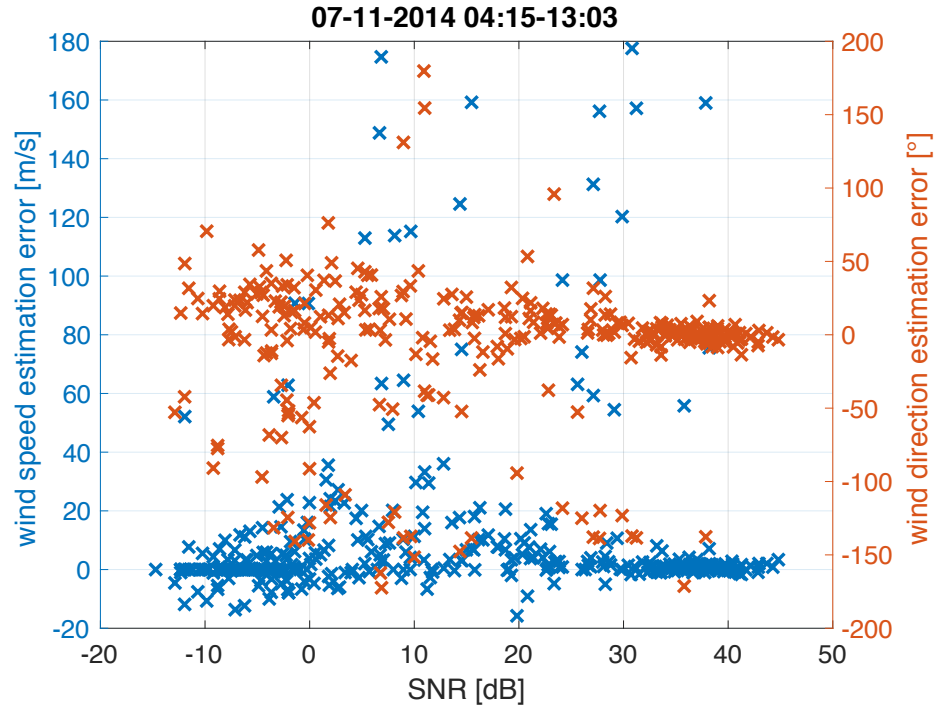

Figure 4.4: This figure shows a scatter plot for the 7.11.2014 relating the SNR to wind speed and direction estimation errors.

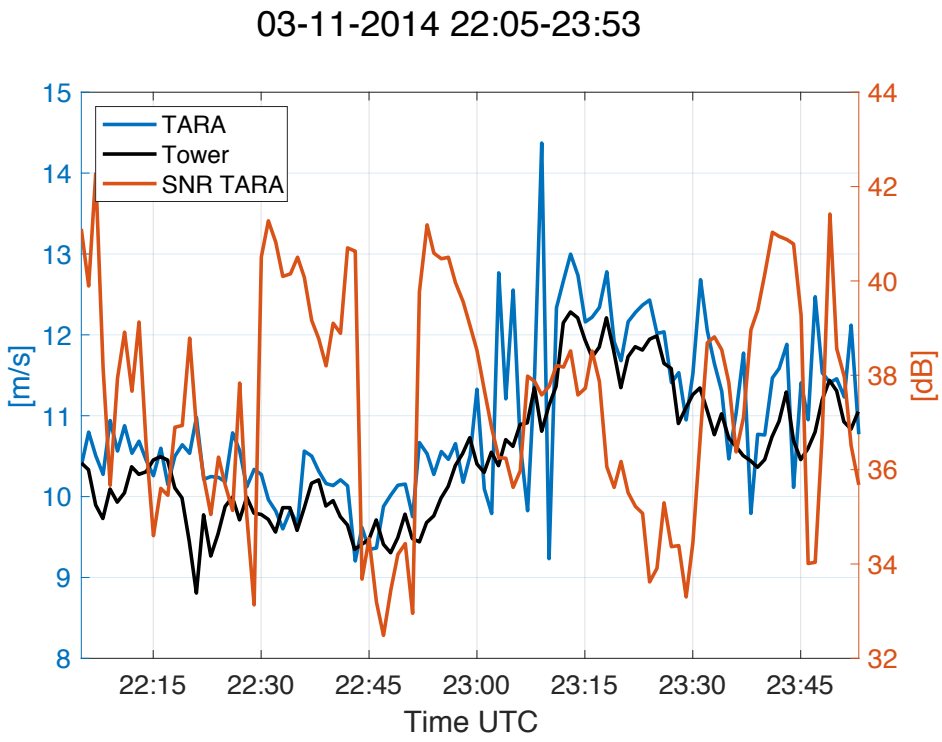

Figure 4.5: This figure shows a plot of the time series for the case study on the 3.11.2014. The blue line shows the wind estimate of TARA and the black line the wind speed measured by the tower. In the same plot the SNR is shown with the scale on the right side of the plot in dB.

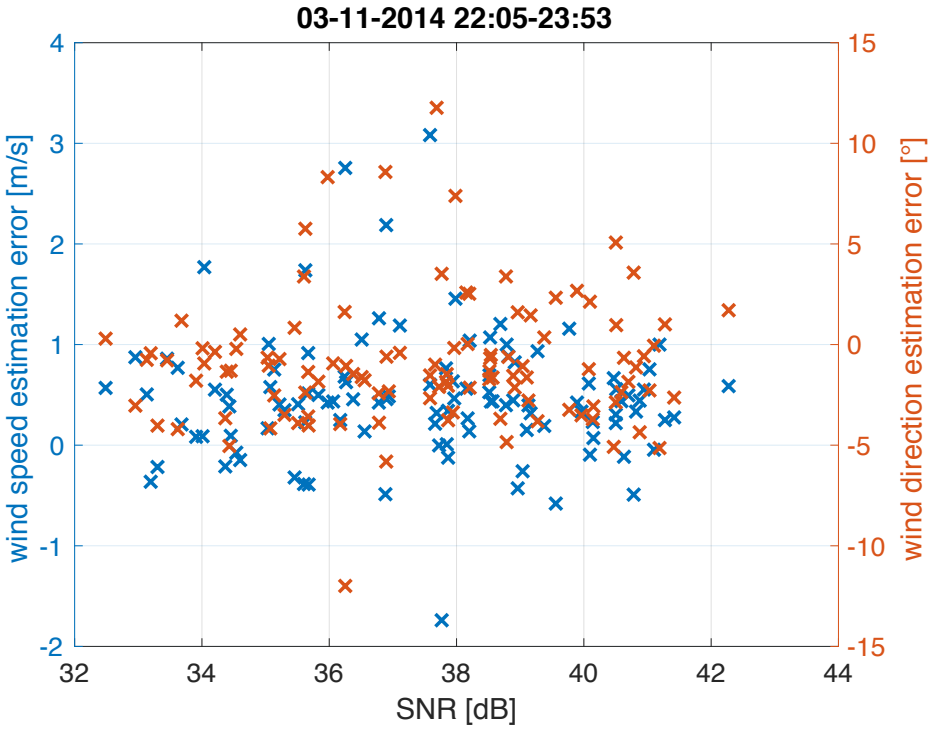

Figure 4.6: This figure shows a scatter plot for the 3.11.2014 relating the SNR to wind speed and direction estimation errors.

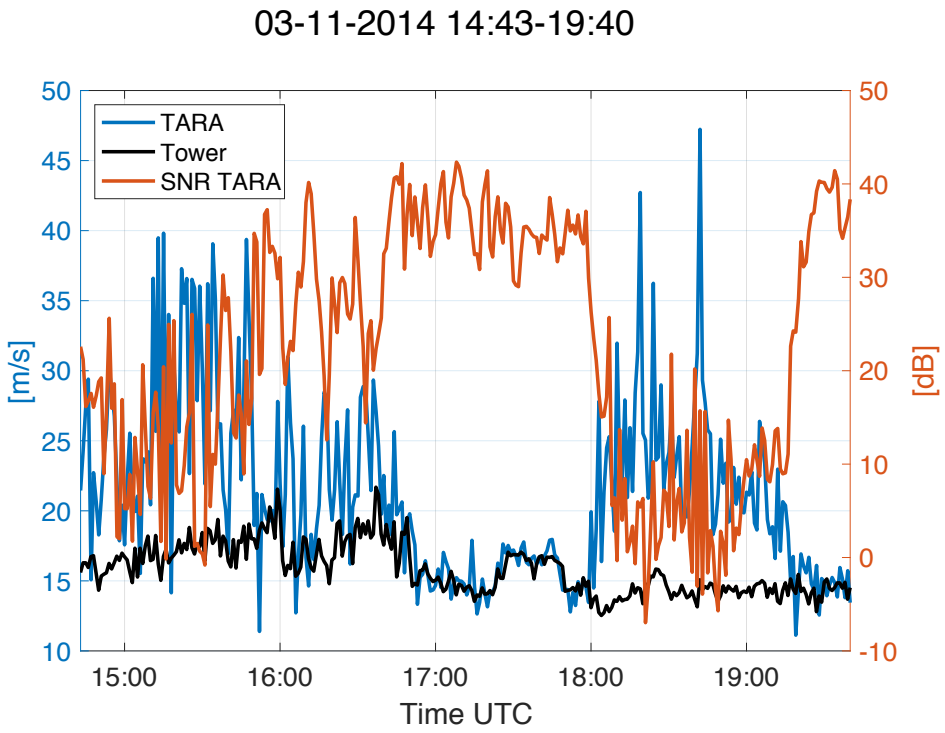

Figure 4.7: This figure shows a plot of the time series for the second case study on the 3.11.2014. The blue line shows the wind estimate of TARA and the black line the wind speed measured by the tower. In the same plot the SNR is shown with the scale on the right side of the plot in dB.

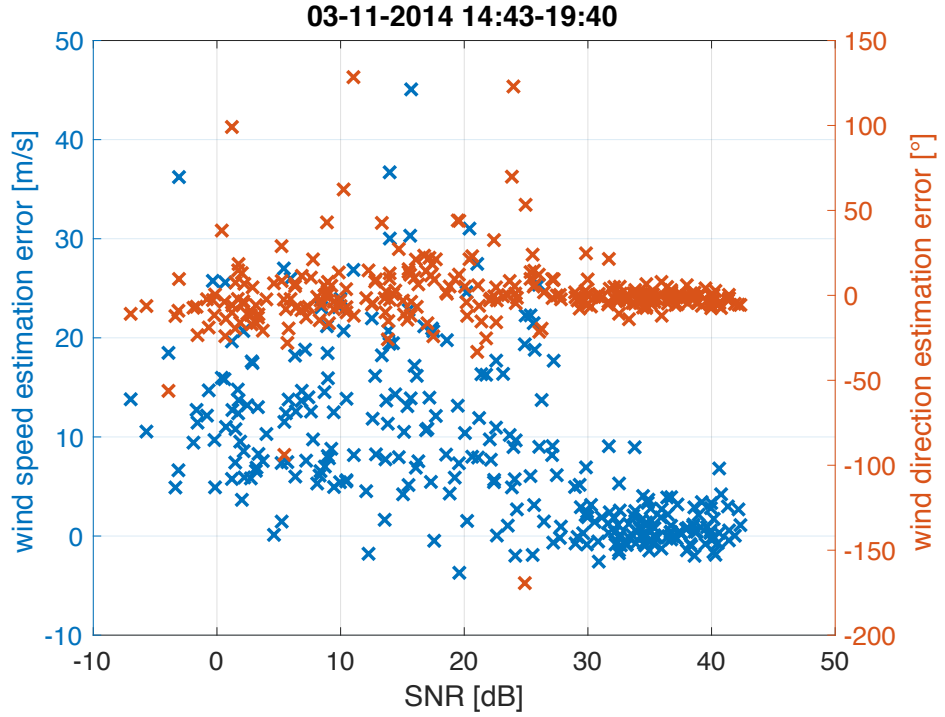

Figure 4.8: This figure shows a scatter plot for the 3.11.2014 relating the SNR to wind speed and direction estimation errors.

4.3. Re-estimation Wind Using Averaged Mean Doppler Velocities

To increase the SNR, averaging can be carried out. There are two ways of averaging that can be performed. Either the wind estimates can directly be averaged or the mean Doppler velocities can be averaged first and the wind estimated using the averaged Doppler velocities.

Because of the non-linearity of the equations of the wind speed and direction estimation, these two averaging procedures will lead to different results at low SNR. This different outcomes are discussed in this section. However in a first subsection the time series of the mean Doppler velocities for the three case studies will be presented.

4.3.1. Mean Doppler Velocities for All Case Studies

As mentioned above the averaged mean Doppler velocities for the three beams will be used to re-estimate the wind for TARA. The three time series considered are shown below in Figures 4.9, 4.10 and 4.11. The figures contain two parts. The top plot shows the time series of the wind speed and the bottom part shows the mean Doppler velocities averaged over a time interval of one minute. One important fact that can be seen in the three figures is that the the accuracy of the wind estimation seems to be related to the variability of the mean Doppler velocities for the three beams.

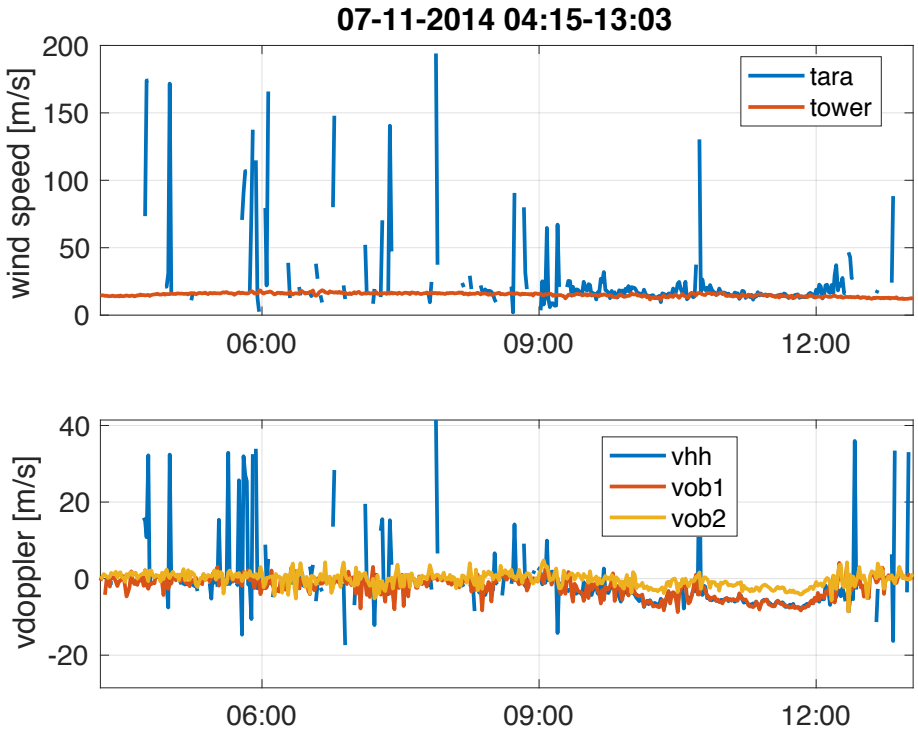

Figure 4.9: This figure shows the time series recorded on 7.11.2014 during ACCEPT-campaign. The top plot shows the wind speed of the tower and TARA and the bottom plot shows the time series of the mean Doppler velocities for all three beams of TARA. Vhh stands for main beam mean Doppler velocity, Vob1 corresponds to offset beam 1 and vob2 to offset beam 2.

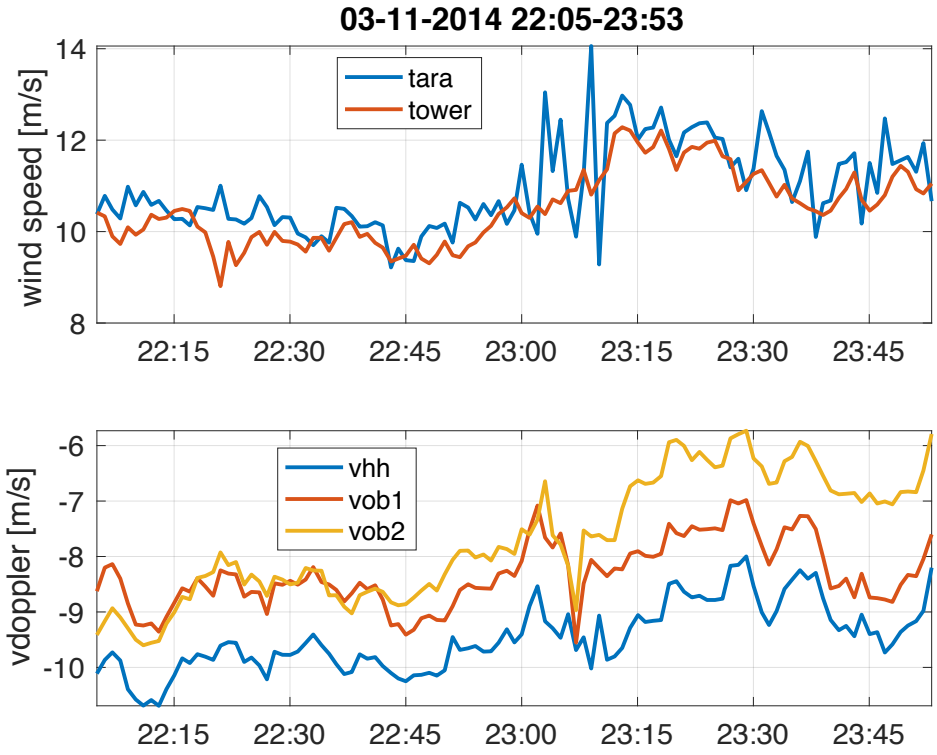

Figure 4.10: This figure shows the time series recorded on 3.11.2014 during ACCEPT-campaign. The top plot shows the wind speed of the tower and TARA and the bottom plot shows the time series of the mean Doppler velocities for all three beams of TARA. Vhh stands for main beam mean Doppler velocity, Vob1 corresponds to offset beam 1 and vob2 to offset beam 2.

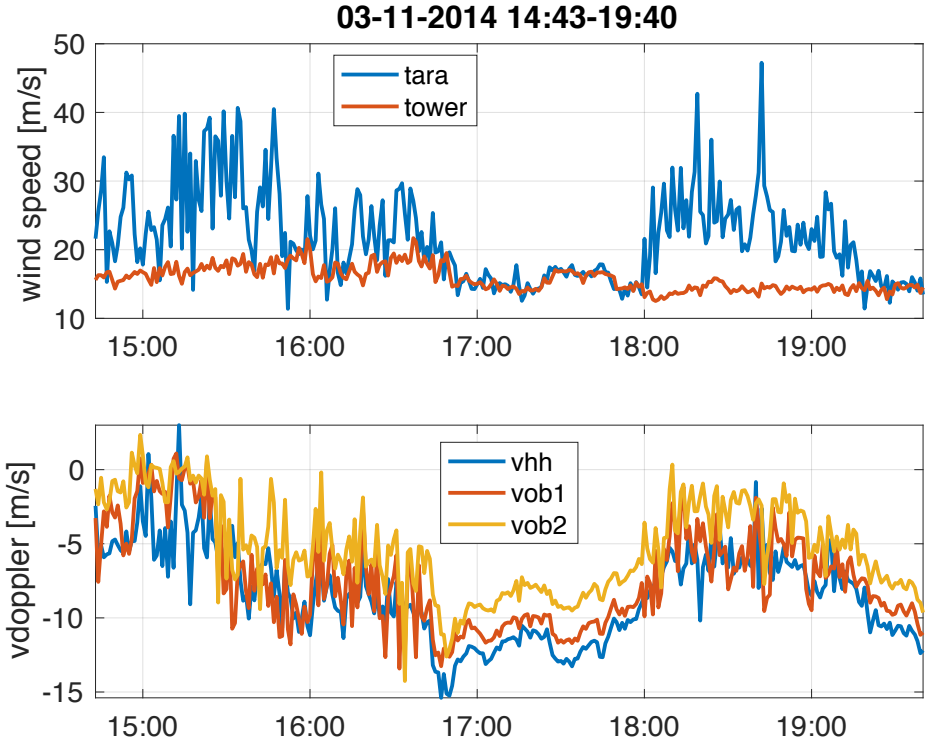

Figure 4.11: This figure shows the time series recorded on 3.11.2014 during ACCEPT-campaign. The top plot shows the wind speed of the tower and TARA and the bottom plot shows the time series of the mean Doppler velocities for all three beams of TARA. Vhh stands for main beam mean Doppler velocity, V_{OB1} corresponds to offset beam 1 and V_{OB2} to offset beam 2.

4.3.2. Results of the Re-estimation

As mentioned above the wind was re-estimated using the one minute averaged mean Doppler for the three beams. The results differ for the three case studies and the exact numbers can be found in Table 4.1 below.

For the 7.11.2014 (see Figure 4.12) the re-estimation resulted in some large outliers being removed while others with values up to 200 m/s remained. This can also be seen in the histograms presented in Figure 4.13. For the 3.11.2014 one case showed almost no differences between the averaged wind estimates compared to the re-estimation using the averaged mean Doppler velocities which was the case study of rain (see Figure 4.14). The histograms presented in Figure 4.15 also show that there were only small changes in the distribution of the wind speed and direction estimation errors. For the last case study (see Figure 4.16) the wind speed estimation seems to be more close to the tower observations, but the variation are still large. For the wind direction the errors seem not to have changed a lot. These changes can also be seen in the histograms in Figure 4.17. The spread of the wind speed estimation error has moved from more positive errors to a distribution more centred around zero, while the wind direction error distribution only slightly shifted to more negative values.

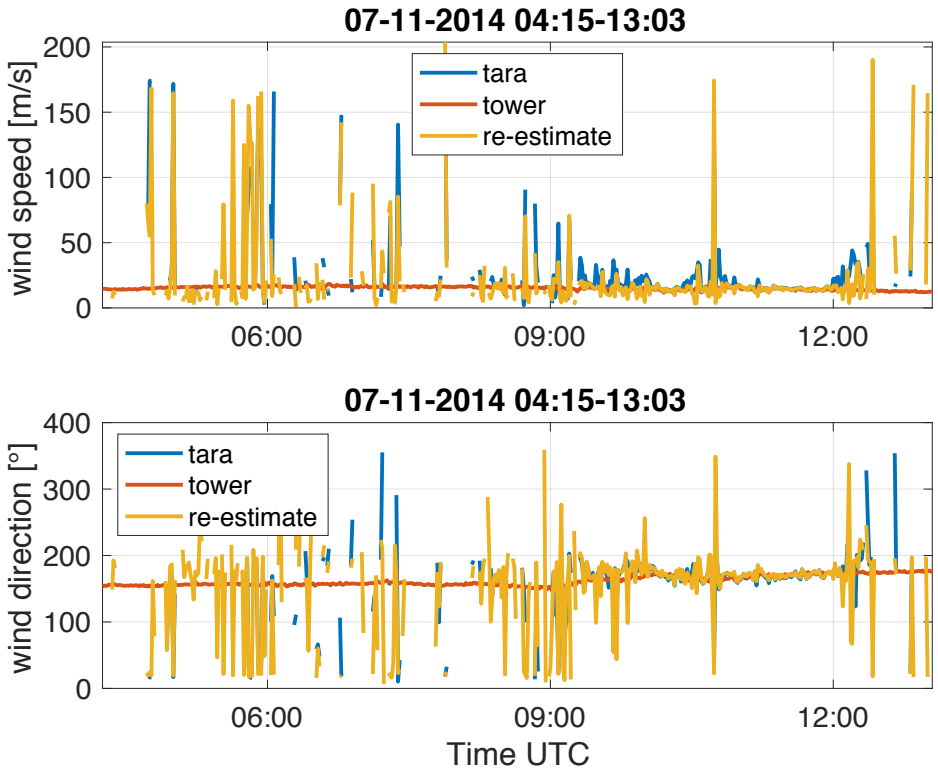

Figure 4.12: This figure shows the results of re-estimating the wind speed and direction using the averaged mean Doppler velocities of the three beams averaged over one minute.

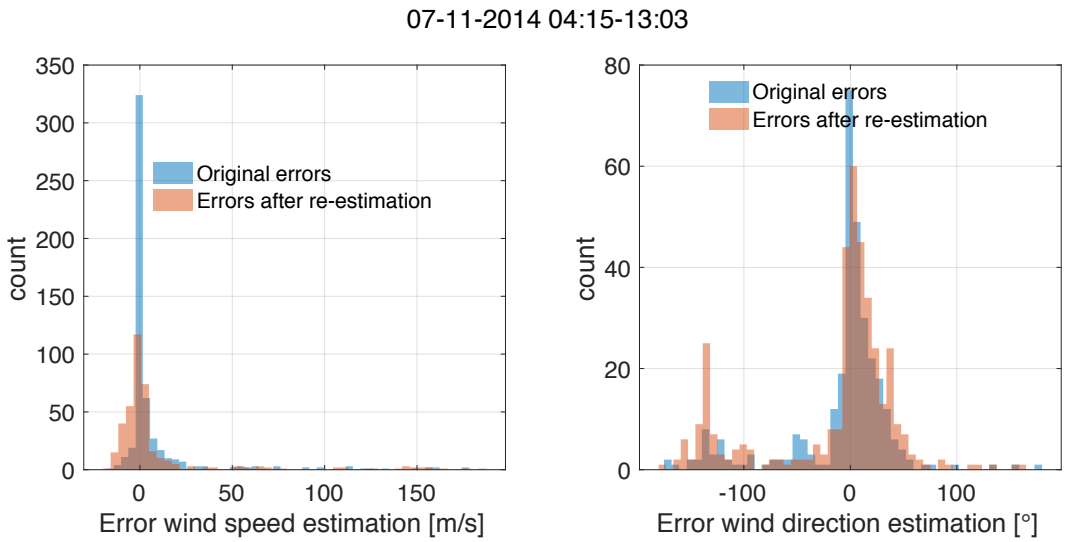

Figure 4.13: This figure shows two histograms for the 7.11.2014. The left side shows the distribution of the errors in wind speed estimation before and after re-estimating the wind with the averaged mean Doppler velocities. The right side shows the same but for the wind direction.

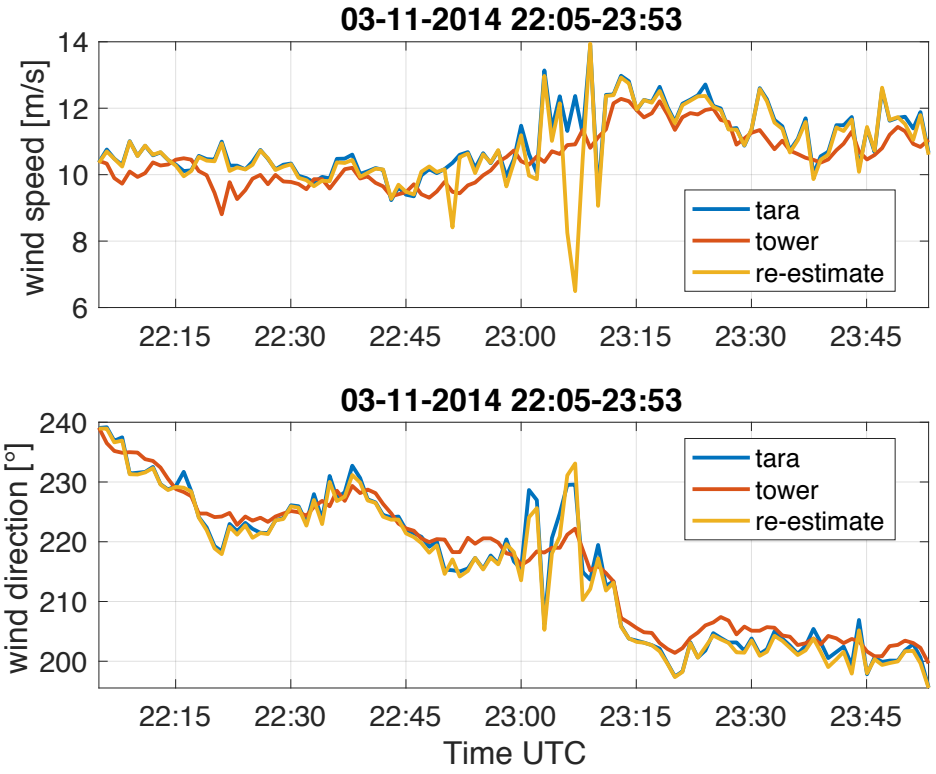

Figure 4.14: This figure shows the results of re-estimating the wind speed and direction using the averaged mean Doppler velocities of the three beams averaged over one minute.

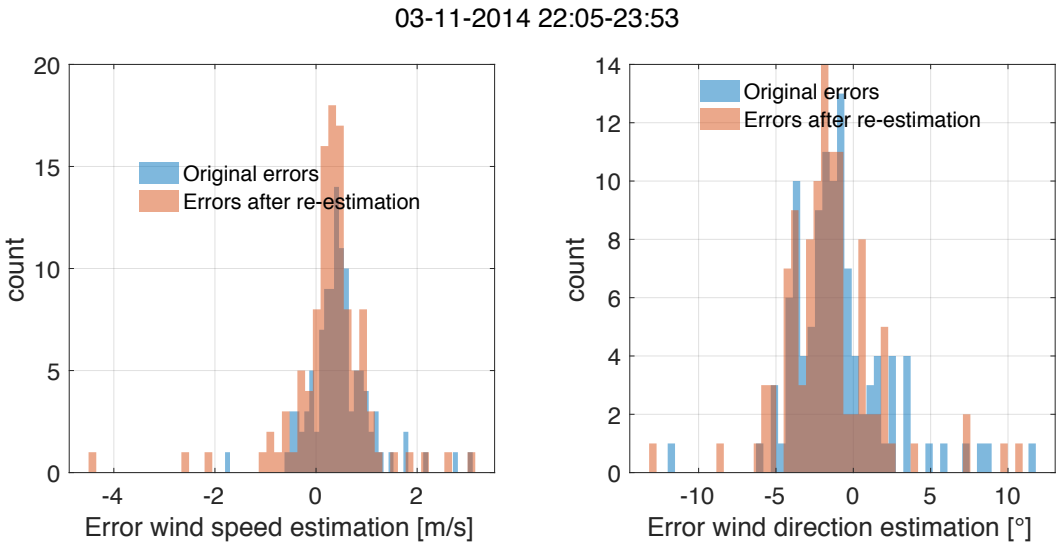

Figure 4.15: This figure shows two histograms for the 3.11.2014. The left side shows the distribution of the errors in wind speed estimation before and after re-estimating the wind with the averaged mean Doppler velocities. The right side shows the same but for the wind direction.

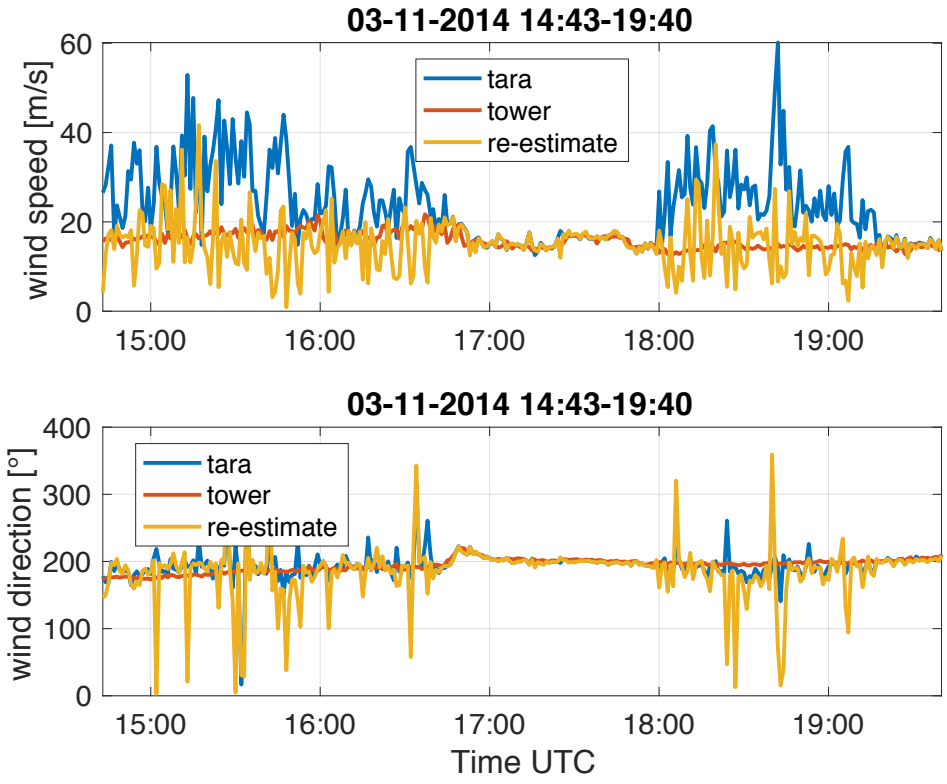

Figure 4.16: This figure shows the results of re-estimating the wind speed and direction using the averaged mean Doppler velocities of the three beams averaged over one minute.

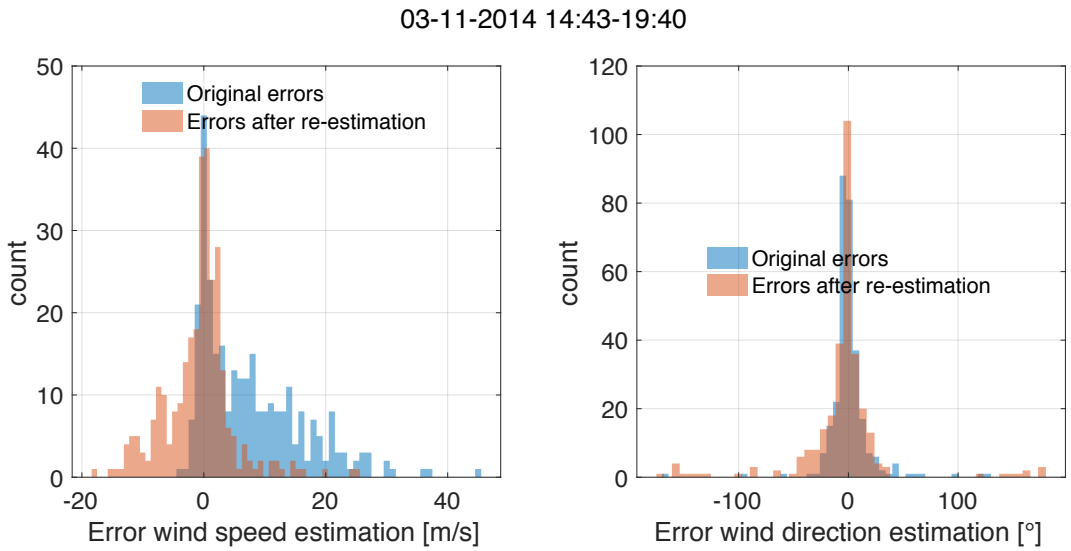

Figure 4.17: This figure shows two histograms for the 3.11.2014. The left side shows the distribution of the errors in wind speed estimation before and after re-estimating the wind with the averaged mean Doppler velocities. The right side shows the same but for the wind direction.

Looking at Table 4.1 the result which can be observed in the three Figures 4.12, 4.14 and 4.16 are quantified. While for the 7.11.2014 the RMSE for the wind speed and wind direction as well as the mean error in wind direction estimation actually increased due to the re-estimation. Only the mean error for the wind speed slightly decreased. For one of the case studies on the 3.11.2014 ([start_22.04.57], rain) the values remained almost the same. For the second one both RMSE as well as the mean error in wind speed decreased and only the mean error in wind direction increased.

Table 4.1: The two tables below show the difference in RMSE and mean estimation error between the original time series averaged at 1 minute and the re-estimated wind speed and direction using the mean Doppler velocities that were averaged at one minute.

original		rmse		mean error	
		wind speed [m/s]	wind direction [°]	wind speed [m/s]	wind direction [°]
07.11.14	[start_04.14.40]	35.1	49.8	13.4	-7.7
03.11.14	[start_22.04.57]	0.8	3.3	0.5	-1.0
03.11.14	[start_14.42.28]	11.3	20.9	7.6	0.6

re-estimate		rmse		mean error	
		wind speed [m/s]	wind direction [°]	wind speed [m/s]	wind direction [°]
07.11.14	[start_04.14.40]	35.2	63.6	8.9	-14.3
03.11.14	[start_22.04.57]	0.9	3.5	0.3	-1.5
03.11.14	[start_14.42.28]	5.8	42.6	-0.7	-4.6

To conclude, while for some case studies the averaging of the mean Doppler velocities and re-estimating the wind might actually improve the results, other cases need another solution. In particular, as shown by the results when only considering the wind estimation during precipitation (identified by melting layer presence) in the previous section, it is important to find a way of effectively removing the unusable data while keeping as much as possible the usable data. To ensure that later on also the vertical profiles of the horizontal wind estimation done by TARA can be used, a method based only on properties of TARA-data needs to be developed.

As mentioned before there seems to be a relationship between the variability of the mean Doppler velocities of three beams and the accuracy of the wind estimate. In order to explore this possibility, the correlation of the mean Doppler velocities are considered in the next section.

4.4. Covariance and Correlation for Clear Air Removal

This and the following section will introduce other techniques than the methods based on the SNR or the presence of the melting layer (see Chapter 3) that are investigated to remove wind estimation during clear air measurements.

With the use of matlab functions cov, corrcov, the correlation as well as the covariance matrix for the mean Doppler velocities of the three beams was calculated using averaging periods of one minute. This averaging period was performed to compare the filtering results with the time series of the tower as well as to make sure that there is enough data considered. The 1-minute averaging was chosen instead of 10-minutes because there would be a lot of variability smoothed out when using 10-minute averages. With a measurement per 3 seconds, the 1-minute averaging will include approx. 20 measurements. Figures 4.18, 4.19 and 4.20 show the three case studies so far.

In the title of the three figures, the overall correlations for the complete time series are found. A summary of the values are found in Table 4.2. The case on the 7.11.2014 is presented in Figure 4.18. While the overall correlation is low, the correlation for the time between 11:00 and 12:00 is close to 1. The cases on the 3.11.2014 are presented in Figures 4.19 and 4.20. Both cases show a value of close to 1 for the overall correlation of the time series.

Figure 4.18: This figure includes five plots of the same time series on the 7.11.2014. The top plot shows the wind speed estimate of TARA as well as the measurement of the tower. The second plot shows the 1-minute averaged mean Doppler velocities. The plot in the middle shows the variances over 1 minute for the mean Doppler velocities of the three beams. The fourth plot shows the covariance of the three beams. The last plot shows the correlations for the mean Doppler velocities between the three beams.

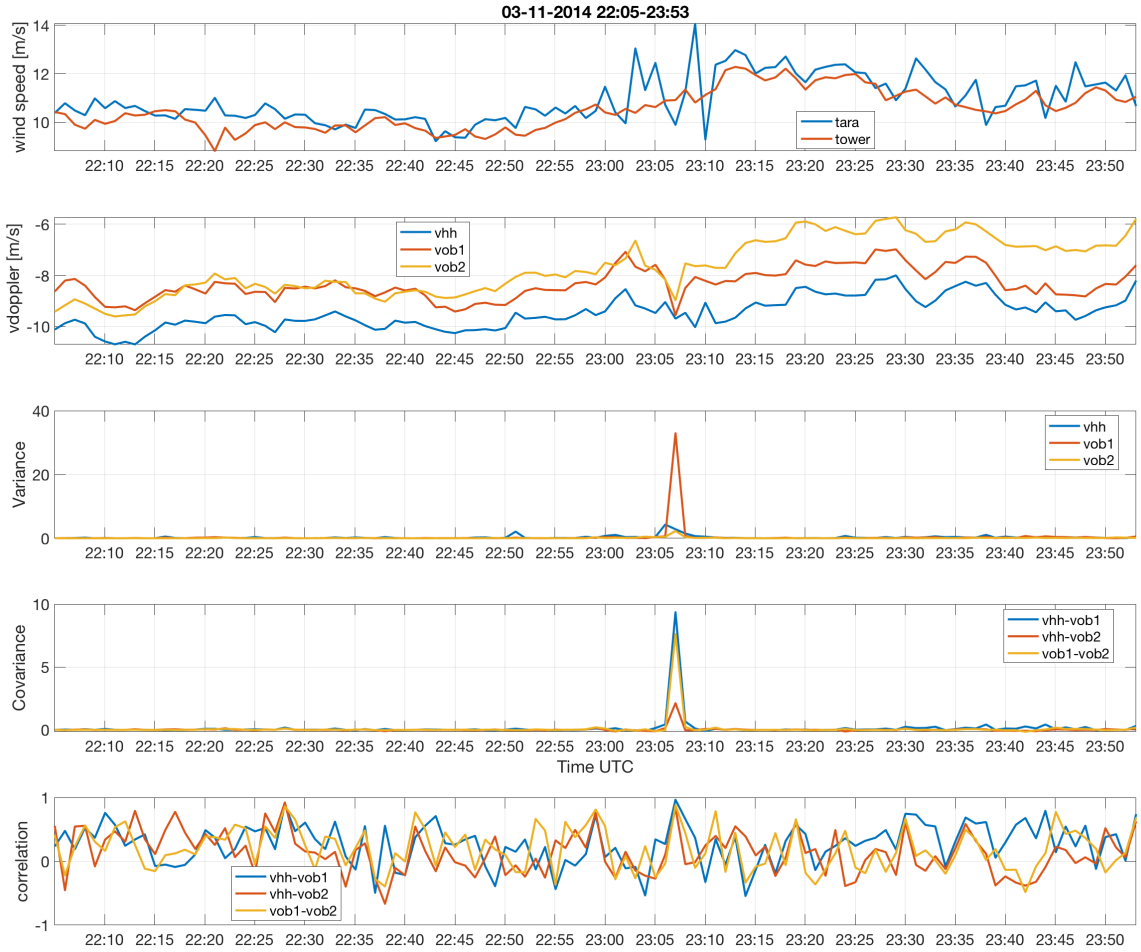

Figure 4.19: This figure includes five plots of the same time series on the 3.11.2014 during rain. The top plot shows the wind speed estimate of TARA as well as the measurement of the tower. The second plot shows the 1-minute averaged mean Doppler velocities. The plot in the middle shows the variances over 1 minute for the mean Doppler velocities of the three beams. The fourth plot shows the covariance of the three beams. The last plot shows the correlations for the mean Doppler velocities between the three beams.

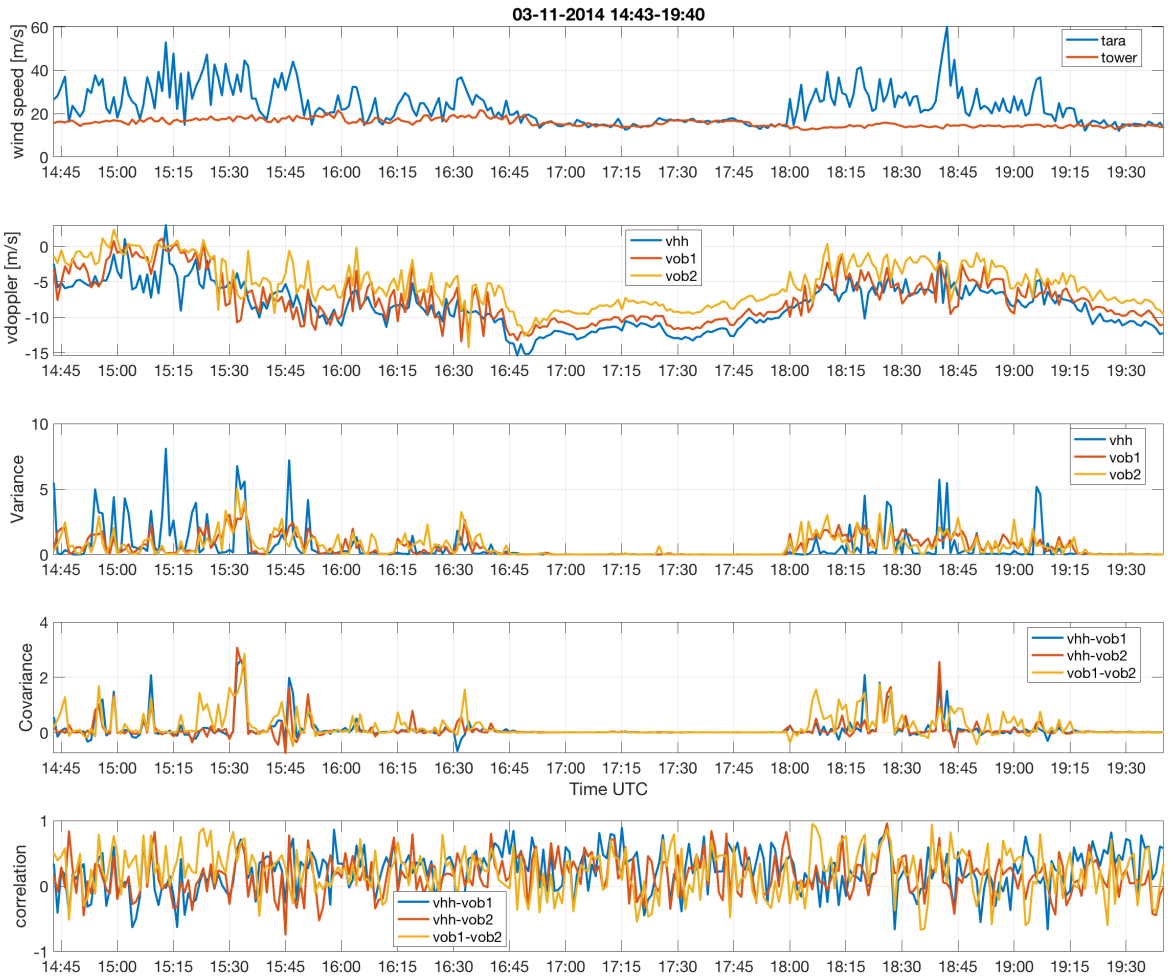

Figure 4.20: This figure includes five plots of the same time series on the 3.11.2014. The top plot shows the wind speed estimate of TARA as well as the measurement of the tower. The second plot shows the 1-minute averaged mean Doppler velocities. The plot in the middle shows the variances over 1 minute for the mean Doppler velocities of the three beams. The fourth plot shows the covariance of the three beams. The last plot shows the correlations for the mean Doppler velocities between the three beams.

As can be seen from the high variability of the correlation coefficients when looking at the Figures for all three case studies (Figures 4.18, 4.19 and 4.20), using only one minute of data for the correlation is not possible. At this time resolution the correlation seems to vary randomly. This was not expected to happen when the wind estimation is good. When only selecting the time period of the wind estimation for the calculation of the correlation, the values are close to one (see Table 4.2 for detailed numbers). This can be seen for all three case studies. But this is not always the case as was discovered when checking other cases. During stable conditions where the wind speed and direction remain relatively constant the variation and covariance will also be small. For such cases, although the wind estimates are accurate, the correlation will not be useful for the reason of how the correlation is calculated. It can be explained by looking at the definition of the correlation, R_{xy}, defined as the covariance of two variables, $cov(x, y)$, divided by the product of the two standard deviations σ_x and σ_y.

$$R_{xy} = \frac{cov(x,y)}{\sigma_x \sigma_y} \approx \frac{0}{0} \tag{4.1}$$

This problem can be seen in another time step on the 3.11.2014 not considered so far which is presented in Figure 4.21.

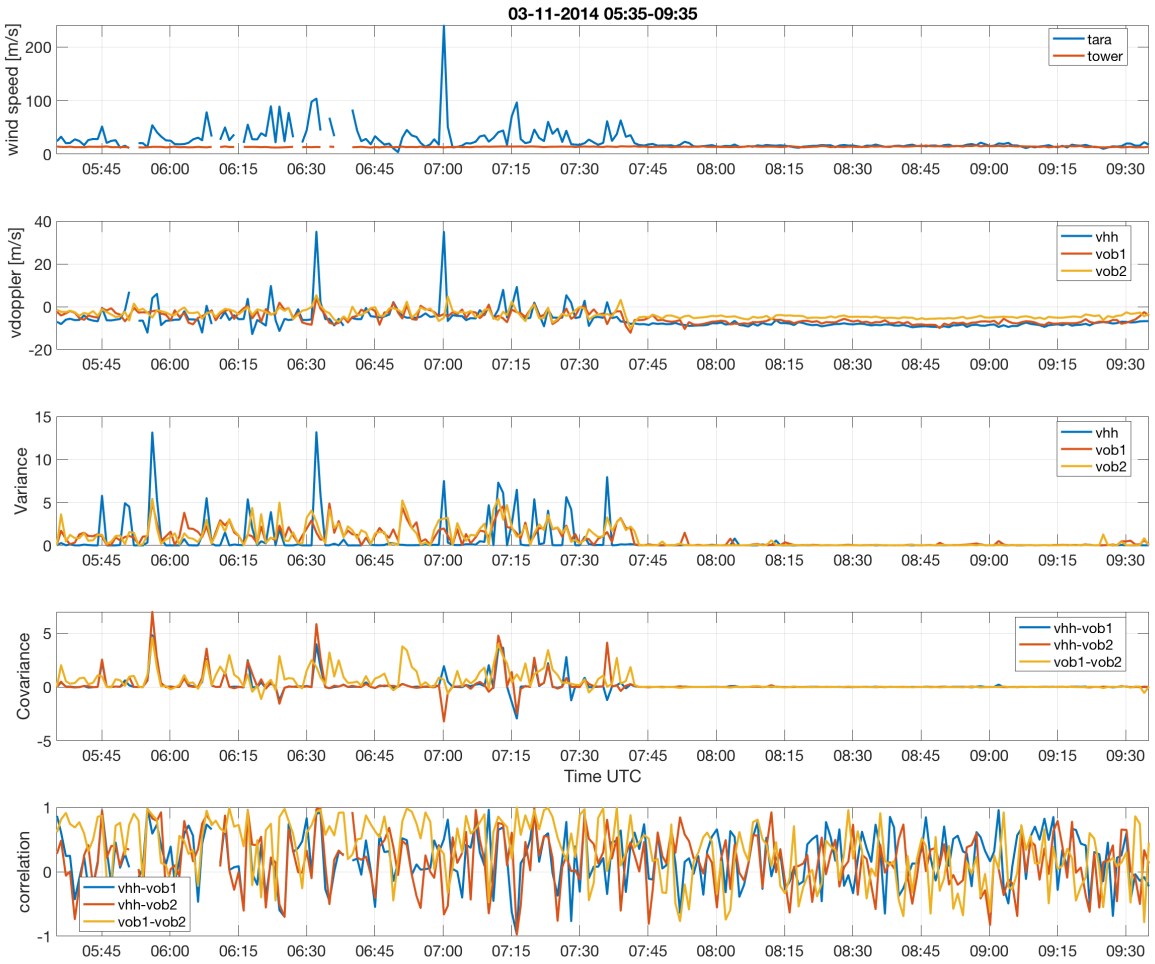

Figure 4.21: This figure includes five plots of the same time series on the 3.11.2014 for an additional time step to illustrate issues when using correlation for stable conditions. The top plot shows the wind speed estimate of TARA as well as the measurement of the tower. The second plot shows the 1-minute averaged mean Doppler velocities. The plot in the middle shows the variances over 1 minute for the mean Doppler velocities of the three beams. The fourth plot shows the covariance of the three beams. The last plot shows the correlations for the mean Doppler velocities between the three beams.

Table 4.2: This table shows the correlations for different time steps during the case studies. The results for the whole time series are in grey.

day	correlations	vhh - vob1	vhh - vob1	vob1 - vob2
07.11.14	04:15-13:03	0.4	0.3	0.7
	11:00 - 12:00	0.9	0.9	0.8
03.11.14	22:05-23:53	0.9	0.9	0.8
	14:43-19:40	0.8	0.8	0.9
	16:50 - 18:00	0.9	0.9	0.8
	05:35 - 09:35	0.5	0.4	0.7
	07:45 - 09:30	0.6	0.6	0.5

A disadvantage is that using a time period of 1 minute to calculate the correlation coefficients is not long enough. But the time span needed also depends on the case. To apply a data selection method based on the correlation of the mean Doppler velocities of the beam would need to be based on an adjustable time resolution to make sure that the best resolution is chosen. But in any case the time resolution will be relatively large to achieve good values for the correlation. Relatively large in this case

means from 30 minutes to up to several hours.

Another approach could be to use the value of the covariance or the variance. The problem with this approach is that this value is not normalized and thus the threshold would have to be determined for each case separately as well as a discussion on how much variance is allowed because there could also be a case with accurate wind estimates but high variability.

To conclude, the method of using variance or covariance is not very useful in selecting the accurate wind estimates at high time resolution which is needed for microphysical studies.

4.5. Coefficient of Variation

Because the correlation of the mean Doppler velocities for the three beams did not prove to be useful for the data selection, another approach was chosen. This was based on the fact that from looking at the time series comparing the wind speed and the mean Doppler velocities the variability seemed to be a good indicator of accurate wind estimation. Following this observation, as a next approach to the data selection it was chosen to normalize the standard deviation, σ, by the mean, μ, using a 1-minute averaging period.

$$C_V = \frac{\sigma}{\mu} [-] \tag{4.2}$$

This is also called the calculation of the coefficient of variation, C_V, which does not have a unit. This makes it possible to compare different cases and to apply the same threshold to all cases (Brown, 1998).

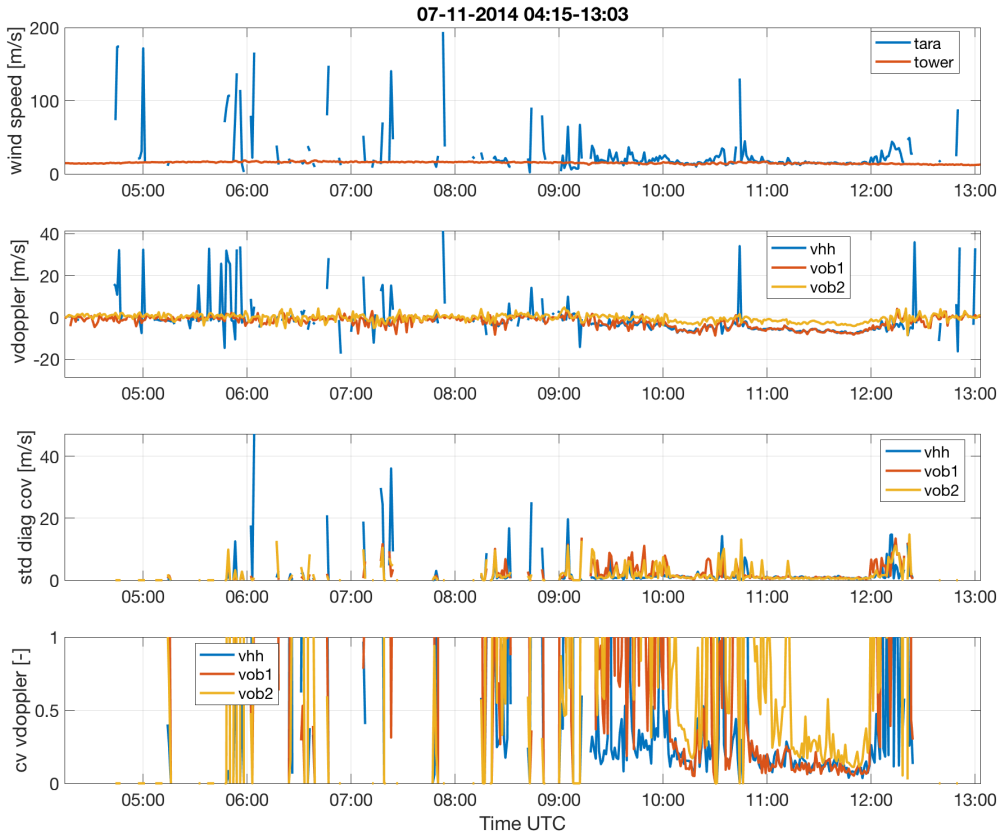

Figure 4.22: This figure includes five plots of the same time series. The top plot shows the wind speed estimate of TARA as well as the measurement of the tower. The second plot shows the 1-minute averaged mean Doppler velocities. The third plot shows the standard deviations over 1 minute for the mean Doppler velocities of the three beams. The last plot shows the coefficient of variation (standard deviation normalized by the mean) of the three beams. It was chosen to use the absolute value of the mean of the mean Doppler velocities because otherwise problems arise while using the mean value for the three beams which is required for the threshold definition.

Figures 4.22, 4.23 and 4.24 show the three case studies considered. In each figure five plots are shown. The top plot is the wind speed estimated by TARA compared to the tower measurements. It was chosen to only show the wind speed and not also the wind direction as both the variables show the same pattern of accuracy. The pattern is the same because both wind speed and direction are calculated using the same V and U. Due to the different ways of calculation, the error propagation is not the same (see Chapter 2.4.2). This equality of pattern of error means that it is therefore not necessary to show both wind speed and direction in both cases. The second plot shows the mean Doppler velocities of the three beams. The middle plot shows the standard deviation for the three beams. The bottom two plots show the coefficient of variation, first for all three beams and then the mean which will be used for the threshold application. While the mean values for the Doppler velocities are negative and that also means that there would be negative values for the coefficient of variation, it was chosen to use the absolute value. In addition there are problems in case the mean for the three beams would be used when there are negative and positive outliers of the same magnitude. When considering a mean in such a case, the coefficient of variation would become very low and using a threshold, wrong wind estimates would be kept. However, for the final data selection using the coefficient of variation, it was decided to use the maximum value for the three beams. This ensures that all the values are below the threshold. Instead of using a negative and positive threshold, it was decided to use the absolute value for the maximum coefficient of variation with one positive threshold, because this leads to the same result.

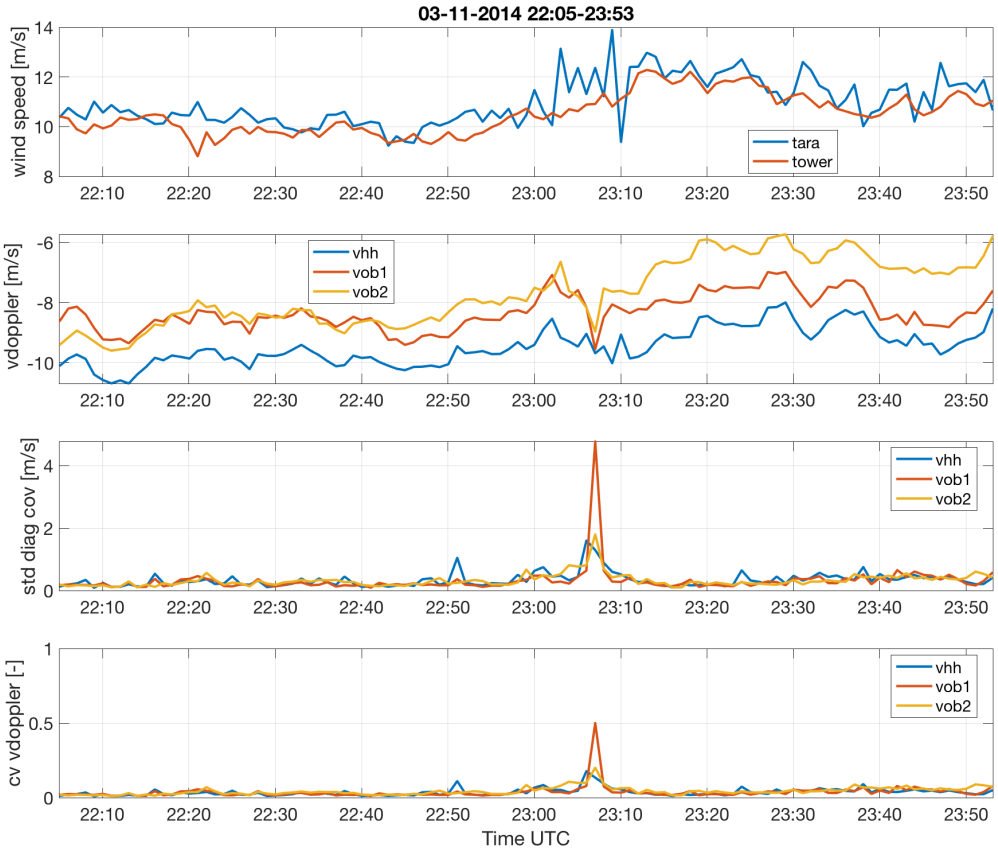

Figure 4.23: This figure includes five plots of the same time series. The top plot shows the wind speed estimate of TARA as well as the measurement of the tower. The second plot shows the 1-minute averaged mean Doppler velocities. The third plot shows the standard deviations over 1 minute for the mean Doppler velocities of the three beams. The last plot shows the coefficient of variation (std normalized by the mean) of the three beams. It was chosen to use the absolute value of the mean of the mean Doppler velocities because otherwise problems arise while using the mean value for the three beams which is required for the threshold definition.

Comparing the three figures shows that the low values (below 1) do correspond with the accurate wind speed estimation in all cases. In contrast to the results of the covariance, variance and correlation calculations, for the coefficient of variation, this relation is also visible using a time resolution of 1 minute.

However, now a threshold to be applied needs to be chosen. The method to chose this threshold is in an iterative process of lowering the limit of the threshold until the maximum of the wind estimation error is below a certain value. This is applied to all usable cases during ACCEPT-campaign and then the results are checked again using the mean value for all thresholds found in the first step. This approach will be discussed in detail in the next subsection.

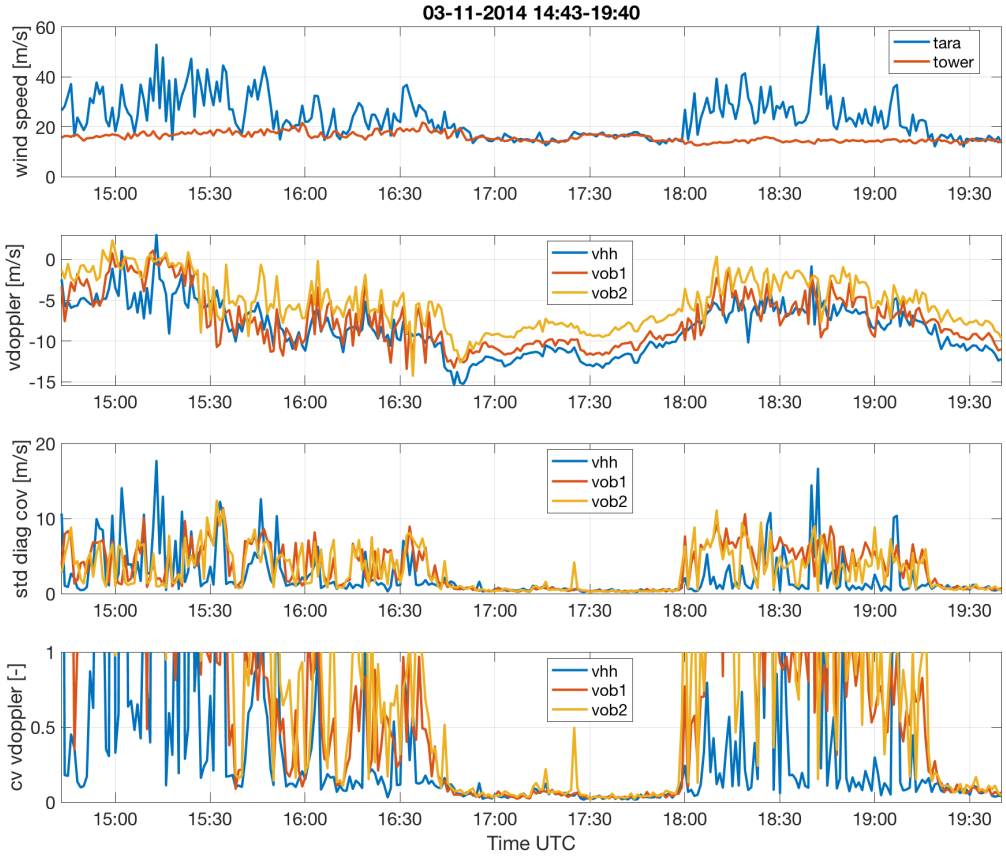

Figure 4.24: This figure includes five plots of the same time series. The top plot shows the wind speed estimate of TARA as well as the measurement of the tower. The second plot shows the 1-minute averaged mean Doppler velocities. The third plot shows the standard deviations over 1 minute for the mean Doppler velocities of the three beams. The last plot shows the coefficient of variation (std normalized by the mean) of the three beams. It was chosen to use the absolute value of the mean of the mean Doppler velocities because otherwise problems arise while using the mean value for the three beams which is required for the threshold definition.

4.5.1. Threshold Coefficient of Variation

As mentioned above, when looking at the time series of the three case studies, the coefficient of variation seems to be a promising criteria of selection of usable data which is only based on TARA and the application is possible at a 1-minute time averaging interval.

To define what threshold should be applied, a mean value for the usable cases of the ACCEPT-campaign was defined. This was done in an iterative procedure, that includes a check of maximum error in the time series in every iteration. If the maximum is above a certain value, the threshold in coefficient of variation is lowered until the maximum error is below a certain value. This was done for the wind speed and direction error separately. For the wind speed the maximum errors used were 2, 5, 10 and 15 m/s while for the direction 5, 10, 15 and 20° were chosen. The maximum threshold for the coefficient of variation is chosen at 1, because this is the limit of large where the standard deviation becomes larger than the mean value of the wind speed. It was also chosen to apply the threshold on the maximum of the three coefficient of variation values instead of the mean, because this ensures that the values for all three beams are below the threshold. This threshold was iteratively lowered, checking the maximum in wind speed or direction error for each iteration.

Figures 4.25 and 4.26 show the mean values for the usable cases of the whole ACCEPT-campaign.

The detailed results for the mean values shown in Figures 4.25 and 4.26 can be found in Appendix B.

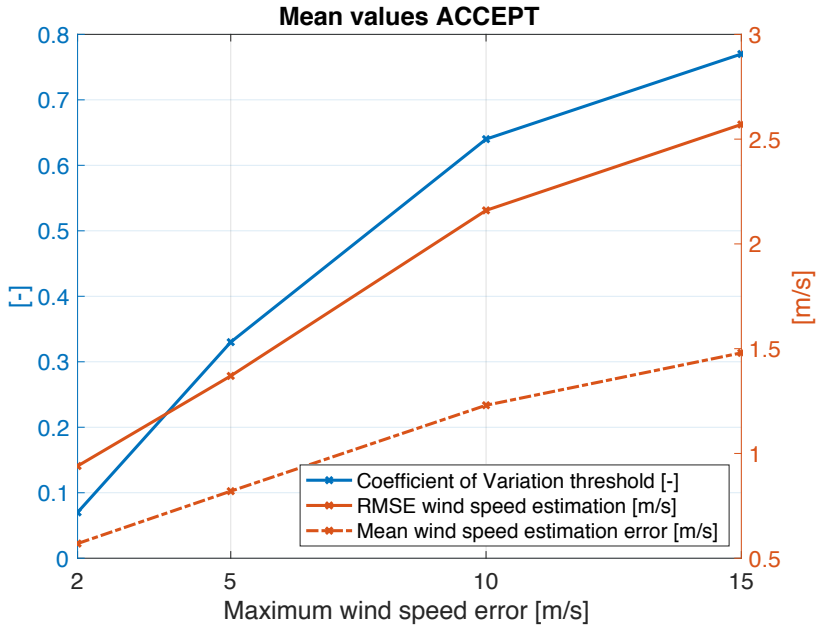

Figure 4.25: This figure shows the effect of using different maximum wind speed estimation errors on the selection of the coefficient of variation threshold in form of a mean value for all the usable cases during the ACCEPT-campaign.

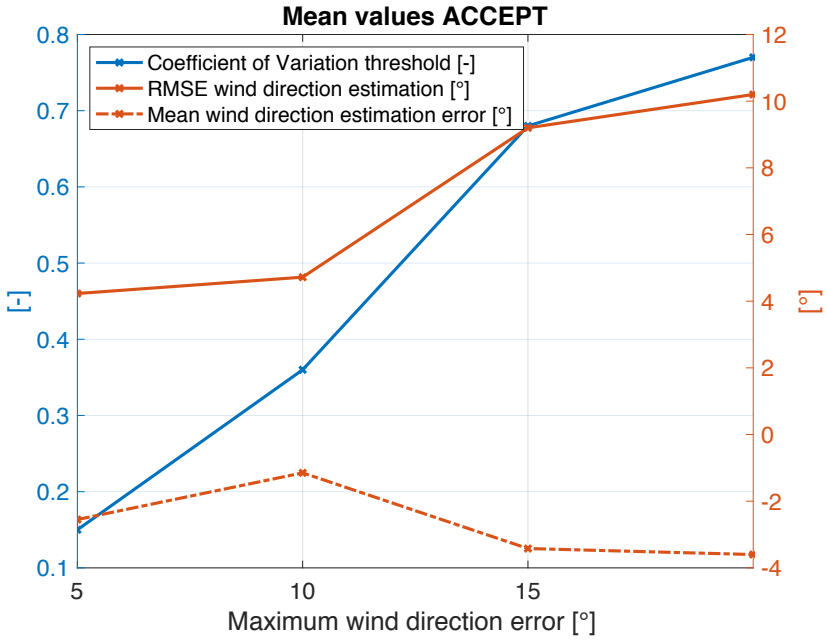

Figure 4.26: This figure shows the effect of using different maximum wind direction estimation errors on the selection of the coefficient of variation threshold in form of a mean value for all the usable cases during the ACCEPT-campaign.

For the wind speed, the RMSE and mean error are below 2 m/s with the maximum wind speed error of 5 m/s. For the wind direction it can be seen that already with a maximum of 15° wind direction error the RMSE and mean direction estimation errors are below 10°. However, the threshold in coefficient of variation is 0.33 for the wind speed and 0.67 for the wind direction using 5 m/s and 15° for the maximum errors as a cut-off in the iterative process of coefficient of variation threshold retrieval. This is the reason

why a maximum direction error of 10° was chosen. As can be seen in Figure 4.26, the threshold in this case is 0.36, which is closer to the one for the wind speed. This decision of using a maximum wind direction error based on a threshold of coefficient closer to the one of the wind speed is reasonable because the two components are closely related, but have a different error propagation. The iterative way of deriving the coefficient of variation threshold was then repeated using both the maximum error of wind speed and direction in combination to define mean values taking into account both wind speed and direction. This is done to ensure that both wind speed and direction maximum estimation error are considered. The results of this are summarized in Tables 4.3 and 4.4. The results for all cases used to define the mean threshold can be found in Appendix B.

So far, the focus was on the mean values obtained considering all the usable cases of the ACCEPT-campaign. Table 4.3 shows a summary of the results for each case study comparing the original results to the filtering using a coefficient of variation threshold on the three case studies. Each sub-table includes the RMSE and mean error for wind speed and direction error. The first sub-table shows the original values calculated including all data for the three case studies. The middle two tables show the results when either applying a maximum wind speed error or maximum wind direction error for the iterative definition of the threshold for the coefficient of variation. The last table shows the results of defining the threshold for the coefficient of variation using both a a maximum wind speed and direction error.

From the sub-tables it can be seen that all ways of defining the threshold improve the results for the cases on 7.11.2014 and on the 3.11.2014 [start_14.42.28]. The rain case on the 3.11.2014 [start_22.04.57] shows also small improvements when applying a maximum error in wind speed as well as a maximum wind direction error. The definition of the threshold based on both the maximum error in wind speed and direction ensures that the lowest threshold is used that is needed to ensure that both components are below a maximum error defined. As can be seen in the three sub-tables on the coefficient of variation selection, the combination leads to choosing the smallest of both thresholds.

Table 4.3: The four tables below show the difference in RMSE and mean estimation error between the original time series averaged at 1 minute and the application of the coefficient of variation thresholds to the 1-minute averaged mean Doppler velocities. The middle two tables show the results for applying the maximum wind speed and direction errors to determine the threshold in coefficient of variation iteratively. The last table shows the threshold results the combination of both maximum wind speed and direction estimation error.

original		rmse		mean error	
		ws [m/s]	wd [°]	ws [m/s]	wd [°]
07.11.14	[start_04.14.40]	35.1	49.8	13.4	-7.7
03.11.14	[start_22.04.57]	0.8	3.3	0.5	-1.0
03.11.14	[start_14.42.28]	11.3	20.9	7.6	0.6

cv threshold defined by max 5 m/s ws error		rmse		mean error		lim coeff of variation
		ws [m/s]	wd [°]	ws [m/s]	wd [°]	
07.11.14	[start_04.14.40]	1.3	4.9	0.6	-0.3	0.9
03.11.14	[start_22.04.57]	0.8	3.3	0.5	-1.0	1
03.11.14	[start_14.42.28]	1.6	3.5	0.6	-1.8	0.3

cv threshold defined by max 10° wd error		rmse		mean error		lim coeff of variation
		ws [m/s]	wd [°]	ws [m/s]	wd [°]	
07.11.14	[start_04.14.40]	1.3	4.6	0.6	-0.7	0.75
03.11.14	[start_22.04.57]	0.5	2.6	0.4	-1.4	0.05
03.11.14	[start_14.42.28]	1.7	3.9	0.7	-1.7	0.5

coefficient of variation combination ws and wd		rmse		mean error		lim coeff of variation
		ws [m/s]	wd [°]	ws [m/s]	wd [°]	
07.11.14	[start_04.14.40]	1.3	4.6	0.6	-0.7	0.75
03.11.14	[start_22.04.57]	0.5	2.6	0.4	-1.4	0.05
03.11.14	[start_14.42.28]	1.6	3.5	0.6	-1.8	0.3

Using the mean of all usable cases (see Appendix B), the threshold for the coefficient of variation to be applied to the total campaign was found to be 0.22. This threshold will be applied to the wind speed and direction time series in the following subsections. The results are then compared when the maximum errors in wind speed and direction would be used for the case studies.

Table 4.4: shows the mean results for the whole ACCEPT-campaign using a combination of maximum wind speed or direction estimation error. Detailed results can be found in the Table in Appendix B.

combination	original rmse		lim	rmse		mean error	
5 m/s and 10°	ws [m/s]	wd [°]		ws [m/s]	wd [°]	ws [m/s]	wd [°]
mean	13.67	27.75	0.22	1.28	4.22	0.80	-1.52

4.5.2. Results Using Coefficient of Variation on Wind Speed

In the previous subsection a mean threshold for the coefficient of variation for the whole ACCEPT-campaign was found to be 0.22. This subsection contains a comparison of applying this general threshold to the three case studies and compare the results with choosing the threshold for each case study separately using a combination of maximum error in wind speed allowed of 5 m/s and direction 10°.

For the case study on the 7.11.2014 (see Figures 4.27 and 4.28) the difference in resulting mean wind speed estimation error is 0.3 m/s and 0.4 m/s for the RMSE of the wind speed estimation error while the difference for the threshold in coefficient applied is 0.53. For one case study on the 3.11.2014 (see Figures 4.29 and 4.30) there is a difference of 0.3 in the resulting RMSE and 0.1 for the mean error values and the difference in the threshold applied is 0.17. For the second case study on the 3.11.2014 (see Figures 4.31 and 4.32) there is a difference of 0.1 for RMSE and no difference for the mean error while the difference in threshold is 0.08. The results including the ones for the wind direction are found in detail in Table 4.3.

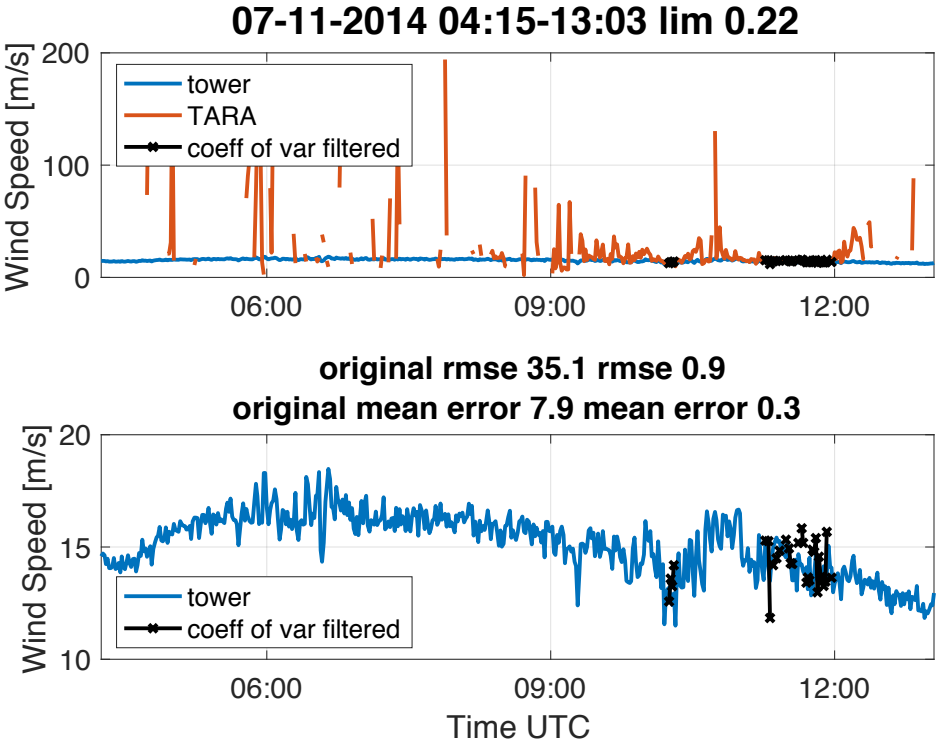

Figure 4.27: This figure shows the result of applying the total threshold in coefficient of variation of 0.22 on the wind speed time series of the 7.11.2014. The top plot shows all data for TARA while in the bottom plot only the data remaining after applying the threshold is presented to be able to look at the results at a more suitable scale.

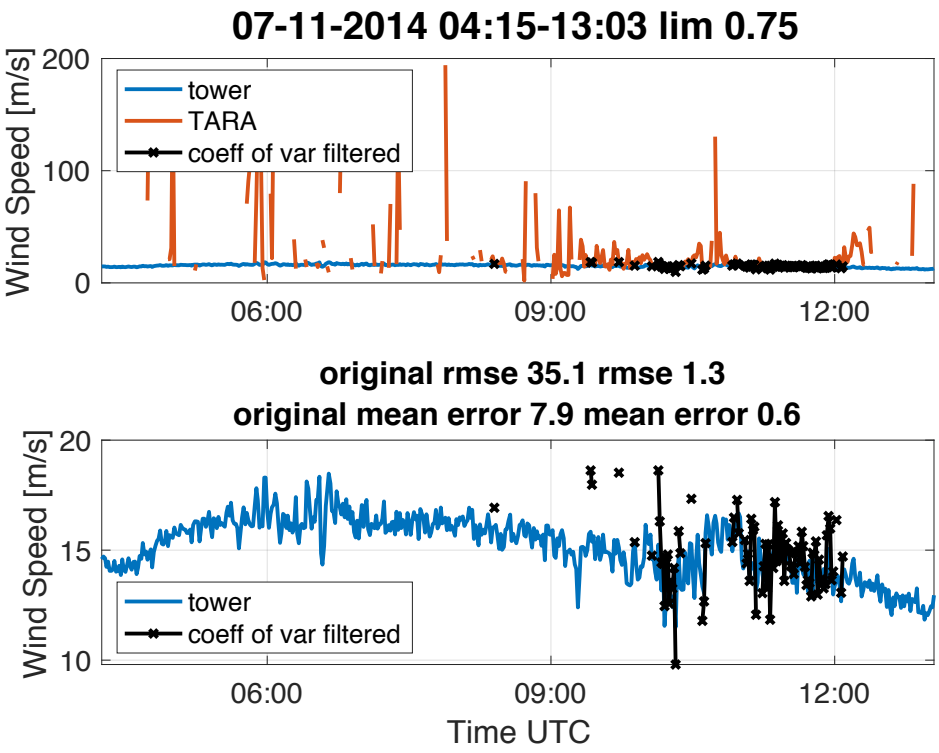

Figure 4.28: This figure shows the result of applying a maximum wind speed error of 5 m/s and maximumg wind direction error of 10° on the wind speed time series of the 7.11.2014. The top plot shows all data for TARA while in the bottom plot only the data remaining after applying the threshold is presented to be able to look at the results at a more suitable scale.

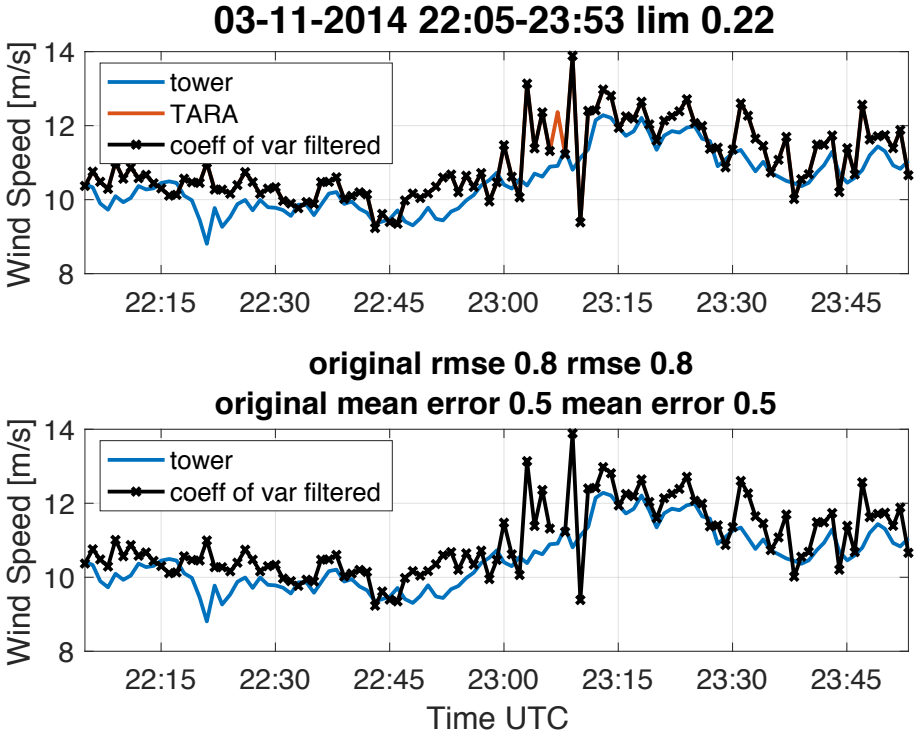

Figure 4.29: This figure shows the result of applying the mean total threshold in coefficient of variation of 0.22 on the wind speed time series of the 3.11.2014. The top plot shows all data for TARA while in the bottom plot only the data remaining after applying the threshold is presented to be able to look at the results at a more suitable scale.

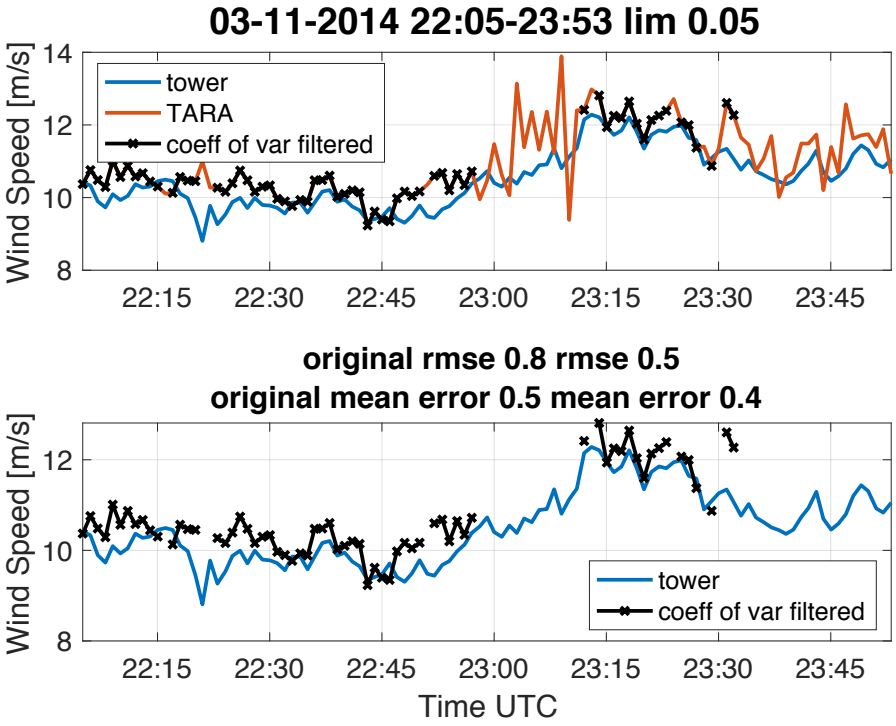

Figure 4.30: This figure shows the result of applying a maximum wind speed error of 5 m/s and a maximumg wind direction error of 10° on the time series of the 3.11.2014. The top plot shows all data for TARA while in the bottom plot only the data remaining after applying the threshold is presented to be able to look at the results at a more suitable scale.

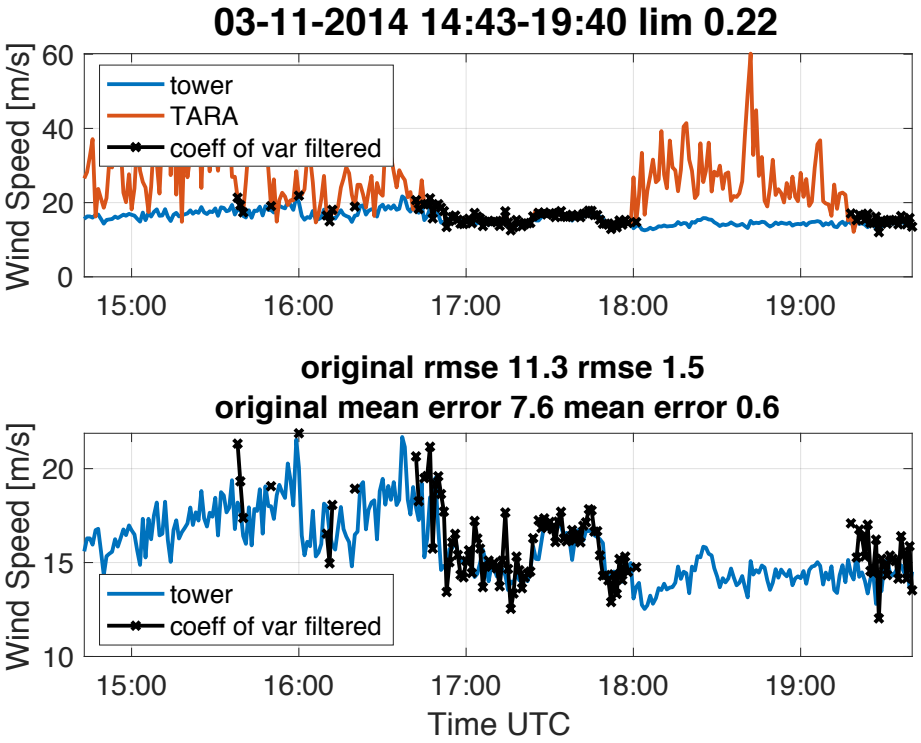

Figure 4.31: This figure shows the result of applying the mean total threshold of coefficient of variation of 0.22 on the time series of the 3.11.2014. The top plot shows all data for TARA while in the bottom plot only the data remaining after applying the threshold is presented to be able to look at the results at a more suitable scale.

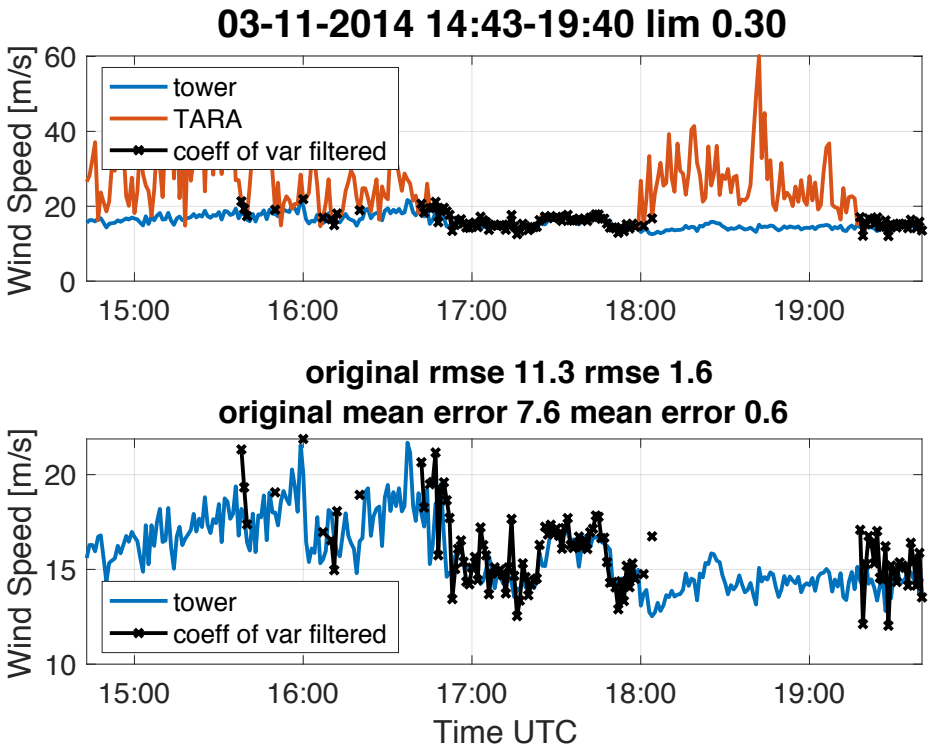

Figure 4.32: This figure shows the result of applying a maximum wind speed error of 5 m/s and maximum wind direction error of 10° on the time series of the 3.11.2014. The top plot shows all data for TARA while in the bottom plot only the data remaining after applying the threshold is presented to be able to look at the results at a more suitable scale.

4.5.3. Results Using Coefficient of Variation on Wind Direction

As found with the results of comparing the mean threshold for the usable cases during the ACCEPT-campaign, the same threshold for the coefficient of variation of 0.22 was also used for time series of the three case studies. The results are as expected following the wind speed results as these two components depend on the same variables U and V. A summary of the improvements in RMSE and mean estimation error for the wind speed and direction can be found in Table 4.3 in the next subsection.

While the errors and thus the data removed are expected to be removed at the same places as for the wind speed, the wind direction estimation errors will be different to the result from the wind speed. This is due to the fact that although wind speed and direction are calculated using the same data, the formulas and thus the error propagations will be different (see Subsection 2.4.2).

For the 7.11.2014, the difference in RMSE is 0.3° and the mean error is larger by 1.8° when using the mean threshold of 0.22 (see Figures 4.33 and 4.34). For the rain case on 3.11.2014 the RMSE is larger by 0.6° and the mean error smaller by 0.4° when using the mean threshold of 0.22 in coefficient of variation (see Figures 4.35 and 4.36). The second case on the 3.11.2014 shows no difference in RMSE and the mean error (see Figures 4.37 and 4.38) while the threshold is different by 0.08. Although some of the values have increased when using the mean value for the threshold in coefficient of variation compared to the one for the individual cases, the results are within the acceptable range of 5-10° wind direction error.

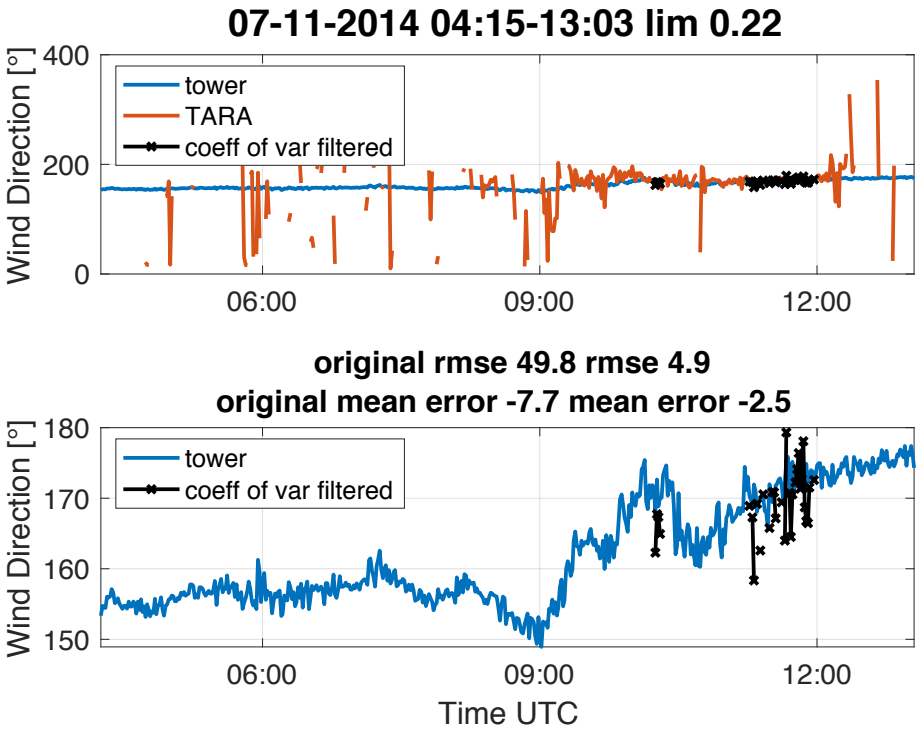

Figure 4.33: This figure shows the result of applying the mean total threshold in coefficient of variation of 0.22 on the wind direction time series of the 7.11.2014. The top plot shows all data for TARA while in the bottom plot only the data remaining after applying the threshold is presented to be able to look at the results at a more suitable scale.

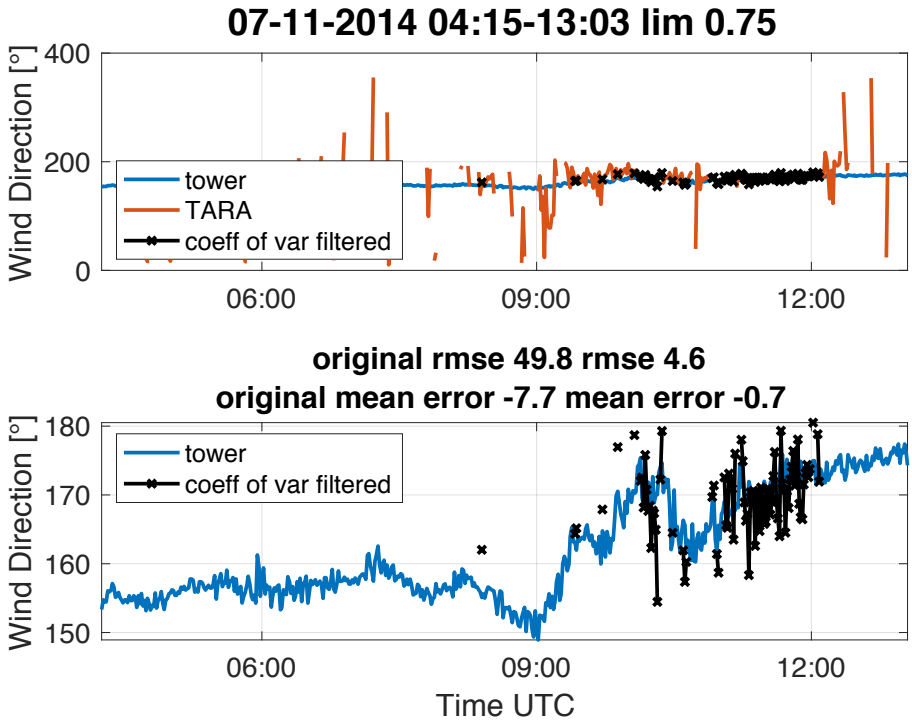

Figure 4.34: This figure shows the result of applying a maximum wind speed error of 5 m/s and maximum error in wind direction of 10° on the wind direction time series of the 7.11.2014. The top plot shows all data for TARA while in the bottom plot only the data remaining after applying the threshold is presented to be able to look at the results at a more suitable scale.

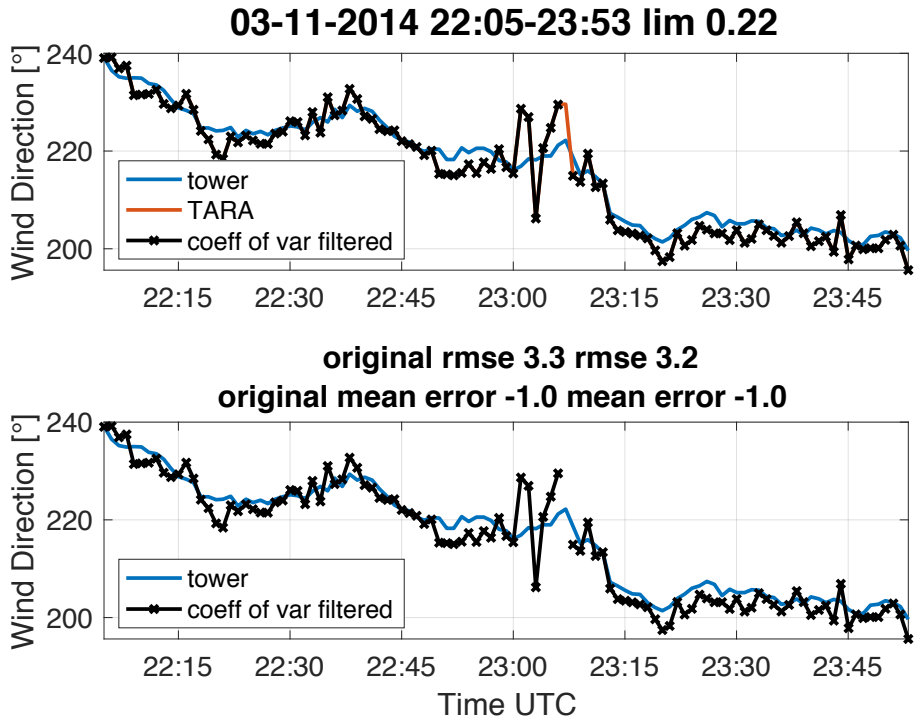

Figure 4.35: This figure shows the result of applying the mean total coefficient of variation threshold of 0.22 on the wind direction time series of the 3.11.2014. The top plot shows all data for TARA while in the bottom plot only the data remaining after applying the threshold is presented to be able to look at the results at a more suitable scale.

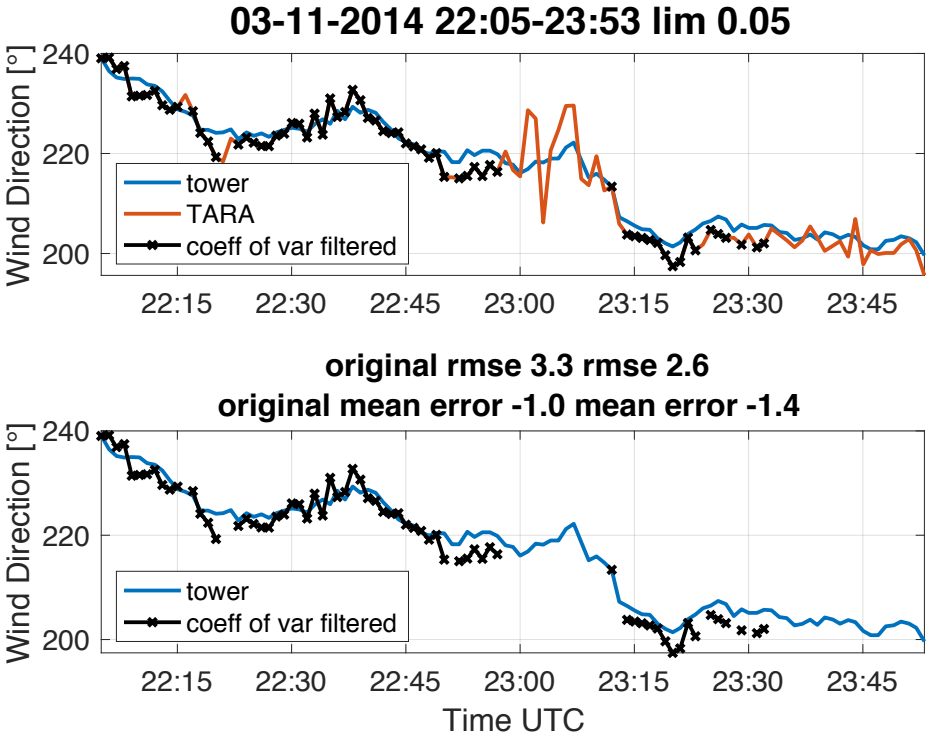

Figure 4.36: This figure shows the result of applying a maximum wind speed error of 5 m/s and maximum wind direction estimation error of 10° on the wind direction time series of the 3.11.2014. The top plot shows all data for TARA while in the bottom plot only the data remaining after applying the threshold is presented to be able to look at the results at a more suitable scale.

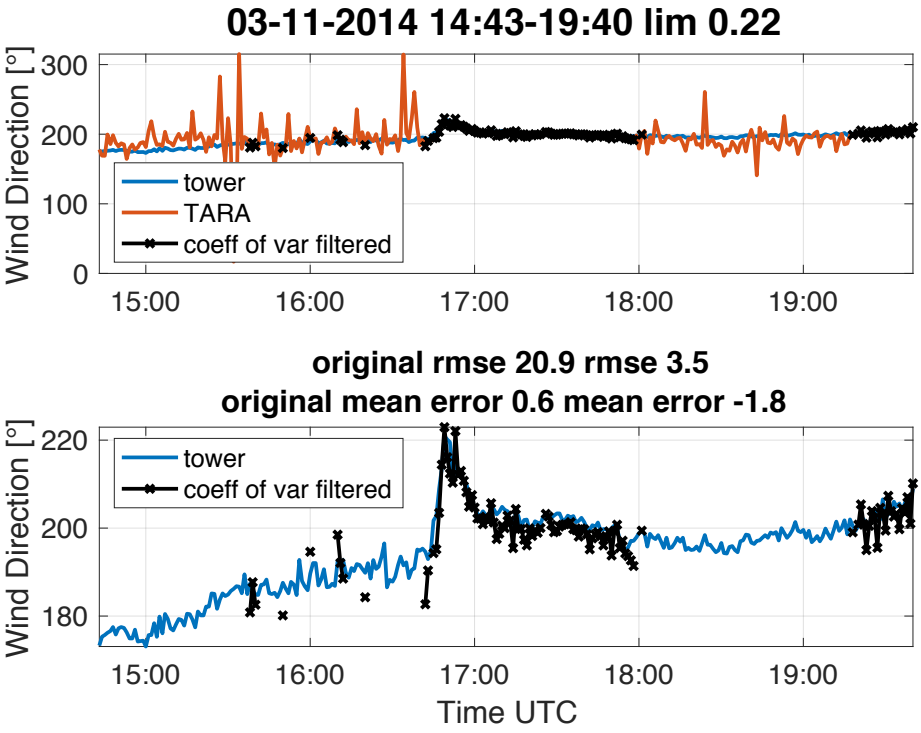

Figure 4.37: This figure shows the result of applying the mean threshold of coefficient of variation of 0.22 on the wind direction time series of the 3.11.2014. The top plot shows all data for TARA while in the bottom plot only the data remaining after applying the threshold is presented to be able to look at the results at a more suitable scale.

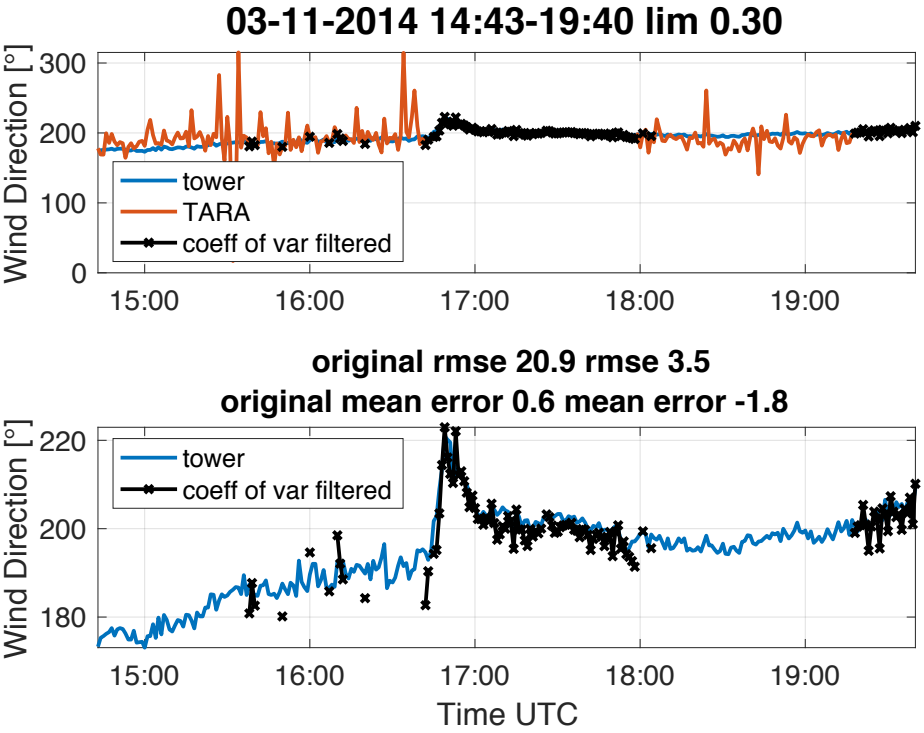

Figure 4.38: This figure shows the result of applying a maximum wind speed error of 5 m/s and maximum wind direction error of 10° on the wind direction time series of the 3.11.2014. The top plot shows all data for TARA while in the bottom plot only the data remaining after applying the threshold is presented to be able to look at the results at a more suitable scale.

4.5.4. Comparison to Results of Rain Selection

Table 4.5 contains three sub-tables. Each table compares the case studies to the mean values for all usable cases of the ACCEPT-campaign. The first table shows the original results for RMSE and mean error in wind speed and direction. The second table shows the same, but using the rain selection that was used for the quality assessment described in Chapter 3. The third table shows the results when applying a threshold in coefficient of variation of 0.22.

The results for the rain case on the 3.11.2014 [start_22.04.57] which only contains usable data are the same for all three methods. This shows that using the coefficient of variation usable data are not removed. For the cases of the 7.11.2014 and the second one on the 3.11.2014 comparing the rain selection to the coefficient of variation threshold showed improvements. In both cases, the RMSE were reduced to below 2 m/s and 5° in wind speed and direction error, when using the coefficient of variation threshold.

This comparison shows the potential of using the coefficient of variation of the mean Doppler velocities for the selection of the usable wind estimates. An advantage of this approach is that it can be performed at high time resolution and independently of other sensors. Although these results are promising, there are some drawbacks to using this method. When calculating the coefficient of variation, the standard deviation is calculated over the period of 1 minute. In a case where there is not a lot of data during 1 minute, the calculation of the standard deviation is possible but not usable. Another problem could be found when the mean of the mean Doppler velocities over 1 minute is close to zero. This problem could be solved by introducing a constant bias to the Doppler velocities. A constant bias would ensure that there are no cases where the standard deviation is divided by a mean which is zero.

Table 4.5: Table showing the results of the wind estimation during precipitation obtained during the ACCEPT-campaign. The first table shows the original values for RMSE and mean error for the three case studies and the mean for all usable cases. The second table does the same during precipitation. The last table shows the result for applying the coefficient of variation threshold of 0.22 to the individual cases and the mean values. A detailed table can be found in Appendix C.

original		rmse		mean error	
		wind speed [m/s]	wind direction [°]	wind speed [m/s]	wind direction [°]
07.11.14	[start_04.14.40]	35.1	49.8	13.4	-7.7
03.11.14	[start_22.04.57]	0.8	3.3	0.5	-1.0
03.11.14	[start_14.42.28]	11.3	20.9	7.6	0.6
mean all usable cases		13.7	27.8	6.6	-6.1

rain		rmse		mean error	
		wind speed [m/s]	wind direction [°]	wind speed [m/s]	wind direction [°]
07.11.14	[start_04.14.40]	3.5	5.6	1.4	0.1
03.11.14	[start_22.04.57]	0.8	3.3	0.5	-1.0
03.11.14	[start_14.42.28]	3.7	7.0	1.5	-1.2
mean all usable cases		3.0	7.6	1.4	-1.2

coefficient of variation threshold 0.22		rmse		mean error	
		wind speed [m/s]	wind direction [°]	wind speed [m/s]	wind direction [°]
07.11.14	[start_04.14.40]	0.9	4.9	0.3	-2.5
03.11.14	[start_22.04.57]	0.8	3.2	0.5	-1.0
03.11.14	[start_14.42.28]	1.5	3.5	0.6	-1.8
mean all usable cases		1.8	5.5	1.0	-1.7

4.5.5. Results Unusable Cases

So far only the cases selected as usable based on quicklooks and original RMSE were donsidered for the coefficient of variation threshold definition and application. However it is important to make sure that the unusable cases also show improvements when the coefficient of variation threshold is applied to the mean Doppler velocities.

Table 4.6 shows that there was a significant improvement in RMSE and mean error for both wind speed and direction when applying a coefficient of variation threshold of 0.22. But the improvement is not as significant as for the usable cases (see Table 4.5). The detailed results can be found in Appendix D. When looking at separate cases, large errors are mainly obtained when there is not a lot of data, i.e. clear air measurements. In the case of the calculation of the coefficient of variation using very little data, the possibility of a smaller or unreliable standard deviation is larger and this could result in small coefficient of variation. Thus this means that some unusable data is kept. For other cases the improvements are significant. To conclude, while the method seems to work well when there is a significant amount of data, a way needs to be found to identify these situations more reliably. A suggestion would be to add a criteria based on the amount of data in a certain time period at a certain height.

Table 4.6: Table showing the results of the wind estimation during precipitation obtained during the ACCEPT-campaign. The mean values for the application of the threshold of coefficient of variation are shown for all cases previously chosen to be unusable. The detailed results can be found in the tables in Appendix D.

mean	rmse ws [m/s]	rmse wd [°]	mean error ws [m/s]	mean error wd [°]
original data	25.5	40.2	15.3	-11.1
cv threshold 0.22	3.6	14.6	2.5	-7.3

4.6. Vertical Profiles

An improved data selection could open up the possibility to use TARA as a wind profiler at CESAR. While the measurements up to 200 m above the ground from the meteorological tower are validated, there is no data available in the database which would make it possible to look at vertical profiles of the horizontal wind. During the ACCEPT-campaign radiosonde launches also took place. Figures 4.41, 4.42, 4.43 and 4.44 show these radiosonde measurements in combination with wind profiler data, the tower data and vertical profiles measured by TARA. The wind profiler data on the 7.11.2014 was provided by Henk Klein Baltink (KNMI). The profiles are averaged over 30 minutes. This was done due to the fact that the wind profiler data is only available at 30 minutes averaging. Although there were three radiosonde launches on the 7.11.2014, only two of them are shown, because the third one was performed when there were no measurements from TARA (See Figure 4.39). While all other data is averaged over the same time periods as the wind profiler, this is not possible for the radiosonde. This is due to the fact that the radiosonde constantly changes position and therefore only takes point measurements. This means that the comparison of the radiosonde with the other sensors can only be done qualitatively and will be most accurate at the first time steps for each radiosonde launch.

Figures 4.39 and 4.40 show the radiosonde paths as well as the height-time profiles of the SNR. In Figure 4.39 all three radiosonde launches are included, while Figure 4.40 shows a zoom of the same plot.

Vertical profiles of the wind speed shown in Figures 4.41, 4.42, 4.43 and 4.44 are composed of different data sources. The same vertical profile is shown for the radiosonde for the whole period of one radiosonde launch. There are two different parts of wind profiler data. One profile is near the surface while the other starts at higher altitudes. Until 200 m the profile measured by the tower is shown. There are two profiles from TARA presented. One shows the original profile of the wind estimation. The second one shows the result of applying the coefficient of variation on 1 minute averaging periods at each height. This was then again averaged over a time period of 30 minutes.

During the first radiosonde launch (see Figures 4.41 and 4.42) both the original and the profile using the coefficient of variation filtering for TARA show a lot of variability compared to the rest of the profiles during the first three time steps. For all time steps, some improvement can be seen for the corrected TARA profile. But even though there were improvements, the variability and difference are still relatively large compared to the wind profiler and radiosonde . This is caused by a lack of data because during the first three time steps (08:15 - 09:15) there are clear air measurements or light precipitation (see Figure 4.40). For the last time step (09:45) there is some rain which leads to an improvement of the results.

During the second radiosonde launch, the correction of the TARA profiles using the coefficient of variation was more effective (see Figures 4.43 and 4.44). This is due to the fact, that there is rain during all time steps considered (see Figure 4.40). The corrected profiles are either much closer to the profiles measured by the other sensors (10:15, 11:15 and 11:45) or some small parts of the profile were removed where the data is not usable (10:45).

To conclude, the qualitative comparison of the vertical profiles of the horizontal wind speed showed positive results for the rain periods, while the removal of unusable data is not working well when there are insufficient amounts of data.

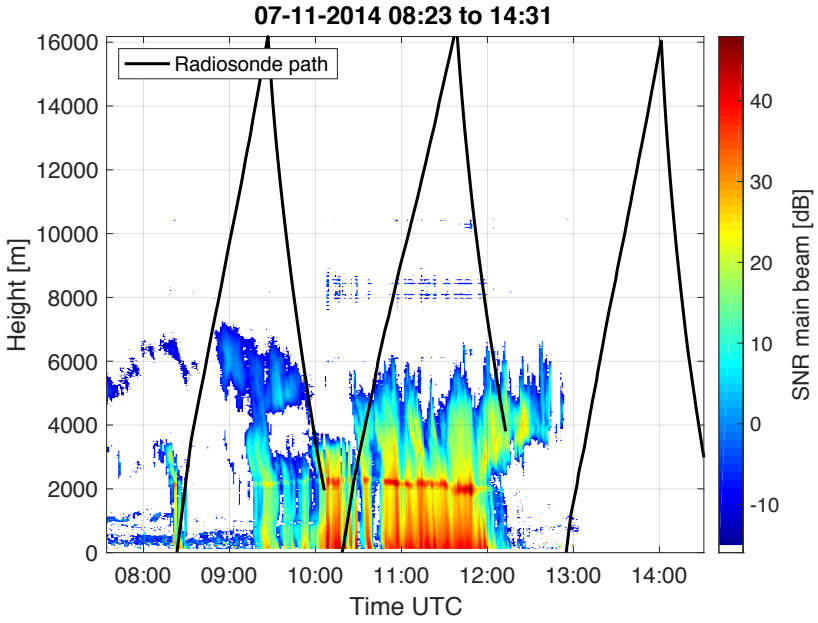

Figure 4.39: Shows the SNR of the main beam for the 7.11.2014. Additionally, the radiosonde paths for the three sondes that were launched on 7.11.2014 are shown. The time indicated in the title represents the time span of the three radiosonde launches.

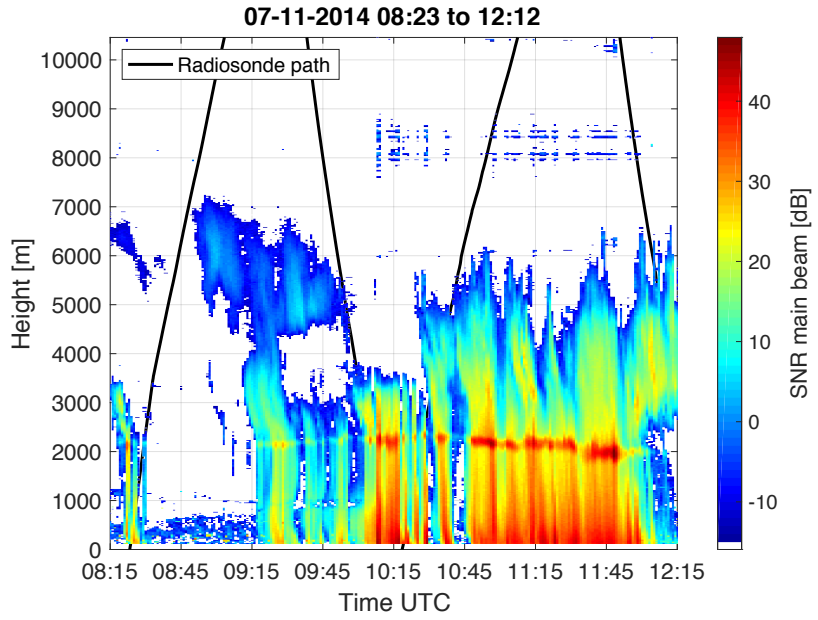

Figure 4.40: Shows a zoomed in part of the SNR of the main beam for the 7.11.2014. Additionally, the radiosonde paths are shown. The time indicated in the title represents the time span of the two radiosonde launches.

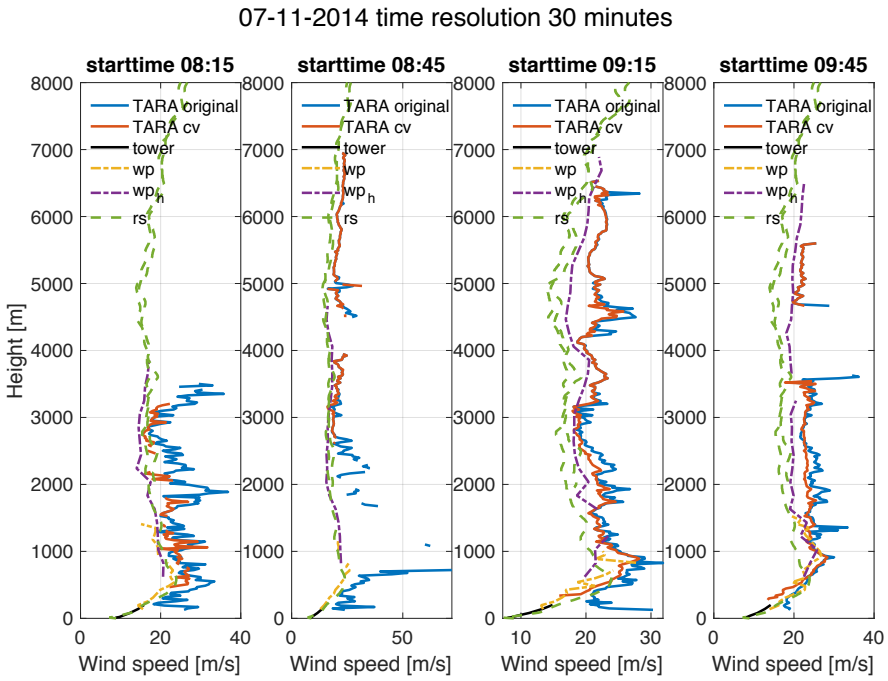

Figure 4.41: This figure shows the vertical profile of the horizontal wind as observed by TARA, the tower, a radiosonde and the wind profiler. The time span is given by the radiosonde while the time resolution of 30 minutes is given by the wind profiler. There are two different profiles for TARA, one showing the original data and one the data selected using a coefficient of variation threshold of 0.22. cv = coefficient of variation, wp = wind profiler measurements near the ground, wp_h = wind profiler measurements starting at higher altitudes, rs = radiosonde.

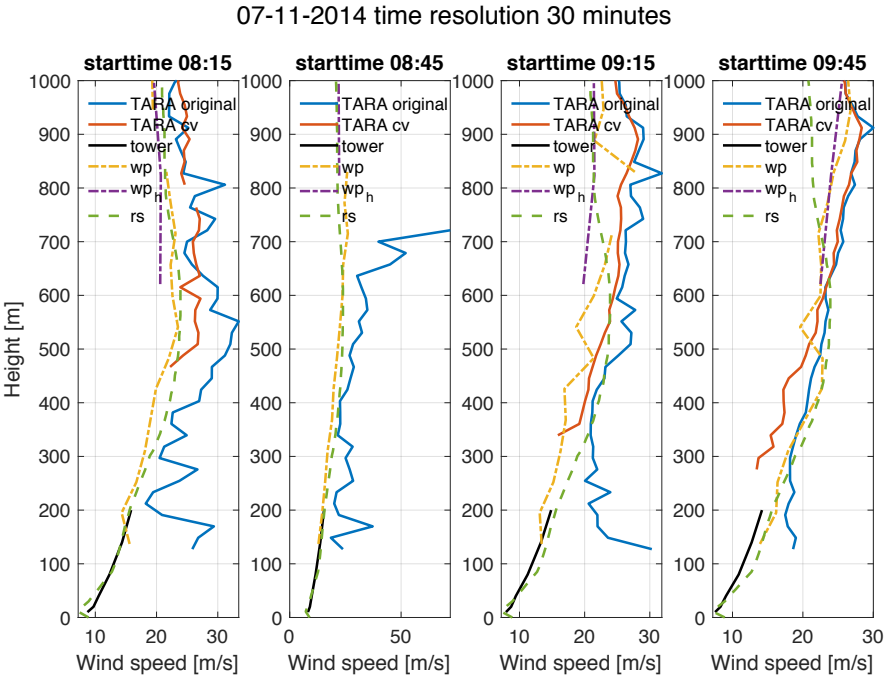

Figure 4.42: This figure shows the same vertical profiles of the horizontal wind as observed by TARA, the tower, a radiosonde and the wind profiler as Figure 4.41.For a better scale, the height is restricted to 1 km for this figure. The time span is given by the radiosonde while the time resolution of 30 minutes is given by the wind profiler. There are two different profiles for TARA, one showing the original data and one the data selected using a coefficient of variation threshold of 0.22. cv = coefficient of variation, wp = wind profiler measurements near the ground, wp_h = wind profiler measurements starting at higher altitudes, rs = radiosonde.

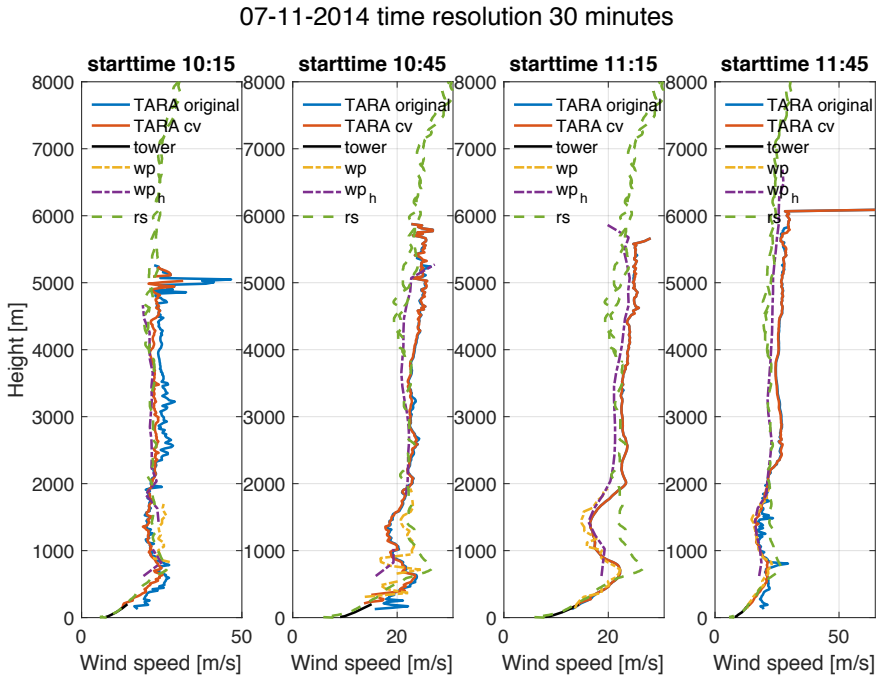

Figure 4.43: This figure shows the vertical profile of the horizontal wind as observed by TARA, the tower, a radiosonde and the wind profiler. The time span is given by the radiosonde while the time resolution of 30 minutes is given by the wind profiler. There are two different profiles for TARA, one showing the original data and one the data selected using a coefficient of variation threshold of 0.22. cv = coefficient of variation, wp = wind profiler measurements near the ground, wp_h = wind profiler measurements starting at higher altitudes, rs = radiosonde.

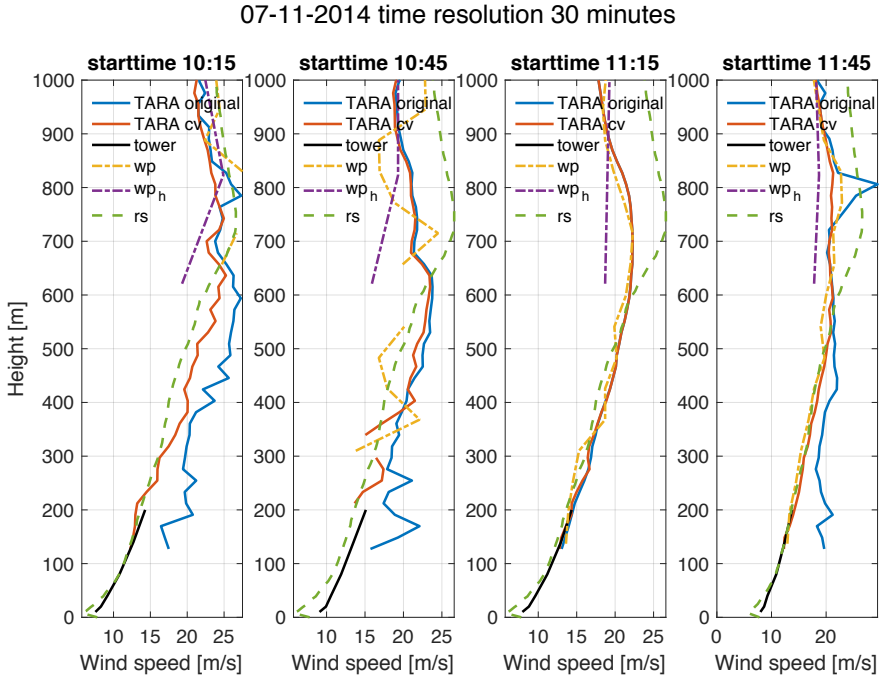

Figure 4.44: This figure shows the same vertical profile of the horizontal wind as observed by TARA, the tower, a radiosonde and the wind profiler as Figure 4.43. For a better scale, the height is restricted to 1 km for this figure. The time span is given by the radiosonde while the time resolution of 30 minutes is given by the wind profiler. There are two different profiles for TARA, one showing the original data and one the data selected using a coefficient of variation threshold of 0.22. cv = coefficient of variation, wp = wind profiler measurements near the ground, wp_h = wind profiler measurements starting at higher altitudes, rs = radiosonde.

5

Conclusions

This research had two main research questions, which will be treated separately in the two sections of this chapter. One section is about the quality assessment of the TARA wind estimation results and the other focusses on the data selection for the TARA wind estimates based on TARA only. In this chapter the main conclusions for the two parts will be drawn including a summary of the results found. While some valuable conclusions could be made, it became obvious during the research that there is a lot of work that can be done in the future on the topic of wind estimation using TARA. Recommendations on how the results of the research done could be improved are provided in Chapter 6.

5.1. Assessment Wind Estimation TARA

At first the goal of this thesis was to obtain vertical profiles of the horizontal wind at high time resolution using the rain radar TARA. These profiles could be used to continue the vertical profile which is obtained up to 200 m using a meteorological tower. However, before this report not much detailed analysis of the results of the wind estimation was performed. Because of this in a first step an evaluation of the wind estimation had to be performed.

Using the data obtained during ACCEPT-campaign in October and November 2014 an analysis of the wind estimation using TARA was performed at a height of 200 m above the surface. This height was chosen because it is the highest point of the tower where wind speed and direction are observed at 1- and 10-minute averages as well as the first reliable results of TARA are found at this height above the surface.

In a first step the clear air measurements needed to be removed. This was first attempted by using a SNR-threshold. This approach was not as successful as initially expected due to the fact that some large outliers had high SNR-values. This was mainly during clear air measurements and probably caused by residual clutter. Because of this while increasing the SNR-threshold, more usable data was removed while the large outliers remained and thus worsening the result. During rain a high SNR-value is a useful indication for good wind estimates but in order to be able to use the SNR as a criteria, clear air measurements had to be removed effectively first.

As developing an effective data filtering method proved to be challenging, the decision was made to check the wind estimation results during conditions which the TARA algorithm was designed for – during precipitation. A rough method was used to select data based on melting layer presence, which meant that if there were a certain amount of SNR-values above a certain threshold detected, the whole time step was kept. Thus, the clear air was removed by selecting only the rain periods in order to be able to assess the quality of the wind estimation during precipitation. This method of selection of precipitation time steps was useful in order to calculate the RMSE and mean errors for wind speed and direction estimation at a height of 200 m above the surface using the tower measurements as the ground truth. The results of the quality assessment of the wind estimation during precipitation showed that at 10-minute resolution, the mean RMSE is 1.3 m/s for the wind speed and 2.8° for the direction. For the time resolution of 1 minute, the mean RMSE became 2.4 m/s and 8.3°. These values are in agreement with 1-2 m/s acceptable error for the wind speed and 5-10° acceptable error in wind direction.

The results for the rain periods during ACCEPT-campaign at 200 m above the ground were promising, but there were some consistent biases found in the data. One possible cause could be the assumptions of equal dynamics and microphysics in the three beams. For this reason it was decided to investigate the impact of the assumption of equal microphysics for the three beams which is not the case in a non-homogeneous medium. An error simulation was carried out, changing the fall velocity for one of the offset beams and re-estimating the wind using the assumption of equal fall velocity. Other sources of error would also possible, i.e. that the positive bias is a statistical artefact in the form that any error in U and V will result in a positive error for the wind speed while this is not the case for the wind direction (see Subsection 2.4.2 for details on how wind speed and direction are calculated from the components U and V). However the simulation of errors using different fall velocities for one of the beams could reproduce the positive bias in wind speed estimation as well as show the dependence of direction for the wind speed and direction estimation error. These error simulations showed the impact of the assumptions made for equal microphysics in the three beams which could be approached by looking at differences in reflectivity in the three beams. Another factor which also needs to be considered is the assumption of equal dynamics for the three beams. In this case it would become a lot more challenging if not impossible to detect such errors using TARA only. This is because each beam only measures one radial velocity and only the combination of them assuming equal dynamics and microphysics makes it possible to estimate the wind using the algorithm applied for TARA.

To conclude, the clear air measurements were effectively removed in an automated way using a rough rain period selection method. While there is room for improvement in the data selection, this approach made it possible to conclude that the wind estimation during precipitation and near the ground using TARA is working well.

5.2. Data Selection

Following the first assessment of the wind estimation results using TARA-data with a rough selection of rain events and concluding that the quality of the wind estimation during rain is sufficient, it was decided that priority will further be given to improve the selection of usable data. This selection needed to be based on TARA only. The time series of the mean Doppler velocities was used for this approach.

A first attempt to improving the data selection was done using the correlation of the three mean Doppler velocities. While the correlations over some parts were good it was not possible to use the correlation coefficients over shorter parts of the time series effectively as a selection criteria. Thus it was concluded that this method was not useful for the data selection. This was because of different reasons. First, the time resolution needed to be largely degraded because of the amount of data needed for the calculation of the coefficients. One approach to solve this problem would be to use a moving window that shifts by the wanted time resolution. Another reason to not use the correlation was that during very stable situations where the mean Doppler velocities are relatively constant, the correlation values are again low.

During the analysis of the time series it was found that accurate wind estimates during precipitation require a large value of SNR ($\geq$ 30 dB). One way to get a higher value for the SNR is to average over longer time periods. This is the reason why a re-estimation of the wind using averaged mean Doppler velocities was performed. While this could improve the results for some cases, in other cases this approach was not successful.

Another aspect that became obvious during the inspection of the time series of the mean Doppler velocities along with the wind estimation time series was that the wind estimation accuracy corresponds with large or small variability of the measurement. For this reason it was decided to use the coefficient of variation for the mean Doppler velocities. This coefficient is defined as normalizing the standard deviation with the mean. Using this a threshold was defined for the whole ACCEPT-campaign. The results of this method compared to the results of the assessment of the wind estimation during rain were mostly better or equal. At 1-minute resolution, the mean RMSE is 1.8 m/s and 5.5° for the wind speed and direction, respectively. This method of using the coefficient of variation threshold was additionally performed on the cases selected as unusable. The mean values in RMSE as well as mean errors could significantly be reduced also in these cases.

A qualitative comparison was then done for the vertical profiles comparing the tower, radiosonde and wind profiler to the original and coefficient of variation filtered TARA-data. These types of profiles could be useful for studies which do not depend on very high time resolution.

However vertical profiles of the horizontal wind measured by TARA must also be investigated at higher time resolutions, namely 1 and 10 minutes.

To conclude, the results of using the coefficient of variation threshold for the selection of the usable data from the TARA wind estimation showed promising results. However there is still a need to remove cases with insufficient amounts of data reliably.

6

Recommendations

Following from the conclusions of the previous chapter, recommendations and next steps that could be taken to improve the research done so far are discussed in this chapter. Although, the wind estimation is working well during precipitation, there are still some factors which were not considered or could be assessed in more detail. These include the selection of usable cases, assumptions made by the algorithm, errors in the mean Doppler velocities and the application of the coefficient of variation to other three-beam rain radars.

While the selection of usable cases was done manually for the assessment of the wind estimation algorithm performance, the selection could be improved by checking the amount of data for an averaging interval. This approach would make it possible to remove large outliers which result from clutter during clear air measurements. One important aspect that could be improved is the selection of usable case studies. In particular, an improvement in data selection could be achieved based on the amount of data present for a certain averaging period and height. In combination with the filtering based on the coefficient of variation for the mean Doppler velocities, this approach could further improve the results for the automatic selection of usable data and case studies. Furthermore to make the selection of the threshold of coefficient of variation more robust, a mean value from a larger amount of case studies would be more reliable.

The algorithm used to estimate the wind is based on the assumption that the three beams of TARA measure the same dynamics as well as microphysics. While this is the case in very stable conditions, this might not always be the correct assumption, especially with increasing beam divergence further away from the radar. The simulation of errors showed that only a small assumption error in one of the beams – caused by the equal microphysics assumption of the wind estimation algorithm – can cause large errors in wind estimation. A more extensive simulation that also looks at the effects of different dynamics measured by the three beams could further be performed. Following an extensive error simulation, an attempt to correct errors caused by the algorithm due to fall velocity differences could be investigated by relating the fall velocity to reflectivity differences in the separate beams.

Another aspect that was not considered in this research are errors which affect the mean Doppler velocities. It was assumed that these were correct and the purpose of this study was to assess how the results are affected by the algorithm that estimates the wind from the mean Doppler velocities. A better correction for clutter suppression in the offset beams as well as the possibility of implementing a different algorithm for clear air measurements could be steps towards a more accurate wind estimation performed using TARA. A part which was not considered during this research is improving the clutter suppression in the offset beams as well as looking at the errors introduced while calculating the mean Doppler velocities for the three beams. An improvement in reliability of the Doppler velocities would also have an impact on the accuracy of the wind estimation as well as the data selection.

For TARA the use of the coefficient of variation showed promising results. One idea would be to apply this to other three-beam rain radars. Due to the fact that the selection is based on the mean Doppler velocities measured by the radar this should also work for any other system. However an evaluation of the performance of the method should be done for each system as differences in i.e. elevation of the main beam could result in errors which are different from the ones found for TARA.

Bibliography

Balaji, B., Prabha, Thara V., Jaya Rao, Y., Kiran, T., Dinesh, G., Chakravarty, Kaustav, Sonbawne, S. M., and Rajeevan, M., 2017. Potential of collocated radiometer and wind profiler observations for monsoon studies. *Atmospheric Research*, 194(January):17–26.

Benjamin, Stanley G., Schwartz, Barry E., Szoke, Edward J., and Koch, Steven E., 2004. The value of wind profiler data in U.S. weather forecasting. *Bulletin of the American Meteorological Society*, 85 (12):1871–1886.

Bosveld, Fred C. Cabauw In-situ Observational Program 2000 – Now: Instruments, Calibrations and Set-up. Technical report, 2018.

Brown, Charles E., 1998. Coefficient of Variation. *Applied Multivariate Statistics in Geohydrology and Related Sciences*, pages 155–157.

Brukx, Patrick. *Dealisasing of radar Doppler velocities to improve wind estimations*. Msc thesis, Delft University of Technology, 2015.

Dotzek, Nikolai and Friedrich, Katja, 2009. Downburst-producing thunderstorms in southern Germany: Radar analysis and predictability. *Atmospheric Research*, 93(1-3):457–473.

Doviak, Richard J. and Zrnic, Dusan S., 2006. *Doppler Radar and Weather Observations*. Courier Corporation, second edi edition.

Gage, K.S., Balsley, B.B., Ecklund, W.L., Carter, D.A., and Mcafee, J.R., 1991. Wind Profiler-Related Research in the Tropical Pacific. *Journal of Geophysical Research*, 96:3209–3220.

Gunter, W. Scott and Schroeder, John L., 2015. High-resolution full-scale measurements of thunderstorm outflow winds. *Journal of Wind Engineering and Industrial Aerodynamics*, 138:13–26.

He, Y. C., Chan, P. W., and Li, Q. S., 2016. Observations of vertical wind profiles of tropical cyclones at coastal areas. *Journal of Wind Engineering and Industrial Aerodynamics*, 152:1–14.

Heijnen, S H, Ligthart, L P, and Russchenberg, H. W.J., 2000. First measurements with TARA; an S-band transportable atmospheric radar. *Physics and Chemistry of the Earth, Part B: Hydrology, Oceans and Atmosphere*, 25(10-12):995–998.

Marshall, John and Plumb, R. Alan, 2008. *Atmosphere, Ocean, and Climate Dynamics - An Introductory Text*. Elsevier Inc.

Milrad, Shawn, 2018. Chapter 12 - Radar Imagery. In *Synoptic Analysis and Forecasting - An Introductory Toolkit*, pages 163–177. Elsevier Inc.

Nash, J and Oakley, T J, 2001. Development of COST 76 wind profiler network in Europe. *Physics and Chemistry of the Earth, Part B: Hydrology, Oceans and Atmosphere*, 26(3):193–199.

Park, S.-G and Lee, Dong-Kyou, 2009. Retrieval of High-Resolution Wind Fields over the Southern Korean Peninsula Using the Doppler Weather Radar Network. *Weather and Forecasting*, 24(1): 87–103.

Pfitzenmaier, Lukas, Dufournet, Yann, Unal, Christine M H, and Russchenberg, Herman W J, 2017. Retrieving Fall Streaks within Cloud Systems Using Doppler Radar. *Journal of Atmospheric and Oceanic Technology*, 34(4):905–920.

Pfitzenmaier, Lukas, Unal, Christine M.H., Dufournet, Yann, and Russchenberg, Herman W.J., 2018. Observing ice particle growth along fall streaks in mixed-phase clouds using spectral polarimetric radar data. *Atmospheric Chemistry and Physics*, 18(11):7843–7862.

Shu, Z. R., Li, Q. S., He, Y. C., and Chan, P. W., 2017. Vertical wind profiles for typhoon, monsoon and thunderstorm winds. *Journal of Wind Engineering and Industrial Aerodynamics*, 168:190–199.

Unal, C. M. H. Geometrical transformations to estimate the 3D wind from the 3 mean Doppler velocities measured by the 3 beams of TARA, MB, OB1 and OB2 - Notes. Technical report.

Unal, Christine, 2009. Spectral polarimetric radar clutter suppression to enhance atmospheric echoes. *Journal of Atmospheric and Oceanic Technology*, 26(9):1781–1797.

Unal, Christine, 2015. High-resolution raindrop size distribution retrieval based on the doppler spectrum in the case of slant profiling radar. *Journal of Atmospheric and Oceanic Technology*, 32(6):1191–1208.

Unal, Christine, Dufournet, Yann, Otto, Tobias, and Russchenberg, Herman, 2012. The new real-time measurement capabilities of the profiling TARA radar. *The Seventh European Conference on Radar in Meteorology and Hydrology*.

Unal, Christine M.H. and Moisseev, D. N., 2004. Combined Doppler and polarimetric radar measurements: Correction for spectrum aliasing and nonsimultaneous polarimetric measurements. *Journal of Atmospheric and Oceanic Technology*, 21(3):443–456.

Vaughan, G and Hooper, D, 2015. Mesosphere – Stratosphere – Troposphere and Stratosphere – Troposphere Radars and Wind Profilers. *Encyclopedia of Atmospheric Sciences 2nd Edition*, 4: 1825–1833.

Wilczak, J. M., Strauch, R. G., Ralph, F. M., Weber, B. L., Merritt, D. a., Jordan, J. R., Wolfe, D. E., Lewis, L. K., Wuertz, D. B., Gaynor, J. E., McLaughlin, S. a., Rogers, R. R., Riddle, a. C., and Dye, T. S., 1995. Contamination of Wind Profiler Data by Migrating Birds: Characteristics of Corrupted Data and Potential Solutions. *Journal of Atmospheric and Oceanic Technology*, 12(3):449–467.

Zhong, Shiyuan, Fast, Jerome D., and Bian, Xindi, 1996. A Case Study of the Great Plains Low-Level Jet Using Wind Profiler Network Data and a High-Resolution Mesoscale Model. *Monthly Weather Review*, 124:785–806.

Appendices

A

RMSE Wind Speed and Direction

Table A.1: Table showing the results of the wind estimation during the ACCEPT-campaign at a time resolution of 60 seconds. The table includes RMSE and mean error for wind speed and direction as well as the mean wind speed and direction of the tower and TARA.

matlab code rain_v2, Resolution 60s		original data				mean wind speed		mean wind direction	
date [mm_dd]	TARA-5_cycle_Processed_Data	rmse ws [m/s]	rmse wd [°]	mean error ws [m/s]	mean error wd [°]	tower [m/s]	TARA [m/s]	tower [°]	TARA [°]
11_12	[start_04.00.47]	31.1	37.4	11.2	1.0	11.3	22.2	175.8	180.5
11_09	[start_21.23.26]	20.3	35.1	5.4	-2.4	8.6	14.1	206.1	191.8
11_07	[start_04.14.40]	34.7	50.4	12.3	-7.7	15.2	27.3	161.9	159.8
11_03	[start_00.04.47]	6.7	17.5	5.1	-9.2	12.9	18.1	206.9	197.7
	[start_05.34.35]	22.5	36.3	9.8	-0.4	13.7	23.5	191.9	191.3
	[start_12.48.52]	9.1	16.5	6.2	3.7	15.4	21.6	183.0	186.7
	[start_13.38.43]	3.9	8.4	2.3	0.4	15.5	17.8	180.2	180.6
	[start_14.42.28]	8.1	18.3	5.4	-1.5	15.8	21.2	194.3	192.7
	[start_19.45.12]	1.4	3.4	0.4	-1.2	12.3	12.8	210.0	208.8
	[start_22.04.57]	0.8	3.5	0.4	-1.3	10.5	10.9	216.6	215.3
11_02	[start_16.26.03]	22.8	31.6	10.6	-6.5	13.6	24.2	201.8	192.3
10_24	[start_00.01.54]	6.9	10.6	5.1	-4.0	11.0	16.1	197.9	193.9
	[start_19.53.58]	1.1	3.6	0.7	-2.4	10.7	11.4	200.1	197.7
	[start_21.33.42]	4.7	14.3	3.7	-10.3	10.5	14.3	208.8	198.6
10_22	[start_00.07.41]	9.6	65.2	2.1	-29.9	17.0	19.1	312.3	267.1
	[start_02.24.15]	23.7	58.7	8.1	-17.9	15.5	23.6	313.9	279.6
10_21	[start_05.48.36]	7.7	34.4	4.3	-5.2	15.7	19.9	226.5	216.9
	[start_14.16.59]	22.6	65.4	13.5	-29.6	16.9	30.5	291.9	253.6
	[start_20.29.08]	8.2	30.4	3.5	-7.0	18.5	22.0	305.2	294.6
	[start_22.14.34]	3.4	16.3	1.0	-4.9	15.2	16.3	309.4	304.5
10_16	[start_00.03.56]	10.5	19.3	2.7	-1.1	9.0	11.8	185.3	183.0
10_12	[start_15.25.39]	13.7	41.0	6.1	0.0	11.7	17.8	78.5	83.3
	mean	12.4	28.1	5.5	-6.2	13.5	18.9	216.3	207.7

Table A.2: Table showing the results of the wind estimation during precipitation during the ACCEPT-campaign at a time resolution of 60 seconds. The table includes RMSE and mean error for wind speed and direction as well as the mean wind speed and direction of the tower and TARA.

matlab code rain_v2, Resolution 60s		rain events				mean wind speed		mean wind direction	
date [mm_dd]	TARA-5_cycle_Processed_Data	rmse ws [m/s]	rmse wd [°]	mean error ws [m/s]	mean error wd [°]	tower [m/s]	TARA [m/s]	tower [°]	TARA [°]
11_12	[start_04.00.47]	5.0	15.3	1.8	2.4	11.2	12.9	183.4	185.8
11_09	[start_21.23.26]	0.8	2.0	0.6	-1.9	8.5	9.1	199.7	197.8
11_07	[start_04.14.40]	2.0	5.8	0.9	0.8	14.4	15.3	169.6	170.4
11_03	[start_00.04.47]	0.9	3.9	0.4	-1.3	11.5	11.9	208.9	207.6
	[start_05.34.35]	2.1	4.9	1.3	-0.3	14.0	15.3	190.0	189.7
	[start_12.48.52]	3.9	22.1	2.0	-12.3	15.7	17.7	182.7	170.4
	[start_13.38.43]	2.0	4.1	1.4	0.0	15.5	16.9	179.9	179.8
	[start_14.42.28]	2.8	8.9	1.1	-2.7	16.0	17.1	199.8	197.1
	[start_19.45.12]	1.4	3.4	0.4	-1.3	12.4	12.8	209.8	208.6
	[start_22.04.57]	0.8	3.5	0.4	-1.3	10.5	10.9	216.6	215.3
11_02	[start_16.26.03]	1.5	4.1	0.6	-1.9	13.3	13.9	207.6	205.8
10_24	[start_00.01.54]	2.4	4.2	1.8	0.6	10.5	12.2	194.7	195.4
	[start_19.53.58]	1.1	3.6	0.7	-2.4	10.7	11.4	200.1	197.7
	[start_21.33.42]	1.0	3.2	0.6	-2.0	10.8	11.4	203.9	201.8
10_22	[start_00.07.41]	9.3	27.1	3.2	-7.9	17.3	20.6	309.7	301.8
	[start_02.24.15]	2.3	11.5	1.0	-1.6	16.1	17.1	317.5	315.9
10_21	[start_05.48.36]	4.0	18.8	1.5	-0.2	16.1	17.5	217.7	215.9
	[start_14.16.59]	4.1	8.9	1.7	-0.5	17.8	19.5	293.5	293.3
	[start_20.29.08]	1.3	6.4	0.7	-1.2	18.1	18.8	306.1	304.9
	[start_22.14.34]	1.9	10.9	0.6	-3.0	15.4	16.1	310.3	307.4
10_16	[start_00.03.56]	1.3	5.4	0.7	0.9	9.7	10.4	177.4	178.3
10_12	[start_15.25.39]	0.8	4.8	0.6	1.0	12.8	13.4	80.9	81.9
	mean	2.4	8.3	1.1	-1.6	13.6	14.7	216.3	214.7

Table A.3: Table showing the results of the wind estimation during the ACCEPT-campaign at a time resolution of 600 seconds. The table includes RMSE and mean error for wind speed and direction as well as the mean wind speed and direction of the tower and TARA.

matlab code rain_v2, Resolution 600s		original data				mean wind speed		mean wind direction	
date [mm_dd]	TARA-5_cycle_Processed_Data	rmse ws [m/s]	rmse wd [°]	mean error ws [m/s]	mean error wd [°]	tower [m/s]	TARA [m/s]	tower [°]	TARA [°]
11_12	[start_04.00.47]	36.5	48.4	18.8	6.6	11.4	30.2	177.2	184.2
11_09	[start_21.23.26]	9.5	47.5	6.4	7.1	8.6	15.0	206.0	185.1
11_07	[start_04.14.40]	32.3	46.3	16.4	-6.7	15.2	31.6	163.3	156.8
11_03	[start_00.04.47]	5.0	11.1	4.4	-9.6	12.9	17.4	206.9	197.3
	[start_05.34.35]	10.0	5.5	7.4	1.0	13.7	21.1	192.5	193.4
	[start_12.48.52]	6.1	4.0	5.6	3.4	15.4	21.1	184.3	187.7
	[start_13.38.43]	2.8	1.9	2.0	-0.4	15.3	17.3	182.0	181.6
	[start_14.42.28]	6.2	6.0	4.8	-1.5	15.8	20.6	195.1	193.5
	[start_19.45.12]	0.5	2.0	0.4	-1.3	12.3	12.7	210.1	208.7
	[start_22.04.57]	0.5	2.1	0.4	-1.6	10.5	11.0	216.1	214.6
11_02	[start_16.26.03]	29.6	33.2	13.5	-10.2	13.6	27.1	201.8	191.6
10_24	[start_00.01.54]	4.8	5.8	4.2	-4.0	11.1	15.3	198.0	194.0
	[start_19.53.58]	0.6	2.6	0.5	-2.6	10.7	11.2	199.5	196.9
	[start_21.33.42]	3.6	9.9	3.4	-9.0	10.5	13.9	208.9	199.9
10_22	[start_00.07.41]	3.4	52.8	0.5	-32.0	17.0	17.5	312.4	280.4
	[start_02.24.15]	5.7	31.5	3.1	-15.7	15.5	18.7	314.2	298.4
10_21	[start_05.48.36]	5.0	13.4	3.4	-5.4	15.7	19.1	225.7	220.3
	[start_14.16.59]	14.5	46.1	10.2	-24.7	17.2	27.4	292.0	267.3
	[start_20.29.08]	7.0	24.9	3.6	-9.0	18.7	22.2	305.0	296.0
	[start_22.14.34]	0.9	2.6	0.7	-1.2	15.2	15.9	309.5	308.3
10_16	[start_00.03.56]	8.2	13.4	3.7	-2.1	9.0	12.8	185.8	183.5
10_12	[start_15.25.39]	8.7	28.6	5.3	-7.5	11.7	17.0	79.7	79.4
	mean	9.2	20.0	5.4	-5.8	13.5	18.9	216.6	210.0

Table A.4: Table showing the results of the wind estimation during precipitation during the ACCEPT-campaign at a time resolution of 600 seconds. The table includes RMSE and mean error for wind speed and direction as well as the mean wind speed and direction of the tower and TARA.

matlab code rain_v2, Resolution 600s		rain events				mean wind speed		mean wind direction	
date [mm_dd]	TARA-5_cycle_Processed_Data	rmse ws [m/s]	rmse wd [°]	mean error ws [m/s]	mean error wd [°]	tower [m/s]	TARA [m/s]	tower [°]	TARA [°]
11_12	[start_04.00.47]	1.1	1.9	1.0	0.6	11.1	12.1	184.3	184.9
11_09	[start_21.23.26]	0.4	1.7	0.4	-1.7	8.5	8.9	199.6	197.9
11_07	[start_04.14.40]	1.1	2.9	0.8	-0.4	14.3	15.2	171.1	170.7
11_03	[start_00.04.47]	0.4	1.3	0.4	-1.1	11.4	11.8	207.2	206.1
	[start_05.34.35]	1.4	1.9	1.2	-1.0	14.1	15.3	190.7	189.7
	[start_12.48.52]	5.8	3.3	5.3	2.5	15.7	20.9	184.6	187.1
	[start_13.38.43]	1.1	1.5	1.0	-1.3	15.3	16.4	181.7	180.4
	[start_14.42.28]	1.6	3.2	1.0	-2.3	15.9	16.9	200.0	197.6
	[start_19.45.12]	0.5	2.0	0.4	-1.3	12.3	12.7	210.1	208.7
	[start_22.04.57]	0.5	2.1	0.4	-1.6	10.5	11.0	216.1	214.6
11_02	[start_16.26.03]	1.4	2.8	0.9	-2.5	13.4	14.3	206.8	204.4
10_24	[start_00.01.54]	1.4	0.8	1.4	0.8	10.4	11.8	195.5	196.3
	[start_19.53.58]	0.6	2.6	0.5	-2.6	10.7	11.2	199.5	196.9
	[start_21.33.42]	0.5	1.8	0.5	-1.8	10.8	11.3	203.9	202.1
10_22	[start_00.07.41]	1.6	1.7	1.3	-0.4	17.9	19.2	308.2	307.8
	[start_02.24.15]	1.8	12.1	1.2	-3.8	15.9	17.1	317.6	313.8
10_21	[start_05.48.36]	2.1	4.3	1.4	-2.1	16.1	17.5	214.1	211.9
	[start_14.16.59]	2.3	3.4	1.9	1.0	17.9	19.8	293.2	294.2
	[start_20.29.08]	0.8	4.0	0.6	-2.5	17.9	18.5	306.1	303.7
	[start_22.14.34]	0.9	2.6	0.7	-1.2	15.2	15.9	309.5	308.3
10_16	[start_00.03.56]	0.8	2.7	0.7	0.1	9.8	10.5	178.3	178.4
10_12	[start_15.25.39]	0.6	1.6	0.6	-0.3	12.8	13.4	82.2	81.9
	mean	1.3	2.8	1.1	-1.0	13.5	14.6	216.4	215.3

B

Comparison Thresholds Coefficient of Variation

Table B.1: Table showing the results of using different maximum wind speed errors for the time series when lowering the threshold of coefficient of variation iteratively.

coefficient of variation results		max ws error ->	2 m/s			5 m/s			10 m/s			15 m/s		
date [mm_d	TARA_5_cycle Processed_Data	original rmse	lim	rmse ws	me ws	lim	rmse ws	me ws	lim	rmse ws	me ws	lim	rmse ws	me ws
11_12	[start_04.00.47]	31.8	0.10	0.6	0.4	0.45	1.4	0.9	0.75	1.9	1.2	0.95	2.9	1.7
11_09	[start_21.23.26]	20.4	0.05	0.5	0.5	0.15	0.7	0.6	0.30	1.3	0.8	1.00	3.3	1.9
11_07	[start_04.14.40]	35.1	0.35	1.0	0.4	0.90	1.3	0.6	0.90	1.3	0.6	1.00	1.7	0.8
11_03	[start_00.04.47]	8.1	0.00	NaN	NaN	0.05	0.9	0.4	0.35	4.2	3.0	0.55	4.6	3.5
	[start_05.34.35]	24.8	0.10	0.9	0.6	0.10	0.9	0.6	0.30	2.5	1.4	0.75	3.7	2.3
	[start_12.48.52]	12.7	0.10	NaN	NaN	0.50	1.7	1.2	1.00	3.6	2.4	1.00	3.6	2.4
	[start_13.38.43]	4.7	0.15	1.3	0.5	1.00	2.1	1.5	1.00	2.1	1.5	1.00	2.1	1.5
	[start_14.42.28]	11.3	0.05	0.8	-0.1	0.30	1.6	0.6	0.70	2.6	1.2	0.85	3.3	1.6
	[start_19.45.12]	1.5	0.05	1.0	0.4	0.20	1.2	0.4	1.00	1.5	0.5	1.00	1.5	0.5
	[start_22.04.57]	0.8	0.05	0.5	0.4	1.00	0.8	0.5	1.00	0.8	0.5	1.00	0.8	0.5
11_02	[start_16.26.03]	23.4	0.00	NaN	NaN	0.10	1.4	0.6	0.10	1.4	0.6	0.25	2.5	1.4
10_24	[start_00.01.54]	10.5	0.05	NaN	NaN	0.20	2.1	1.7	0.75	3.6	3.1	0.75	3.6	3.1
	[start_19.53.58]	1.1	0.05	0.9	0.5	1.00	1.1	0.7	1.00	1.1	0.7	1.00	1.1	0.7
	[start_21.33.42]	7.1	0.05	1.1	0.8	0.10	2.0	1.4	0.75	3.7	3.1	1.00	4.5	3.7
10_22	[start_00.07.41]	9.7	0.05	1.3	1.3	0.05	1.3	1.3	0.85	3.3	0.1	0.85	3.3	0.1
	[start_02.24.15]	25.1	0.05	1.0	0.3	0.20	1.4	0.7	0.50	1.8	0.9	0.95	3.0	1.5
10_21	[start_05.48.36]	9.8	0.05	0.8	0.0	0.10	1.9	0.8	0.20	2.1	0.7	0.20	2.1	0.7
	[start_14.16.59]	24.9	0.00	NaN	NaN	0.10	1.6	0.8	0.35	2.3	1.4	0.35	2.3	1.4
	[start_20.29.08]	8.0	0.05	1.0	0.8	0.15	1.4	0.8	0.15	1.4	0.8	0.15	1.4	0.8
	[start_22.14.34]	3.6	0.05	1.6	1.4	0.45	1.8	0.8	1.00	2.0	0.7	1.00	2.0	0.7
10_16	[start_00.03.56]	11.1	0.05	0.8	0.7	0.10	0.9	0.6	0.85	1.6	1.0	1.00	1.9	1.2
10_12	[start_15.25.39]	15.1	0.10	0.8	0.6	0.15	0.9	0.6	0.25	1.4	0.8	0.25	1.4	0.8
	mean	13.67	0.07	0.94	0.57	0.33	1.37	0.82	0.64	2.16	1.23	0.77	2.57	1.48

Table B.2: Table showing the results of using different maximum wind direction errors for the time series when lowering the threshold of coefficient of variation iteratively.

coefficient of variation results		max wd error ->	5°			10°			15°			20°		
date [mm_d	TARA_5_cycle Processed_Data	original rmse wd	lim	rmse wd	me wd	lim	rmse wd	me wd	lim	rmse w	me wd	lim	rmse wd	me wd
11_12	[start_04.00.47]	37.8	0.05	2.0	-1.1	0.25	3.8	0.6	0.25	3.8	0.6	0.45	5.4	1.7
11_09	[start_21.23.26]	35.1	1.00	6.2	-4.0	1.00	6.2	-4.0	1.00	6.2	-4.0	1.00	6.2	-4.0
11_07	[start_04.14.40]	49.8	0.15	3.9	-1.9	0.75	4.6	-0.7	0.90	4.9	-0.3	0.90	4.9	-0.3
11_03	[start_00.04.47]	17.1	0.00	NaN	NaN	0.00	NaN	NaN	0.70	11.7	-8.5	0.70	11.7	-8.5
	[start_05.34.35]	35.2	0.10	4.9	-2.7	0.15	4.3	-2.1	0.25	4.8	-0.5	0.75	6.2	0.5
	[start_12.48.52]	19.5	0.25	2.2	0.4	0.50	4.0	1.0	1.00	5.4	-0.4	1.00	5.4	-0.4
	[start_13.38.43]	8.6	0.15	2.4	-1.3	0.35	4.1	0.2	1.00	4.6	0.8	1.00	4.6	0.8
	[start_14.42.28]	20.9	0.05	2.5	-1.8	0.50	3.9	-1.7	0.60	4.7	-1.8	0.60	4.7	-1.8
	[start_19.45.12]	3.5	0.00	NaN	NaN	1.00	3.5	-1.1	1.00	3.5	-1.1	1.00	3.5	-1.1
	[start_22.04.57]	3.3	0.00	NaN	NaN	0.05	2.6	-1.4	1.00	3.3	-1.0	1.00	3.3	-1.0
11_02	[start_16.26.03]	31.6	0.05	4.6	-2.7	0.35	7.2	-4.0	0.75	8.5	-4.8	0.75	8.5	-4.8
10_24	[start_00.01.54]	10.9	0.05	NaN	NaN	0.20	5.5	-3.4	1.00	7.5	-4.5	1.00	7.5	-4.5
	[start_19.53.58]	3.3	0.05	3.2	-2.3	1.00	3.3	-2.0	1.00	3.3	-2.0	1.00	3.3	-2.0
	[start_21.33.42]	13.8	1.00	10.2	-8.2	1.00	10.2	-8.2	1.00	10.2	-8.2	1.00	10.2	-8.2
10_22	[start_00.07.41]	65.5	0.05	5.2	-5.2	0.10	5.4	1.6	1.00	45.1	-25.6	1.00	45.1	-25.6
	[start_02.24.15]	57.2	0.00	NaN	NaN	0.15	5.0	0.3	0.20	5.6	0.1	1.00	22.2	-6.8
10_21	[start_05.48.36]	33.8	0.05	1.4	-0.5	0.05	1.4	-0.5	0.10	6.5	-2.1	0.10	6.5	-2.1
	[start_14.16.59]	62.9	0.05	5.7	-2.6	0.05	5.7	-2.6	0.05	5.7	-2.6	0.20	6.3	-0.7
	[start_20.29.08]	29.5	0.05	2.1	0.5	0.10	4.6	-0.6	0.15	5.6	-0.9	0.15	5.6	-0.9
	[start_22.14.34]	16.1	0.05	7.2	-6.2	0.10	5.3	-2.1	1.00	12.0	-4.0	1.00	12.0	-4.0
10_16	[start_00.03.56]	19.2	0.05	2.8	-2.5	0.15	3.8	-0.9	0.60	4.8	-0.3	0.60	4.8	-0.3
10_12	[start_15.25.39]	35.8	0.05	5.4	-1.0	0.10	4.5	0.0	0.25	6.9	-0.7	0.25	6.9	-0.7
	mean	27.75	0.15	4.23	-2.55	0.36	4.72	-1.51	0.67	7.93	-3.26	0.75	8.85	-3.40

Table B.3: Table showing the results of using a combination of maximum wind speed error of 5 m/s and maximum wind direciton error of 10° when lowering the threshold of coefficient of variation iteratively

coefficient of variation results		original rmse		lim	rmse		mean error	
date [mm_d	TARA_5_cycle Processed_Data	ws [m/s]	wd [°]		ws [m/s]	wd [°]	ws [m/s]	wd [°]
11_12	[start_04.00.47]	31.8	37.8	0.25	1.1	3.8	0.7	0.6
11_09	[start_21.23.26]	20.4	35.1	0.15	0.7	3.1	0.6	-2.6
11_07	[start_04.14.40]	35.1	49.8	0.75	1.3	4.6	0.6	-0.7
11_03	[start_00.04.47]	8.1	17.1	0.00	NaN	NaN	NaN	NaN
	[start_05.34.35]	24.8	35.2	0.10	0.9	4.9	0.6	-2.7
	[start_12.48.52]	12.7	19.5	0.50	1.7	4.0	1.2	1.0
	[start_13.38.43]	4.7	8.6	0.35	2.0	4.1	1.4	0.2
	[start_14.42.28]	11.3	20.9	0.30	1.6	3.5	0.6	-1.8
	[start_19.45.12]	1.5	3.5	0.20	1.2	3.2	0.4	-1.1
	[start_22.04.57]	0.8	3.3	0.05	0.5	2.6	0.4	-1.4
11_02	[start_16.26.03]	23.4	31.6	0.10	1.4	4.1	0.6	-1.7
10_24	[start_00.01.54]	10.5	10.9	0.20	2.1	5.5	1.7	-3.4
	[start_19.53.58]	1.1	3.3	1.00	1.1	3.3	0.7	-2.0
	[start_21.33.42]	7.1	13.8	0.10	2.0	6.5	1.4	-4.3
10_22	[start_00.07.41]	9.7	65.5	0.05	1.3	5.2	1.3	-5.2
	[start_02.24.15]	25.1	57.2	0.15	1.4	5.0	0.6	0.3
10_21	[start_05.48.36]	9.8	33.8	0.05	0.8	1.4	0.0	-0.5
	[start_14.16.59]	24.9	62.9	0.05	1.4	5.7	1.1	-2.6
	[start_20.29.08]	8.0	29.5	0.10	1.1	4.6	0.7	-0.6
	[start_22.14.34]	3.6	16.1	0.10	1.7	5.3	1.1	-2.1
10_16	[start_00.03.56]	11.1	19.2	0.10	0.9	3.5	0.6	-1.2
10_12	[start_15.25.39]	15.1	35.8	0.10	0.8	4.5	0.6	0.0
	mean	13.67	27.75	0.22	1.28	4.22	0.80	-1.52

C

Results Coefficient of Variation Complete ACCEPT-campaign

Table C.1: Table showing the original results of the wind estimation during ACCEPT-campaign without removing statistical outliers at time resolution of 60 seconds.

matlab code rain_v2, Resolution 60s		original data			
date [mm_d	TARA-5_cycle_Processed_Data	rmse ws [m/s]	rmse wd [°]	mean error ws [m/s]	mean error wd [°]
11_12	[start_04.00.47]	31.8	37.8	13.2	1.2
11_09	[start_21.23.26]	20.4	35.1	5.8	-3.0
11_07	[start_04.14.40]	35.1	49.8	13.4	-7.7
11_03	[start_00.04.47]	8.1	17.1	6.1	-8.5
	[start_05.34.35]	24.8	35.2	11.8	-0.1
	[start_12.48.52]	12.7	19.5	8.9	3.4
	[start_13.38.43]	4.7	8.6	2.7	0.4
	[start_14.42.28]	11.3	20.9	7.6	0.6
	[start_19.45.12]	1.5	3.5	0.5	-1.1
	[start_22.04.57]	0.8	3.3	0.5	-1.0
11_02	[start_16.26.03]	23.4	31.6	11.4	-6.4
10_24	[start_00.01.54]	10.5	10.9	7.6	-3.5
	[start_19.53.58]	1.1	3.3	0.7	-2.0
	[start_21.33.42]	7.1	13.8	5.1	-9.4
10_22	[start_00.07.41]	9.7	65.5	2.7	-29.0
	[start_02.24.15]	25.1	57.2	9.3	-19.7
10_21	[start_05.48.36]	9.8	33.8	5.5	-4.2
	[start_14.16.59]	24.9	62.9	15.9	-29.1
	[start_20.29.08]	8.0	29.5	3.6	-7.8
	[start_22.14.34]	3.6	16.1	1.2	-5.2
10_16	[start_00.03.56]	11.1	19.2	3.4	-0.9
10_12	[start_15.25.39]	15.1	35.8	7.7	-2.0
	mean	13.7	27.8	6.6	-6.1

Table C.2: Table showing the results for the wind estimation during ACCEPT-campaign during precipitation without removing statistical outliers at time resolution of 60 seconds.

matlab code rain_v2, Resolution 60s		rain events			
date [mm_d	TARA-5_cycle_Processed_Data	rmse ws [m/s]	rmse wd [°]	mean error ws [m/s]	mean error wd [°]
11_12	[start_04.00.47]	5.7	14.7	2.1	2.1
11_09	[start_21.23.26]	1.0	2.9	0.8	-2.4
11_07	[start_04.14.40]	3.5	5.6	1.4	0.1
11_03	[start_00.04.47]	1.0	3.9	0.5	-1.0
	[start_05.34.35]	2.1	4.4	1.3	-0.4
	[start_12.48.52]	7.9	15.0	4.1	-7.7
	[start_13.38.43]	2.2	5.3	1.5	0.8
	[start_14.42.28]	3.7	7.0	1.5	-1.2
	[start_19.45.12]	1.5	3.5	0.5	-1.2
	[start_22.04.57]	0.8	3.3	0.5	-1.0
11_02	[start_16.26.03]	1.5	3.8	0.7	-1.6
10_24	[start_00.01.54]	3.5	4.8	2.5	0.8
	[start_19.53.58]	1.1	3.3	0.7	-2.0
	[start_21.33.42]	1.0	3.4	0.6	-1.9
10_22	[start_00.07.41]	9.3	27.0	3.4	-7.5
	[start_02.24.15]	2.4	8.1	1.1	-0.5
10_21	[start_05.48.36]	5.3	14.7	2.0	-0.2
	[start_14.16.59]	5.5	8.1	2.5	0.6
	[start_20.29.08]	1.4	6.0	0.8	-1.2
	[start_22.14.34]	1.9	10.9	0.8	-3.2
10_16	[start_00.03.56]	1.9	5.4	0.9	1.1
10_12	[start_15.25.39]	2.0	5.1	1.0	1.2
	mean	3.0	7.6	1.4	-1.2

Table C.3: Table showing the results of the wind estimation during ACCEPT-campaign selecting the data using a coefficient of variation threshold without removing statistical outliers at time resolution of 60 seconds.

Resolution 60s		coefficient of variation threshold 0.22			
date [mm_d	TARA-5_cycle_Processed_Data	rmse ws [m/s]	rmse wd [°]	mean error ws [m/s]	mean error wd [°]
11_12	[start_04.00.47]	1.1	3.8	0.7	0.6
11_09	[start_21.23.26]	1.3	3.6	0.8	-2.8
11_07	[start_04.14.40]	0.9	4.9	0.3	-2.5
11_03	[start_00.04.47]	3.8	10.0	2.4	-6.0
	[start_05.34.35]	2.2	4.7	1.1	-0.9
	[start_12.48.52]	1.3	2.0	1.0	-0.2
	[start_13.38.43]	1.8	3.2	1.2	-1.0
	[start_14.42.28]	1.5	3.5	0.6	-1.8
	[start_19.45.12]	1.2	3.2	0.4	-1.1
	[start_22.04.57]	0.8	3.2	0.5	-1.0
11_02	[start_16.26.03]	2.3	6.0	1.2	-2.9
10_24	[start_00.01.54]	2.3	5.8	1.9	-3.7
	[start_19.53.58]	1.1	3.3	0.7	-2.0
	[start_21.33.42]	2.9	8.8	2.4	-6.9
10_22	[start_00.07.41]	2.3	11.1	1.4	-1.9
	[start_02.24.15]	1.4	5.9	0.7	0.0
10_21	[start_05.48.36]	2.1	7.2	0.8	-0.7
	[start_14.16.59]	1.9	6.3	1.1	-0.6
	[start_20.29.08]	3.4	9.5	1.3	-0.1
	[start_22.14.34]	1.8	5.9	0.8	-1.6
10_16	[start_00.03.56]	1.1	4.0	0.7	-0.6
10_12	[start_15.25.39]	1.3	6.0	0.8	-0.4
	mean	1.8	5.5	1.0	-1.7

D

Coefficient of Variation Results for Unusable Cases

Table D.1: Table showing the original results of the wind estimation during ACCEPT-campaign for cases identified as not being usable for the quality assessment of the wind estimation at time resolution of 60 seconds. This identification was done looking at quicklooks or initial RMSE and mean error results for wind speed and direction estimation errors.

Resolution 60s		original data			
date [mm_d	TARA-5_cycle_Processed_Data	rmse ws [m/s]	rmse wd [°]	mean error ws [m/s]	mean error wd [°]
11_10	[start_00.05.44]	7.2	12.5	4.4	-10.7
	[start_01.42.02]	37.9	38.4	23.5	-7.6
11_07	[start_00.02.13]	9.8	19.2	-0.4	6.8
	[start_13.08.22]	32.2	34.8	18.2	-2.8
11_04	[start_00.02.30]	43.5	43.5	23.2	-6.5
11_03	[start_05.15.36]	21.3	18.5	17.9	1.0
	[start_09.39.56]	16.2	28.5	11.7	7.6
11_01	[start_00.02.46]	31.5	34.8	19.8	-12.8
	[start_16.44.46]	65.9	87.5	45.8	16.7
	[start_19.03.51]	69.7	79.1	45.2	-1.7
10_30	[start_00.02.39]	35.3	50.6	18.8	-5.3
10_29	[start_00.02.12]	11.1	21.9	7.3	-6.5
	[start_06.42.59]	17.3	27.1	12.1	-6.8
	[start_10.20.52]	18.2	55.7	10.9	-11.3
10_24	[start_07.26.39]	14.1	17.4	8.6	0.9
	[start_17.39.19]	7.2	6.0	5.4	-1.9
10_22	[start_06.32.39]	19.9	73.6	11.6	-56.2
	[start_12.36.43]	33.7	82.9	18.3	-58.6
10_21	[start_00.02.25]	19.6	30.7	13.4	-16.9
10_20	[start_00.02.36]	25.6	47.4	18.4	-30.0
10_19	[start_00.02.29]	18.9	28.7	14.1	-17.0
	[start_08.15.23]	25.8	38.3	21.0	-24.9
	[start_12.04.04]	24.6	56.4	17.3	-1.2
10_18	[start_00.02.23]	5.9	8.7	4.7	-2.0
	[start_02.59.55]	8.0	18.7	2.5	9.7
	[start_07.30.24]	22.0	28.3	14.2	3.2
10_17	[start_00.03.49]	55.4	66.3	28.9	-25.5
	[start_05.37.01]	31.1	38.7	21.0	-19.8
10_16	[start_07.14.52]	29.2	44.1	21.2	-19.8
	[start_23.29.41]	16.0	50.7	15.9	-50.4
10_15	[start_00.02.21]	25.0	37.8	17.7	-25.7
	[start_15.55.50]	25.3	38.1	10.4	-2.3
10_14	[start_00.01.55]	31.9	35.2	15.3	1.3
	[start_08.50.05]	12.9	22.7	8.4	3.3
	[start_12.20.27]	17.8	32.4	12.7	-11.1
10_13	[start_00.04.39]	11.6	64.4	6.7	-38.2
	[start_00.42.10]	37.1	87.4	14.4	-31.6
	[start_03.28.30]	41.4	80.5	16.4	-49.1
	[start_06.18.00]	22.6	40.4	13.4	1.8
	[start_07.08.46]	12.3	23.4	6.0	9.8
	[start_07.35.40]	11.3	31.6	7.3	6.5
	[start_08.05.50]	41.0	39.7	16.2	-6.2
	[start_10.21.11]	9.5	11.4	8.9	2.7
	[start_10.33.52]	11.4	11.2	7.8	5.7
	[start_11.15.09]	25.9	26.4	15.3	-0.3
10_12	[start_00.01.53]	46.1	60.4	22.7	-24.9
10_11	[start_00.02.09]	41.0	57.2	22.9	-15.1
	mean	25.5	40.2	15.3	-11.1

Table D.2: Table showing the results of the wind estimation during ACCEPT-campaign using a threshold in coefficient of variation for data selection for cases identified as not being usable for the quality assessment of the wind estimation at a time resolution of 60 seconds. This identification was done looking at quicklooks or initial RMSE and mean error results for wind speed and direction estimation errors.

Resolution 60s		coefficient of variation threshold 0.22			
date [mm_d	TARA-5_cycle_Processed_Data	rmse ws [m/s]	rmse wd [°]	mean error ws [m/s]	mean error wd [°]
11_10	[start_00.05.44]	3.1	9.2	2.3	-7.9
	[start_01.42.02]	3.4	7.6	2.1	-4.4
11_07	[start_00.02.13]	0.7	3.5	0.5	2.8
	[start_13.08.22]	2.2	11.4	0.9	2.2
11_04	[start_00.02.30]	3.7	12.5	3.2	-10.8
11_03	[start_05.15.36]	NaN	NaN	NaN	NaN
	[start_09.39.56]	2.5	5.3	1.7	3.0
11_01	[start_00.02.46]	6.1	14.9	5.6	-13.3
	[start_16.44.46]	1.8	4.9	0.7	0.2
	[start_19.03.51]	4.8	21.0	4.7	-20.8
10_30	[start_00.02.39]	2.9	42.6	0.9	-16.7
10_29	[start_00.02.12]	2.0	8.1	1.7	-7.1
	[start_06.42.59]	1.6	4.6	1.3	-0.5
	[start_10.20.52]	1.4	28.9	0.8	-11.0
10_24	[start_07.26.39]	1.4	3.4	1.0	-0.4
	[start_17.39.19]	1.0	3.9	0.7	-2.1
10_22	[start_06.32.39]	1.8	5.3	1.1	0.1
	[start_12.36.43]	5.3	27.9	2.1	-20.4
10_21	[start_00.02.25]	5.3	15.5	3.8	-10.1
10_20	[start_00.02.36]	4.8	25.7	3.6	-10.5
10_19	[start_00.02.29]	7.7	17.9	7.2	-17.1
	[start_08.15.23]	3.9	13.5	3.0	-12.9
	[start_12.04.04]	6.7	25.3	4.6	-0.4
10_18	[start_00.02.23]	3.4	7.6	2.8	-5.2
	[start_02.59.55]	1.9	6.2	-0.4	5.5
	[start_07.30.24]	13.9	17.8	13.9	-17.8
10_17	[start_00.03.49]	6.4	40.4	6.1	-39.7
	[start_05.37.01]	4.2	33.7	2.2	-9.7
10_16	[start_07.14.52]	6.6	22.6	4.1	-12.8
	[start_23.29.41]		NaN	NaN	NaN
10_15	[start_00.02.21]	2.8	11.1	1.2	-4.7
	[start_15.55.50]	0.7	3.3	0.5	-1.1
10_14	[start_00.01.55]	1.3	3.3	1.3	0.1
	[start_08.50.05]	3.3	4.6	2.1	2.1
	[start_12.20.27]	2.2	6.9	1.4	-2.6
10_13	[start_00.04.39]	0.8	11.9	-0.7	-11.9
	[start_00.42.10]	NaN	NaN	NaN	NaN
	[start_03.28.30]	3.1	4.1	-3.1	4.1
	[start_06.18.00]	2.4	9.6	-1.1	1.2
	[start_07.08.46]	1.6	5.8	1.4	4.9
	[start_07.35.40]	1.3	7.1	0.8	5.6
	[start_08.05.50]	NaN	NaN	NaN	NaN
	[start_10.21.11]	NaN	NaN	NaN	NaN
	[start_10.33.52]	NaN	NaN	NaN	NaN
	[start_11.15.09]	4.5	3.5	4.1	-2.3
10_12	[start_00.01.53]	10.3	56.7	10.3	-56.7
10_11	[start_00.02.09]	3.1	29.2	0.7	0.7
	mean	3.6	14.6	2.5	-7.3